DISSERTATION

THE DEVELOPMENT OF MICROFLUIDIC DEVICES FOR ENVIRONMENTAL AND FOOD QUALITY ANALYSIS

Submitted by

Jana Catherine Jokerst

Department of Chemistry

In partial fulfillment of the requirements

For the Degree of Doctor of Philosophy

Colorado State University

Fort Collins, Colorado

Spring 2012

Doctoral Committee:

Advisor: Charles Henry

Thomas Borch
George Barisas
Steven Strauss
Ronald Tjalkens

ABSTRACT

THE DEVELOPMENT OF MICROFLUIDIC DEVICES FOR ENVIRONMENTAL AND FOOD QUALITY ANALYSIS

Whether termed micro-total analysis systems, lab-on-a-chip, or microfluidic devices, the technologies that define the field of microfluidics have shown great promise for overcoming many challenges in environmental, clinical, and biological analyses. The numerous advantages these devices bring to analysis, such as cost, reduced analysis time, minimal sample and reagent requirements, integration of multiple processing steps in a single device, and the possibility for automation and on-site analysis, make them attractive alternatives to conventional instrumentation. The work comprising this dissertation focuses on novel, miniaturized platforms for both food and water quality analysis. The development of two devices for these applications will be presented: a microchip capillary electrophoresis (MCE) method for the determination of perchlorate in drinking water and a paper-based analytical device (μPAD) for the detection of foodborne, pathogenic bacteria.

Recent advances in microfluidics have had a significant focus in environmental analysis. The portability and rapid analysis these devices provide has brought us closer to on-site monitoring of environmental matrices and real-time measurements in these systems. Perchlorate has gained considerable attention over the past decade as a water contaminant. Prolonged consumption of contaminated drinking water has been linked to impaired thyroid function, leading to a number of adverse health effects. Current detection methods rely on expensive bench-top instruments, housed in a centralized laboratory. While these techniques offer high

sensitivity and low detection limits, they are costly, time-consuming, and do not provide the ability to monitor perchlorate on-site. This dissertation describes the development of a microchip capillary electrophoresis device capable of rapid analysis of ppb levels of perchlorate in drinking water. Unique separation chemistry in which zwitterionic surfactant micelles are incorporated into the running buffer allows for selective analysis of perchlorate. The device performance was tested via analysis of spiked drinking water samples with detection limits of the system below the U.S. Environmental Protection Agency requirement. Further advancement of the device for analysis of more complex environmental samples is also discussed herein.

The remaining chapters present a novel, paper-based device for bacterial detection. Faster, simpler methods of detecting foodborne pathogens are highly desired, particularly in the food industry. Existing methodologies are time-consuming, cumbersome, and require highly trained personnel. Often, several days are required for confirmation of food contamination, and in an industry with time-sensitive products, this delay is a major hindrance. Presented here is a paper-based analytical device (μPAD) developed for more rapid and simple detection of three foodborne pathogens: *Listeria monocytogenes*, *Escherichia coli* O157:H7, and *Salmonella enterica*. The μPAD provides a fast, easy-to-use technology for first-level screening that compliments existing methods. The device comprises a simple spot test on filter paper and utilizes species-specific enzymatic assays for colorimetric bacteria detection. In this work, the device is used to detect the three pathogens in spiked ready-to-eat meat samples. Concentrations as low as 10^1 cfu/cm^2 were detected within an 8-12 h of enrichment. While this first phase of development shows great promise, work is ongoing to enhance assay selectivity and reduce overall analysis time.

ACKNOWLEDGEMENTS

This dissertation would not have been possible without the help and support of many friends, colleagues, and family members. Special thanks are paid to Henry Group members, past and present. Thanks to each of you for helping me through this program. Your constant support, constructive critiques, and the friendly work environment you created will always be remembered. Jaclyn Adkins, I am especially grateful and appreciative of your hard work and cheerful nature. I am honored to have acted as a mentor to such a kind, thoughtful person and talented chemist. Meghan Mensack, I am very fortunate to have had you as a mentor for the past year. Thank you for your words of wisdom and assistance with countless presentations and manuscripts.

I thank my collaborators and graduate committee members for their invaluable input and guidance. Don Cropek, Imee Arcibal, and Larry Goodridge, it was a pleasure working with all of you. I am appreciative of all your hard work and the knowledge I gained from our collaborations. Bledar Bisha, I am forever grateful for your steadfast assistance and insight. Thank you for many enlightening conversations and your masterful instructions in the Microbiology lab.

I thank my wonderful friends and family for their love and support. Mallory Mentele, I would not have made it to the end without you. Your friendship is one of the greatest things I take away from my time at Colorado State University, and I will cherish it always. I thank my husband, Adam Jokerst. Your unwavering support, encouragement, and love give me strength and confidence every day. I am so very blessed to have you in my life.

Finally, I owe great deal of thanks to Dr. Charles Henry, my advisor. Thank you for your guidance, instruction, patience, and understanding. I am inspired by your passion and enthusiasm, and I am honored to have had the opportunity to work for you.

TABLE OF CONTENTS

LIST OF ABBREVIATIONS

BGE	background electrolyte
CCL	Contaminant Candidate List
CDC	Center for Disease Control
CE	capillary electrophoresis
CMC	critical micelle concentration
CZE	capillary zone electrophoresis
CRPG	chlorophenol red galactopyranoside
DOD	Department of Defense
ELISA	enzyme-linked immunosorbent assay
EIC	electrostatic ion chromatography
EOF	electroosmotic flow
FASS	field-amplified sample stacking
HDAPS	hexadecyl-N,N-dimethyl-3-ammonio-1-propane sulfonate
HVPS	high voltage power supply
IC	ion chromatography
IC-MS	ion chromatography-mass spectrometry
LOC	lab-on-a-chip
LOD	limit of detection
MC	magenta caprylate (5-bromo-6-chloro-3-indolyl octanoate)
MCL	maximum contaminant level
MCE	microchip capillary electrophoresis
MEKC	micellar electrokinetic chromatography

NASA	National Aeronautic and Space Administration
NIS	sodium iodide symporter
PCR	polymerase chain reaction
PDMS	poly(dimethylsiloxane)
PDS	propane disulfonate
PI-PLC	phosphatidylinositol-specific, phospholipase C
ppm	parts per million
ppb	parts per billion
RTE	ready-to-eat
S/N	signal-to-noise ratio
TDAPS	tetradecyl-N,N-dimethyl-3-ammonio-1-propane sulfonate
TSH	thyroid stimulating hormone
U.S. EPA	United States Environmental Protection Agency
X-InP	5-bromo-4-chloro-3-indolyl *myo*-inositol phosphate
μPAD	paper-based analytical device
μTAS	micro-total analysis systems

CHAPTER 1. INTRODUCTION TO MICROFLUIDICS FOR THE ANALYSIS OF PERCHLORATE IN WATER

1.1 INTRODUCTION

The field of microfluidics has gained considerable attention over the past few decades because of the abundant and desirable characteristics associated with lab-on-a-chip (LOC) and micro-total analysis systems (μTAS). Over the years, groups have demonstrated the use of microfluidics for a seemingly limitless number of applications. Environmental analysis, in particular, is one of the major fields of study for microfluidic devices. Capabilities these devices afford, such as portability and speed, are particularly attractive for on-site environmental monitoring. While a limited number of devices have been developed for analysis of atmospheric aerosols, the majority of environmentally focused microfluidics have been established for water quality assessment.

In the first few chapters of this dissertation, a novel microchip capillary electrophoresis (MCE) method for the determination of perchlorate in water is presented. Perchlorate is a water contaminant that most often originates from the use of munitions, flares, rocket fuels, and other explosives. It persists in the environment and water table for long periods of time, and consumption of contaminated drinking water can cause very serious health problems. Current analytical techniques involve ion chromatography coupled to mass spectrometry. While these regulatory methods provide sensitive analysis with low detection limits, the instrumentation is

complex and unsuitable for on-site analysis or regular monitoring at a municipal water treatment facility. The MCE device presented here provides rapid detection of perchlorate with detection limits that exceed the US Environmental Protection Agency (U.S. EPA) regulatory limit, making it a good alternative to conventional techniques. This chapter presents an introductory discussion of perchlorate contamination, capillary electrophoresis in microfluidics, and the fundamental concepts on which the MCE method was developed.

1.2 PERCHLORATE

1.2.1. Perchlorate Contamination

Perchlorate is an environmental contaminant known to have deleterious effects on the body's endocrine system. Much of the perchlorate contamination in the U.S. is attributed to the manufacturing of ammonium perchlorate (NH_4ClO_4) as an oxidizer in flares, rocket fuels, propellants, blasting agents, and fireworks.[1] The use of manufactured perchlorate salts is largely tied to the Department of Defense (DOD), the National Aeronautics and Space Administration (NASA), and a number of defense contractors for rockets, missiles, and munitions.[2,3] Moreover, perchlorate can occur naturally in the environment, and traces of perchlorate have been found in natural materials and fertilizers, including Chilean caliche, potash ore, and kelp.[4] Until the 1950's, these natural fertilizers were used across the U.S., introducing perchlorate directly to soils. Due to its high water solubility, stability, and mobility, perchlorate is regarded as a persistent, emerging contaminant, and it may exist in the environment for decades.[5] Perchlorate contamination has been sporadic throughout the U.S. Perchlorate has been detected in drinking water, groundwater, and various food products in more than twenty states.[6] In particular, large areas in the western and southwestern U.S. have reported very high concentrations of perchlorate

in municipal water systems and groundwater.[2,7,8] This geological area and other arid regions are particularly susceptible to accumulation of perchlorate in soils and vegetation due to low precipitation and a relatively deep water table. [9,10] With little annual rainfall, perchlorate persists in these areas rather than being transported downstream.

Human exposure to perchlorate most likely occurs upon ingestion of contaminated water and foods.[11] As awareness of perchlorate contamination increases, monitoring levels in drinking water and food products has become progressively important. Perchlorate contamination has been reported in leafy green vegetables, milk, grains, and fruit.[2,5,11-13] However, drinking water contamination is of particular concern since exposure in this form is more long term.[2,7,11] The U.S. EPA added perchlorate to its Contaminant Candidate List (CCL) for drinking water in 1998 following the discovery of its presence throughout drinking water supplies in the southwest US.[5] More recently, a health advisory was issued for perchlorate, stating 15 ppb is a safe level for all subpopulations.

1.2.2 Perchlorate and Public Health

The human health risk of perchlorate exposure results from the observed affinity between perchlorate and the sodium/iodide symporter (NIS), a membrane protein responsible for the controlled transport of iodide to the thyroid gland for the production of thyroid hormones, thyrosine (T_4) and triiodothyronine (T_3). As a result of this affinity, which can be attributed to the similar hydrated radius and charge of perchlorate and iodide, perchlorate inhibits the uptake of iodide into thyroid follicular cells. With less available iodide for T_3 and T_4 production, the body's homeostatic response is to increase the amount of thyroid stimulating hormone (TSH) generated by the pituitary gland. Disruption of thyroid function, caused by increased levels of

THS and decreased T_3 and T_4 concentrations, can lead to serious adverse health effects, particularly if the thyroid gland is deprived from iodide over a long period of time.[2,3,14,15]

Prolonged exposure to perchlorate in adults has raised major concerns, as insufficient iodide uptake in adults can lead to thyroid conditions, such as goiter, as well as mental retardation in extreme cases.[3,11] Thyroid inhibition in neonates and infants, however, can be far more detrimental. Since the NIS is also expressed in the placenta and in lactating breast tissue, the fetus may be exposed to perchlorate in the womb or from the ingestion of breast milk as an infant.[6] For the fetus and young infants, thyroid hormones are essential for skeletal and neurological development, and iodide deficiency during gestation and infancy has been linked to profound mental and physical deficits in children.[16,17]

1.3 DETERMINATION OF PERCHLORATE IN DRINKING WATER

1.3.1 Conventional Analysis Methods

Currently, the most commonly used technique for perchlorate analysis in water is ion chromatography (IC). IC has been commercially available for over 30 years and is widely accepted as a powerful tool for the analysis of inorganic ions. Determination of trace levels of perchlorate in the environment is a challenging analytical task, and to date, IC is the most suitable technique for identification and quantification of such low concentrations. U.S. EPA method 314.0 employs an anion-exchange column functionalized with alkanol quaternary ammonium groups for trace perchlorate analysis. The mobile phase consists of a sodium hydroxide solution with an organic modifier such as methanol or *p*-cyanophenol, and anions are detected via suppressed conductivity detection within 20 min. Using a large (1000 μL) injection loop, detection limits are in the ppb range.[18] Often the ability to detect trace levels of perchlorate

is enhanced by coupling to mass spectrometry (MS). U.S. EPA method 331.0 employs IC-MS to achieve detection limits as low as 0.005 ppb.

IC is a reliable and practical technique for very sensitive perchlorate analysis; however, several drawbacks exist. Similar to most chromatographic techniques, there is great interest in improving speed and simplifying method development. Separations are relatively slow through the high-pressure resistance columns employed, and method development is hindered by the time required to equilibrate the column with new eluent. Furthermore, the instrumentation is complex and bulky, relinquishing portability. Currently, water samples must be sent to a centralized laboratory for costly and time-consuming analysis. A fast, portable, cost-effective means of perchlorate determination would greatly benefit municipal water systems and the US military.

1.3.2 Capillary Electrophoresis

In the analysis of inorganic ions, capillary electrophoresis (CE) is often used as a complementary technique to IC due to its short analysis time, low cost, separation efficiency, and ease of method development.[19] Unlike chromatography, CE requires no packing material or stationary phase for analyte separation, eliminating band broadening due to multiple flow paths or mass transfer with a stationary phase. Mikkers[20] and Jorgenson[21] are credited with development of conventional CE. In the 1980's, the technique was realized to meet increasing demands for fast separations, high resolution and selectivity, reduced waste management costs, and the ability to analyze a wider range of analytes than contemporary HPLC.

General CE theory centers around two phenomena: the electrophoretic mobility of ions in an applied electric field and the generation of electroosmotic flow (EOF). In normal polarity capillary zone electrophoresis (CZE), the most commonly implemented CE mode, the capillary is filled with a background electrolyte (BGE) and an electric field is generated via cathodic and

anodic electrodes placed at either end of the capillary. When an electric field is applied, charged analytes are separated in the BGE by their individual electrophoretic mobilities. Resulting analyte velocities in the field can be described by equation 1.1 where velocity, v_{ep}, is equal to the intrinsic electrophoretic mobility of an analyte, μ_{ep}, multiplied by the field strength, E.

$$v_{ep} = \frac{q}{f}E \equiv \mu_{ep}E \tag{1.1}$$

The analyte mobility, μ_{ep}, is a function of the analyte charge, q, and the friction coefficient, f, which is described by the Stokes equation:

$$f = 6\pi\eta r \tag{1.2}$$

where the frictional coefficient, f, is calculated for a spherical particle having a hydrodynamic radius r in a solution of viscosity, η.

In CZE, analytes are injected at the anodic end of the capillary, causing positively charged analytes to migrate down the capillary towards the cathode, negatively charged analytes to migrate towards the anode, and neutral analytes to remain stationary at the injection site. Here, a key element of CE theory comes into play: the generation of EOF (μ_{eo}) within the capillary, which enables the detection of all analyte species, regardless of charge. At a pH above ~2, silanol groups on the surface of silica capillaries are deprotonated, and an electrical double layer is formed on the surface consisting of the negatively charged silanol groups and positively charged cations in the BGE. A static, Inner Hemholtz or Stern layer of ions exists at the very surface of the capillary wall while a more diffuse and mobile Outer Hemholtz layer forms distally from the Stern layer as illustrated in Figure 1.1. Under an applied electric field, cations in the Outer Hemholtz layer migrate toward the cathode carrying the waters of hydration or the bulk solution with them, generating electroosmotic flow. The velocity of EOF propels analytes

toward the detector. Consequently, analytes migrate at a new apparent velocity, v_{app}, given by the sum of the electroosmotic flow and the electrophoretic velocities.

$$v_{app} = \mu_{app}E = (\mu_{ep} + \mu_{eo})E \quad (1.3)$$

Since EOF is pH dependent, this factor plays an important role in separation selectivity. When the magnitude of EOF is larger than electrophoretic mobility, all analytes will reach the detector with a net positive apparent mobility, μ_{app}. Typically, detection of analytes is carried out via optical (fluorescence or UV) or conductivity detection.

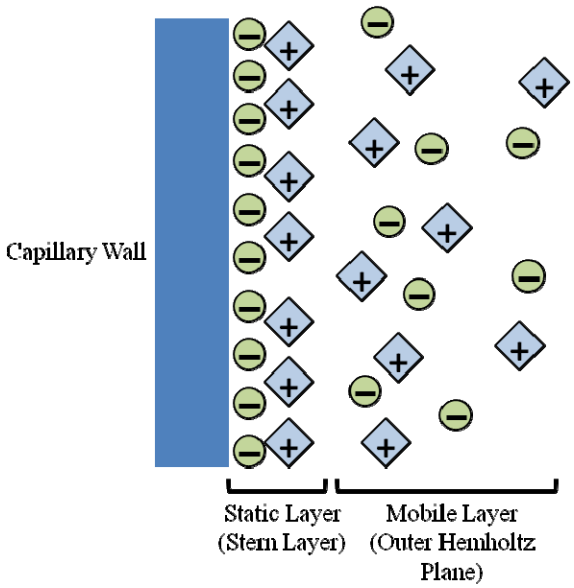

Figure 1.1 An illustration of the electrical double layer that forms in bare-silica capillaries. Under an applied electric field, movement of ions in the mobile layer generates electroosmotic flow in the capillary.

In recent years, CE has been used for the trace determination of perchlorate in drinking and environmental waters[22] as well as explosive devices[23] and post-blast residues.[24] Kiplagat and co-workers developed an electromembrane extraction technique using a supported liquid membrane. A selective extraction is performed across the membrane, effectively preconcentrating perchlorate from tap water, bottled water, rain water, and surface water. The extract was then analyzed via CE with conductivity detection, achieving detection limits as low

as 0.2 ppb in the original sample.[22] Blanco and co-workers presented a sequential injection CE instrument coupled with conductivity detection for the identification of improvised explosive devices which contain perchlorate, a common explosive tracer ion.[23] In this work, soil extracts from controlled detonation sites were analyzed, and using CE, the detection limits for perchlorate were in the ppb range. Another recent study, by Sarazin and co-workers, utilized CE to identify and determine ten anions in post-blast residues from explosive detonators.[24] Limits of detection for perchlorate were 0.5 ppm in this case; however, sample matrices were complex and highly varied, including soil, cloth, glass, plastic, and paper, making the sample preparation more challenging than for aqueous samples.

1.3.3 Selectivity

With particular focus on the separation of inorganic anions, selectivity in CE is largely dependent on the intrinsic ionic mobilities of the anions.[25] There are a number of factors that influence these mobilities, including pH, buffer composition, and EOF modifiers. Electrophoretic mobility of analytes can be changed by altering their mass-to-charge ratio. This can be done by simply changing the buffer pH. For weak acids, a BGE with a pH value near the pK_a of the analytes can greatly reduce mobility.[19,25-27] The addition of a pseudo-stationary phase can also provide additional selectivity in the separation of inorganic anions. Zwitterionic surfactants added to the BGE in concentrations above the critical micelle concentration (CMC) will form micelles in solution that selectively retain polarizable anions.[28] Sulfobetaine-type surfactants have been explored for this purpose.[29,30] These compounds have a bifunctional, hydrophilic head group, composed of a positively charged ammonium group and a negatively charged sulfonate group, attached to a hydrophobic tail. An illustration of CE separations with surfactant micelles is shown in Figure 1.2. The interaction of sulfobetaine surfactants with

anions follows the Hofmeister series, which describes an ions chaotropic character.[29] This interaction is very strong for polarizable anions and can provide a great advantage for anion separations. For example, association constants reported for chloride, nitrate, iodide, and perchlorate with TDAPS micelles are 2.0, 15, 95, and 800 $dm^3 \cdot mol^{-1}$, respectively.[31] Employing this unique and selective chemistry, perchlorate can be separated from competing anions. The optimization of this separation will be discussed in Chapter 2.

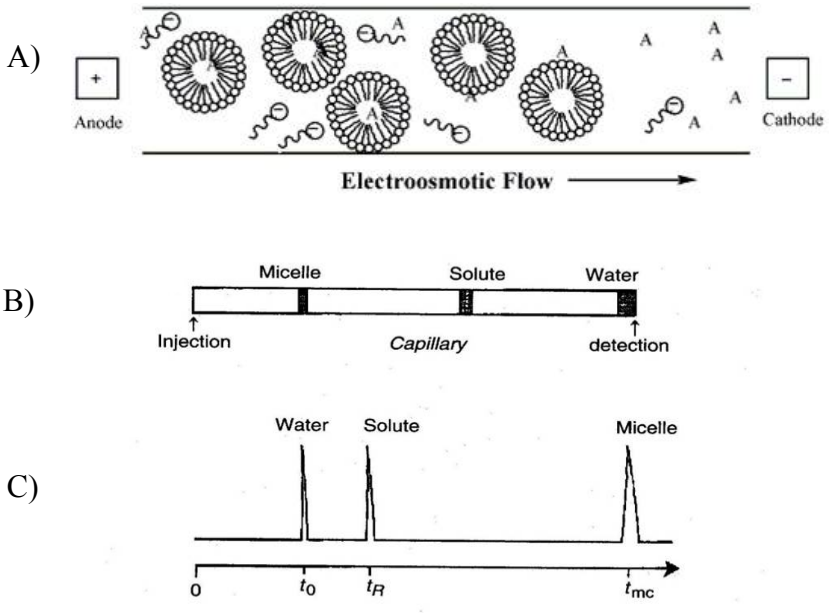

Figure 1.2 A) An illustration of micellar electrokinetic chromatography (MEKC) for separation of a neutral analyte using surfactant micelles. In this case, the micelle is negatively charged and therefore, migrates in the opposite direction of EOF. The neutral analyte is retained by the micelle, and since the velocity of EOF is greater than the velocity of the micelle, the neutral species is carried to the detector. B) Schematic showing the migration behaviors of water, which acts as an EOF marker, the neutral analyte, which has an apparent velocity between that of the EOF and the micelle, and the micelle, which migrates at a velocity that is the difference between EOF and electrophoretic mobility of the micelle. C) The corresponding electropherogram, showing the detection of the neutral analyte and the micelle. (Reprinted from Terabe et al.)[35]

1.3.4 On-Capillary Sample Concentration

Fundamentally, the capillary dimensions employed in CE can restrict the limits of detection achieved. For example, the total volume of sample injected is limited by the small volume of the capillary. Also, optical detection techniques, such as UV detection, are hampered by the reduced pathlength. To overcome these challenges and improve detection limits, on-line sample preconcentration methods such as field-amplified sample stacking (FASS) have been developed.[32,33] FASS is the simplest sample stacking technique, and it was first reported by Mikkers and co-workers in 1979.[20] FASS is achieved by exploiting the differences in ionic strength between the BGE and sample matrix. When analytes are dissolved in a low-conductivity matrix, such as water, a high field strength develops over the high resistance sample plug upon injection. Analytes migrate quickly until they reach the buffer interface. As sample ions reach the high-conductivity BGE, they slow down and stack in a narrow zone, preconcentrating the sample. Since analyte velocity is directly proportional to field strength, the greater the difference in resistance between the BGE and sample matrix, the faster analytes will migrate. A schematic illustrating sample stacking in CE is shown in Figure 1.3.

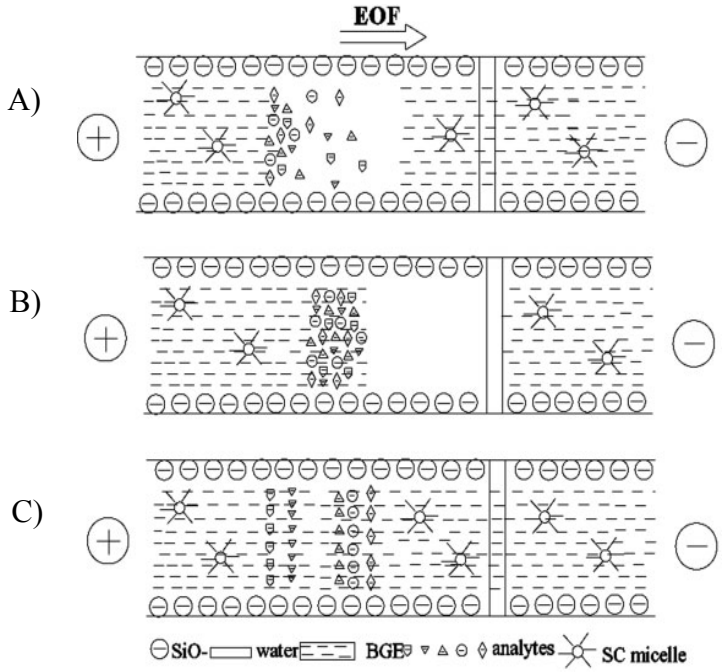

Figure 1.3 Diagram of sample stacking in CZE. A) Anionic analytes dissolved in water, a low-conductivity matrix, are injected as a sample plug. The high field strength generated across the sample plug causes the analytes to "stack" at the sample-BGE interface (B). C) Analytes form narrow zones and are separated based on their apparent electrophoretic mobilities. (Reprinted from Zang et al.)[36]

FASS enhances analyte detection in two ways: by narrowing analyte bands in the capillary and by increasing the amount of sample that can be loaded onto the capillary. By causing analytes to stack in a narrow band, analyte peak widths are reduced and peak heights are increased. In turn, this results in a greater signal-to-noise ratio and lower detection limits. Also, because peak widths are reduced, larger sample volumes can be injected onto the capillary without sacrificing separation efficiency. With a greater mass of analyte loaded onto the capillary, greater signals are achieved.[32] Sample stacking plays an important role in perchlorate analysis, and it will be discussed in upcoming chapters.

1.3.5 Microchip CE

CE is a well established and power technique for anion separations. An added advantage of CE is that it is easily adaptable to a miniaturized, microfluidic format.[37] Microfluidic devices offer numerous advantages to conventional instrumentation, such as reduced sample and reagent volumes, portability, cost effectiveness, and faster analysis times. The idea of micro-total analysis systems (μTAS) was first hypothesized by Manz and coworkers 1990 and describes the concept of full integration of sample preparation, analysis, and detection steps on a single device.[38] In particular, a microfluidic device for perchlorate analysis would allow for on-site, rapid, and inexpensive determination of perchlorate in a variety of water systems.

Microchip CE (MCE) devices have been developed for a broad range of applications. Early MCE devices were fabricated in glass with wet chemical etching techniques.[38,39] Today, fabrication in various polymeric materials, including poly(dimethylsiloxane) (PDMS), using photolithography is more common since the material less expensive and the fabrication is much simpler.[40,41] Basic microchip designs incorporate a "T-shaped" channel configuration with fluid reservoirs at each channel terminus. Electrodes, controlled by an external power supply, are placed in fluid reservoirs to enable the generation of an electric field through the microchip. If conductivity detection is employed, the longer separation channel is bisected by microelectrodes just before the waste reservoir. Electrodes placed in designated sample and buffer reservoirs allow for electrokinetic injection of a sample plug down the separation channel. A representation of a MCE device is shown in Figure 1.4. The development of a microchip CE (MCE) device for perchlorate analysis is presented in Chapter 2.

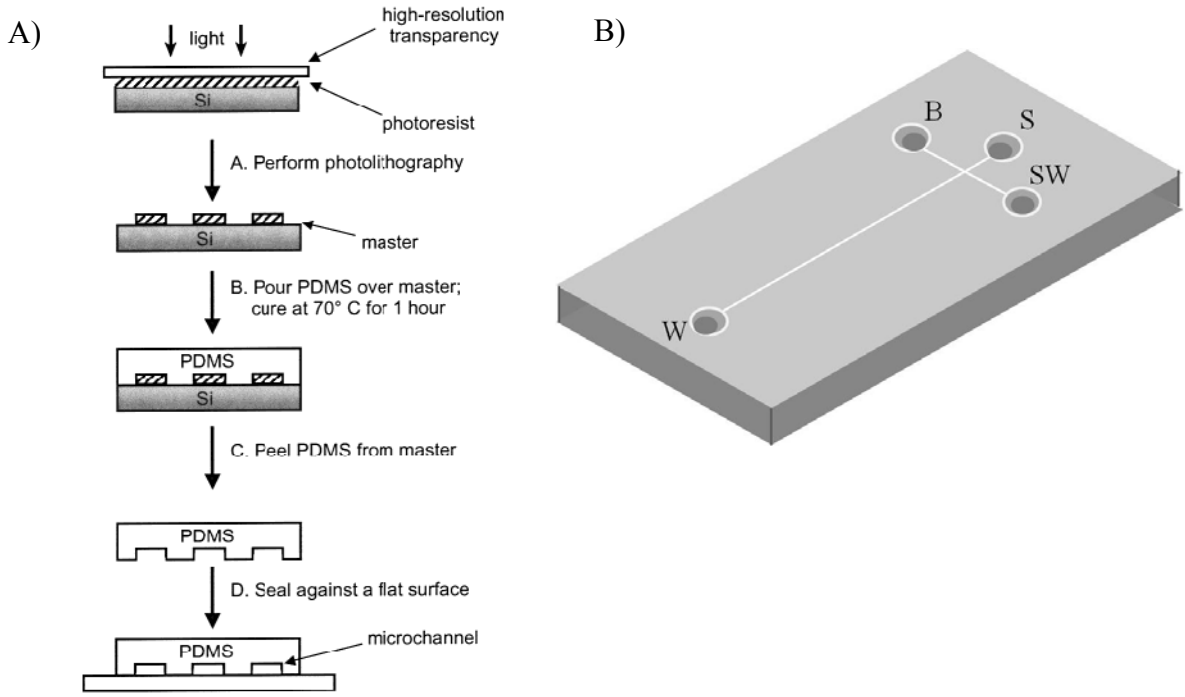

Figure 1.4 A) Schematic showing rapid prototyping of microfluidic devices from PDMS (Reprinted from McDonald et al.)[41] B) Representation of a MCE device, with sample (S), buffer (B), sample waste (SW), and waste reservoirs (W).

1.4 CONCLUSIONS

Perchlorate contamination in drinking and environmental waters is a continuing public health issue. Long-term perchlorate exposure has been associated with very serious health complications, particularly for infants, pregnant women and their fetuses. It is well understood that perchlorate interferes with the uptake of iodide into the thyroid via the sodium iodide symporter, disrupting the production of thyroid hormones. The U.S. EPA has issued a recommended limit for drinking water of 15 ppb, and while the current method of analysis, IC-MS, is sensitive enough for trace detection, a faster, less expensive, and more portable device is desired for monitoring perchlorate contamination. A MCE device has been developed for this

application. The optimization of the method, including the use of unique surfactant chemistry, as well as determination of perchlorate in drinking water samples is presented in Chapter 2. Chapter 3 discusses the next phase of this project and our efforts to expand the utility of the MCE device to more complex, environmental samples.

1.5 REFERENCES

1. Shi, Y.; Zhang, N.; Gao, J.; Li, X.; Cai, Y. *Atmospheric Environment* **2011,** *45* (6), 1323-1327.
2. Greer, M. A.; Goodman, G.; Pleus, R. C. *Environ Health Perspect* **2002,** *110* (9), .
3. Urbansky, E. T.; Schock, M. R., Issues in managing the risks associated with perchlorate in drinking water. *Journal of Environmental Management* **1999,** *56* (2), 79-95.
4. Orris, G. J. H., G. J.; Tsui, D. T.; Eldrige, J. E. *Preliminary analyses for perchlorate in selected natural materials and their derivative products*; US Department of the Interior: Tucson, AZ, 2003.
5. Urbansky, E. T. *Environ Sci & Pollut Res* **2002,** *9*, 187-192.
6. Borjan, M.; Marcella, S.; Blount, B.; Greenberg, M.; Zhang, J.; Murphy, E.; Valentin-Blasini, L.; Robson, M. *Science of The Total Environment* **2011,** *409* (3), 460-464.
7. Tian, K.; Dasgupta, P. K.; Anderson, T. A. *Analytical Chemistry* **2003,** *75* (3), 701-706.
8. Parker, D. R. *Environ. Chem.* **2009,** *6* (1), 10-27.
9. Rao, B.; Anderson, T. A.; Orris, G. J.; Rainwater, K. A.; Rajagopalan, S.; Sandvig, R. M.; Scanlon, B. R.; Stonestrom, D. A.; Walvoord, M. A.; Jackson, W. A. *Environmental Science & Technology* **2007,** *41* (13), 4522-4528.
10. Jackson, W. A.; Bohlke, J. K.; Gu, B. H.; Hatzinger, P. B.; Sturchio, N. C. *Environmental Science & Technology* **2010,** *44* (13), 4869-4876.
11. Charnley, G. *Food and Chemical Toxicology* **2008,** *46* (7), 2307-2315.
12. Andrea B, K. *Analytica Chimica Acta* **2006,** *567* (1), 4-12.
13. Seyfferth, A. L.; Parker, D. R. *J. Agricultural and Food Chemistry* **2006,** *54* (6), 2012-2017.
14. Van Sande, J.; Massart, C.; Beauwens, R.; Schoutens, A.; Costagliola, S.; Dumont, J. E.; Wolff, J. *Endocrinology* **2003,** *144* (1), 247-252.
15. Yu, K. O.; Narayanan, L.; Mattie, D. R.; Godfrey, R. J.; Todd, P. N.; Sterner, T. R.; Mahle, D. A.; Lumpkin, M. H.; Fisher, J. W. *Toxicology and Applied Pharmacology* **2002,** *182* (2), 148-159.
16. Zoeller, R. T.; Rice, D. C. *Regulatory Toxicology and Pharmacology* **2004,** *40* (3), 376-377.
17. Juan, B., Thyroid Hormones and Brain Development, *Vitamins And Hormones*, Gerald, L., Ed. Academic Press: 2005; Vol. Volume 71, pp 95-122.
18. Jackson, P. E.; Gokhale, S.; Streib, T.; Rohrer, J. S.; Pohl, C. A. *Journal of Chromatography A* **2000,** *888* (1–2), 151-158.
19. Pacakova, V.; Stulik, K. *Journal of Chromatography A* **1997,** *789* (1–2), 169-180.
20. Mikkers, F. E.; Everaerts, F. M.; Verheggen, T. P. *Journal of Chromatography A* **1979,** *169*, 11-20.
21. Jorgenson, J. W.; Lukacs, K. D. *Analytical Chemistry* **1981,** *53* (8), 1298-1302.
22. Kiplagat, I. K.; Thi, K. O. D.; Kuban, P.; Bocek, P. *Electrophoresis* **2011,** *32* (21), 3008-3015.
23. Blanco, G. A.; Nai, Y. H.; Hilder, E. F.; Shellie, R. A.; Dicinoski, G. W.; Haddad, P. R.; Breadmore, M. C. *Analytical Chemistry* **2011,** *83* (23), 9068-9075.
24. Sarazin, C.; Delaunay, N.; Varenne, A.; Vial, J.; Costanza, C.; Eudes, V.; Minet, J. J.; Gareil, P. *Journal of Chromatography A* **2010,** *1217* (44), 6971-6978.
25. Lucy, C. A. *Journal of Chromatography A* **1999,** *850* (1-2), 319-337.
26. Smith, S. C.; Khaledi, M. G. *Analytical Chemistry* **1993,** *65* (3), 193-198.

27. Harakuwe, A. H.; Haddad, P. R. *Journal of Chromatography A* **1996,** *734* (2), 416-421.
28. Yokoyama, T.; Macka, M.; Haddad, P. *Analytical Chemistry* **2001,** *371* (4), 502-506.
29. Harrison, C. R.; Sader, J. A.; Lucy, C. A. *Journal of Chromatography A* **2006,** *1113* (1–2), 123-129.
30. Mbuna, J.; Takayanagi, T.; Oshima, M.; Motomizu, S. *Journal of Chromatography A* **2004,** *1022* (1–2), 191-200.
31. Yokoyama, T.; Macka, M.; Haddad, P. R. *Analytica Chimica Acta* **2001,** *442* (2), 221-230.
32. Osbourn, D. M.; Weiss, D. J.; Lunte, C. E. *Electrophoresis* **2000,** *21* (14), 2768-2779.
33. Breadmore, M. C. *Electrophoresis* **2007,** *28* (1-2), 254-281.
34. Terabe, S. *The Chemical Record* **2008,** *8* (5), 291-301.
35. Terabe, S.; Otsuka, K.; Ichikawa, K.; Tsuchiya, A.; Ando, T. *Analytical Chemistry* **1984,** *56* (1), 111-113.
36. Zang, H.; Zhou, L.; Chen, X. *Electrophoresis* **2008**, *29,* 1556-1564.
37. Lander, J. P. *Handbook of Capillary and Microchip Electrophoresis and Associated Microtechniques* CRC Press, Boca Raton, FL, **2008**.
38. Manz, A.; Miyahara, Y.; Miura, J.; Watanabe, Y.; Miyagi, H.; Sato, K. *Sensors Actuators B* **1990**, *1*, 249.
39. Manz, A.; Graber, N.; Widmer, H. M. *Sensors Actuators B* **1990**, *1*, 244.
40. Duffy, D. C.; McDonald, J. C.; Schuller, O. J. A.; Whitesides, G. M. *Analytical Chemistry* **1998**, *70*, 4974-4980.
41. McDonald, J. C.; Whitesides, G. M. *Acc. Chem. Res.* **2002**, *35*, 491-495.

CHAPTER 2. RAPID ANALYSIS OF PERCHLORATE AT PPB LEVELS IN DRINKING WATER USING MICROCHIP CAPILLARY ELECTROPHORESIS

2.1 CHAPTER OVERVIEW

A microchip capillary electrophoresis (MCE) system has been developed for the determination of perchlorate in drinking water. The United States Environmental Protection Agency (U.S. EPA) has proposed health advisory limit for perchlorate in drinking water of 15 parts per billion (ppb), a level requiring large, sophisticated instrumentation, such as ion chromatography coupled with mass spectrometry (IC-MS), for detection. An inexpensive, portable system is desired for routine, on-line monitoring applications of perchlorate in drinking water. Here, we present an MCE method using contact conductivity detection for perchlorate determination. The method has several advantages, including reduced analysis times relative to IC, inherent portability, high selectivity, and minimal sample pretreatment. Resolution of perchlorate from more abundant ions was achieved using zwitterionic, sulfobetaine surfactants, N-Hexadecyl-N,N-dimethyl-3-ammonio-1-propane sulfonate (HDAPS) and N-Tetradecyl-N,N-dimethyl-3-ammonio-1-propane sulfonate (TDAPS). The system performance and the optimization of the separation chemistry, including the use of these surfactants to resolve perchlorate from other anions, are discussed in this work. The system is capable of detection limits of 3.4 ± 1.8 ppb (n=6) in standards and 5.6 ± 1.7 ppb (n=6) in drinking water. This work was published in *Analytical Chemistry* in 2010.[1]

2.2 INTRODUCTION

In recent years, scientific literature and popular media have been pervaded by reports on perchlorate, its persistence in the environment, its detection by various analytical methods, and its effect on human health.[2-12] Long-term exposure can disrupt thyroid hormone production by competitively inhibiting the uptake of iodide into the thyroid. Reduced thyroid hormone production has been linked to a number of developmental and neurological disorders in newborns and infants, such as cerebral palsy and cretinism.[3-6] Such adverse health effects have invoked the need for a method to monitor perchlorate levels in drinking water.

Perchlorate contamination in watersheds is ostensibly attributed to the use of Chilean fertilizers up to the 1950's and the manufacturing of ammonium perchlorate, NH_4ClO_4, in missile and rocket fuels.[5-12] In 2004, California introduced a public health goal of 6 ppb perchlorate in drinking water, and since then, several other states have adopted similar advisory levels.[5,7] While perchlorate exposure is recognized nationally as a water quality issue and human health concern, the toxicity impact is not fully understood. The USEPA has not set regulatory levels of perchlorate in drinking water, but recently issued an Interim Drinking Water Health Advisory, determining that a level of 15 ppb is protective of all subpopulations.[13]

Perchlorate has been mainly analyzed by ion chromatography (IC) with either conductivity detection (CD) or mass spectrometry (MS).[14-17] Currently, USEPA employs methods 314.0, 331.0, and 332.0 for perchlorate analysis. While these methods are capable of detecting and quantifying perchlorate with low detection limits (0.02 – 0.005 ppb), the instrumentation is costly, complex, and lacks portability. A system that can monitor perchlorate levels on-line is desirable, particularly during remediation efforts for contaminated drinking water supplies.

A microchip capillary electrophoresis (MCE) method capable of measuring perchlorate with low sample and reagent consumption, reduced analysis times relative to IC, and low detection limits is presented here. The optimization of the separation chemistry as well as the use of contact conductivity detection, incorporating a bubble cell design, allow for low limits of detection and fast analysis times (approximately 1 min).[18] Two zwitterionic sulfobetaine surfactants, hexadecyl-N,N-dimethyl-3-ammonio-1-propane sulfonate (HDAPS) and tetradecyl-N,N-dimethyl-3-ammonio-1-propane sulfonate (TDAPS), were investigated for the selective manipulation of perchlorate retention times. At concentrations above the critical micelle concentration (CMC), micellar interactions slow the migration of perchlorate, separating the analyte from higher mobility anions commonly found in water. Ultimately, TDAPS provided more reproducible results than HDAPS. Finally, the novel separation chemistry was used to detect perchlorate in drinking water samples with 99% recovery and detection limits of 5.6 ppb.

2.3 EXPERIMENTAL

2.3.1 Materials

All chemicals were reagent grade unless otherwise stated. 100-mm silicon wafers were purchased from University Wafer (Boston, MA). Poly(dimethylsiloxane) (PDMS) and Sylgard 184 elastomer were obtained from Dow Corning (San Diego, CA). SU-8 3025 photoresist was purchased from Microchem (Newton, MA). Sodium fluoride, 1,3-propane disulfonic acid disodium salt, and tetradecyl-N-N-dimethyl-3-ammonio-1-propane sulfonate (TDAPS) were purchased from Sigma-Aldrich (St. Louis, MO). Chloride, nitrate, and sulfate (potassium salt) were obtained from Fisher (Fair Lawn, NJ). Potassium perchlorate was obtained from J.T. Baker (Phillipsburg, NJ). Nicotinic acid was purchased from Fluka (Buchs, Switzerland). Hexadecyl-

N,N-dimethyl-3-ammonio-1-propane sulfonate (HDAPS) was obtained from Anatrace, Inc. (Maumee, OH). Tungsten microwires (13-μm diameter) were purchased from GoodFellow Corp. (Huntingdon, UK). Solutions were prepared in 18.2 MΩ water from a Millipore Milli-Q purification system (Billerica, MA).

2.3.2 Microchip Fabrication

Construction of PDMS microchips was performed using previously reported methodologies.[19-21] Soft lithography techniques were used to fabricate a master microchip mold on silicon wafer. The wafer was spin-coated with SU-8 3025 at 800 rpm and pre-baked at 65°C for 3 min followed by 95°C for 5 min. A photomask was placed on the coated wafer and exposed to light using a UV lamp at 50% intensity for 85s, developing only the microchip features. A second bake step was then performed: 65˚C for 2 min and 95˚C for six minutes. The positive relief was developed by submerging the wafer in propylene glycol methyl ether acetate for 5 min, gently rinsing with isopropanol, and drying under a nitrogen stream. The PDMS microchip is fabricated by pouring a degassed mixture of Sylgard 184 silicone elastomer and curing agent (10:1, w/w) onto the master mold as well as a blank silicon wafer. Scotch tape was used to confine the edges of the wafer, keeping the uncured polymer from running off the wafer surface. PDMS was cured in an 85˚C oven for at least 1 hr. The microchip was assembled by cutting the cured PDMS with a razor blade, gently lifting the excised pieces from the master mold, and inserting microwires into designated channels. The surface of the PDMS microchip and blank were placed in an air plasma cleaner (Harrick PDC-32G Plasma Cleaner/Sterilizer) and oxidized for 45s. Immediately after plasma treatment, the PDMS layers were aligned, and their plasma-treated surfaces were brought into contact to form an irreversible seal. Final channel dimensions were 50 μm x 50 μm as determined by contact profilometry. Microwire

spacing was 120 μm and the waste reservoir was 2 mm after the detection zone. The sample and buffer channels were 2 cm in length, the sample waste was 1.5 cm long, and the separation channel was 5 cm long. Microchips used in this study were designed with a bubble cell for enhanced detection limits. The design, fabrication, and optimization of the bubble cell were previously described.[18] A schematic of the microchip is shown in Figure 2.1.

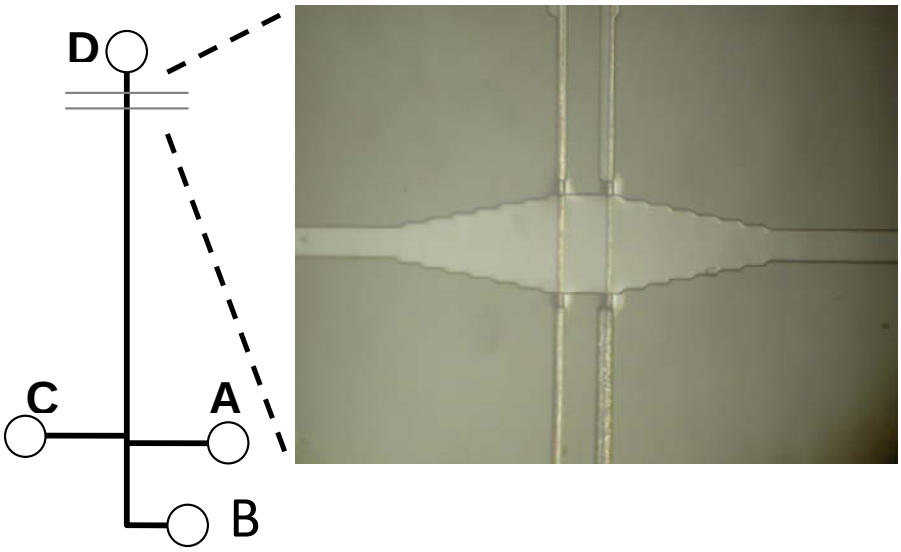

Figure 2.1. Microchip design. The bubble cell region is at the detection zone, seen as the expanded channel width in the photo (right), bisected by two tungsten microwires. Reservoirs are filled as follows: A = sample waste, B = sample, C = buffer, and D = waste.

2.3.3 Instrumentation and Data Acquisition

Contact conductivity detection was performed with a Dionex CD20 conductivity detector as described previously.[18] A National Instruments USB-6210 DAQ and LabView 8.0 software, running a custom Virtual Instrument, were used to monitor the output of the detector at a collection rate of 20 kHz with 2000-point boxcar averaging. No additional data filtration or smoothing was performed. A fifth-order, polynomial baseline fit was subtracted from the raw data to account for baseline drift resulting from reagent evaporation, ion depletion, and

temperature fluctuations. A previously published, custom-built, floating high voltage power supply (HVPS) was used for electrophoresis.[22]

2.3.4 Electrophoresis

Separations were performed in counter-EOF mode, in which the migration of analytes toward the detection zone is opposite the direction of electroosmotic flow (EOF).[23] Microchips were prepared by rinsing for approximately 30 s each with 18.2 MΩ·cm water and buffer. Gated injection was used throughout this study.[24,25] Each sample was made in 18.2 MΩ·cm water and mixed with 10% background electrolyte (BGE) to ensure conductivity consistency.[25] Field-amplified sample stacking (FASS), a sample preconcentration method which exploits the differences in electrical resistance between the low-conductivity sample matrix and high-conductivity BGE, was employed in all separations.[25] Zwitterionic surfactants, HDAPS and TDAPS, were used in the buffer system.[26-29] Propane disulfonate (PDS) was used as an internal standard throughout this work.

Drinking water was collected from a potable water source in the Chemistry building at Colorado State University, Fort Collins, CO. The only sample preparation performed was the addition of 10% BGE. In addition, water samples were spiked with known concentrations of perchlorate for recovery studies.

2.4 RESULTS AND DISCUSSION

2.4.1 System Optimization

Several factors were considered when optimizing separation conditions, including buffer pH, field strength, injection time, and sulfobetaine surfactant composition and concentration. The use of sulfobetaine surfactants is based on previous work by Lucy[30] and Haddad[31] focusing

on the ability of zwitterionic head groups to interact with the polarizable perchlorate ion. Nicotinic acid (10 mM) was chosen as the background electrolyte because of its relatively low pH (3.6) at this concentration, and its lack of electrochemically active functional groups.[32-34] Using an electrolyte with a low pH causes partial protonation of the silanol groups on the surface of PDMS, reducing the EOF. Additionally, low pH is integral in preventing interference by other anionic compounds in the sample. Compounds with pK_a values greater than the buffer pH will be partially- or fully-protonated, slowing their migration toward the detector or preventing their detection entirely. The EOF was approximately $-1.2 \pm 0.5 \times 10^{-5}$ $cm^2 \cdot V^{-1} \cdot s^{-1}$ and was calculated from the migration time of the internal standard.[35]

Sulfobetaine surfactants were used as BGE additives to improve the resolution of perchlorate from other anions. A series of electropherograms collected as a function of TDAPS surfactant concentration are shown in Figure 2.2. In the absence of surfactant, perchlorate migrates faster than the internal standard. While perchlorate is resolved from chloride, nitrate, and sulfate, the resolution was deemed insufficient for real samples where the concentrations of these anions will exceed perchlorate by at least 1000-fold. At concentrations above the CMC, micelles selectively interact with perchlorate, reducing its apparent mobility.[30,31] Therefore, the migration time of perchlorate could be manipulated by varying surfactant concentration. Initially, HDAPS was tested because of its low CMC (0.1 mM).[28] HDAPS appeared to be an excellent initial candidate for this separation, however, over time it was found to produce inconsistent migration times. Specifically, the average retention time of perchlorate was 73 s but the RSD was 48% (Figure 2.3). The cause of the instability is not understood at this point but is likely the poor reproducibility of HDAPS-PDMS adsorption.[36,37]

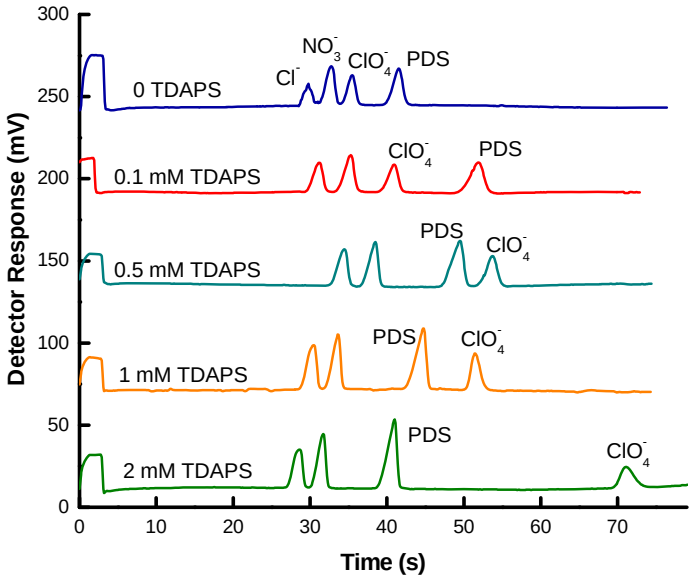

Figure 2.2. Electropherograms showing the changes in perchlorate retention with increasing TDAPS concentrations. Resolution for perchlorate and PDS is 1.87 ± 0.21, 2.84 ± 0.19, and 10.1 ± 0.23 when the TDAPS concentration is 0.5 mM, 1.0 mM and 2.0 mM, respectively. Sample contains 5 µM analytes: 0.17 ppm chloride, 0.31 ppm nitrate, 0.50 ppm perchlorate, and 1.2 ppm PDS in 18.2 MΩ·cm water. Conditions: 10 mM nicotinic acid BGE, -350 V/cm, 3.0 s injection. Detector range: 100 µS

We next tested TDAPS. Similar to HDAPS, TDAPS was selected for its relatively low CMC (0.4 mM).[31] Furthermore, TDAPS has been used successfully by the Henry group in other types of separations.[38] The optimization of TDAPS concentration in the BGE is shown in Figure 2.2. Perchlorate is effectively separated from chloride and nitrate, and migrates slower than the internal standard when the TDAPS concentration is > 0.5 mM. Under these conditions, sulfate co-migrates with chloride and was omitted for clarity. The optimal concentration of TDAPS, based on resolution and peak shape, was determined to be 1.0 mM. Employing this buffer system, a significant improvement in reproducibility was observed. The average retention time for perchlorate was 53.5 s with an RSD of 8.6%. While baseline resolution for perchlorate was achieved without TDAPS, a higher resolution is needed for real samples in which sulfate,

chloride, and nitrate concentration could easily exceed 1 ppm and therefore, interfering with the detection of low concentrations of perchlorate.

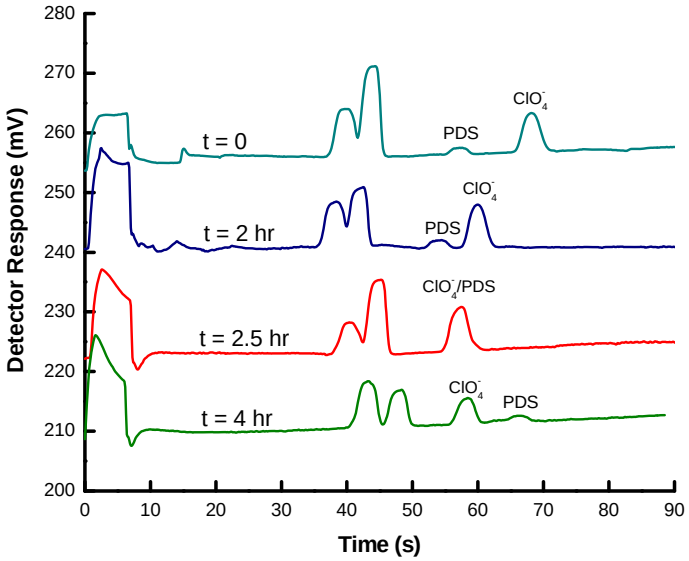

Figure 2.3. Electropherograms showing irreproducibility of the perchlorate retention time and the electroosmotic flow after 4 hr when HDAPS is used in the BGE. Conditions: 10 mM nicotinic acid, 0.5 mM HDAPS BGE, -350 V/cm, 5.0 s injections. Detector range: 100 µS.

In addition to surfactant studies, field strength and injection time were also investigated. These parameters were optimized for both standards and drinking water samples. A field strength of -200 V/cm was used for optimizing surfactant concentrations, however, in later experiments, the field strength was increased to reduce analysis time. The progression of electropherograms from -200 V/cm to -500 V/cm for standards can be seen in Figure 2.4. Analysis time is reduced as field strength increases, however, a significant increase in noise was observed at field strengths > -400 V/cm. The optimal field strength was determined to be -350 V/cm and was used throughout the remainder of this work. Increasing the field strength from -200 V/cm to -350 V/cm reduced the analysis time from 100 s to approximately 60 s. In contrast, current IC techniques require run times of 15 to 30 min.[17]

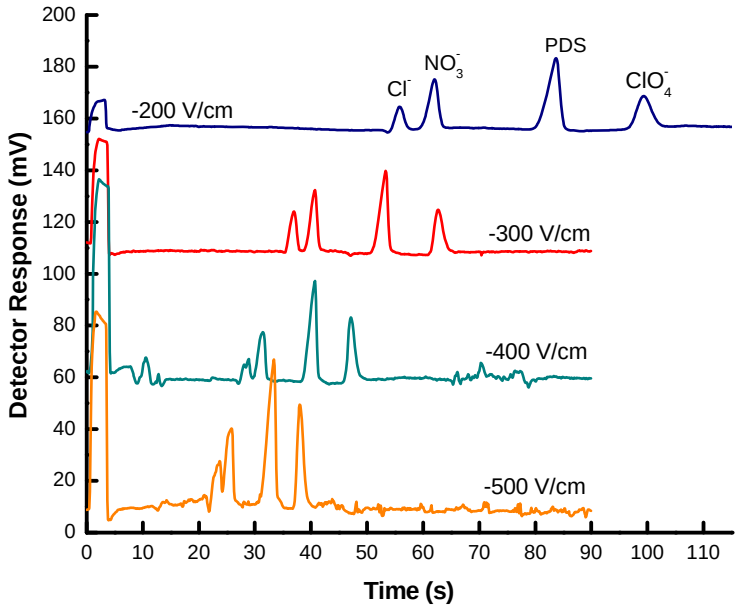

Figure 2.4. Electropherograms showing the changes in the separation with increasing field strength. Sample contains 5 µM analytes: 0.17 ppm chloride, 0.31 ppm nitrate, 0.50 ppm perchlorate, and 1.2 ppm PDS in 18.2 MΩ·cm water. Conditions: 10 mM nicotinic acid, 1 mM TDAPS BGE, 3.0 s injection. Detector range: 100 µS.

Increased injection times result in a greater amount of sample introduced into the separation channel for gated injections. Since chloride and sulfate have the highest ion mobilites in drinking water, more chloride and sulfate will be introduced into the microchip compared to other anions in a single injection (Figure 2.5). The large peaks generated from chloride, nitrate, and sulfate in higher ionic strength matrices, such as drinking water, can interfere with perchlorate analysis when injection times are long (> 10 s). Additionally, peak shapes are compromised due to effects of a larger sample plug. The best injection time for standards ranges between 1 and 5 s, while the optimal injection time for drinking water samples was 10 s.

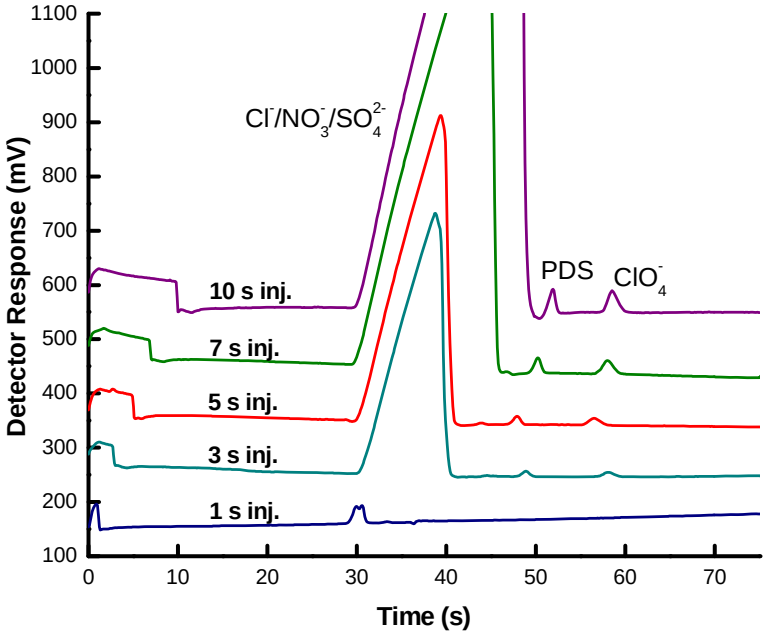

Figure 2.5. Electropherograms showing the changes in peak areas with increasing injection time. Sample contains 100 ppb perchlorate and 0.124 ppm PDS in drinking water. The peak area for perchlorate increased from 11.4 mV·s ± 0.06, to 18.9 mV·s ±0.02, to 34.9 mV·s ± 0.02, to 50.8 mV·s ± 0.08 for 3.0 s, 5.0 s, 7.0 s, and 10 s injections, respectively. Conditions: 10 mM nicotinic acid, 1 mM TDAPS BGE, -350 V/cm. Detector range: 100 µS.

2.4.2 Limit of Detection for Perchlorate in Standards

The limit of detection for perchlorate in standards was determined utilizing the optimized separation conditions. Standards were prepared in 18.2 MΩ·cm water and then diluted with 10% (v/v) BGE to provide consistent sample conductivity. Electropherograms showing the separation of PDS and perchlorate at concentrations between 1 ppb and 50 ppb are shown in Figure 2.6. The LOD was 3.4 ± 1.8 ppb for perchlorate (34 nM ± 18 nM), S/N = 3. A calibration curve for this data is also shown in Figure 2.6. The linear rage for perchlorate was 5 to 1000 ppb (R^2 = 0.9982). The detection limit and linear range are within the USEPA proposed health advisory limits and are comparable to that achieved by IC-CD systems.

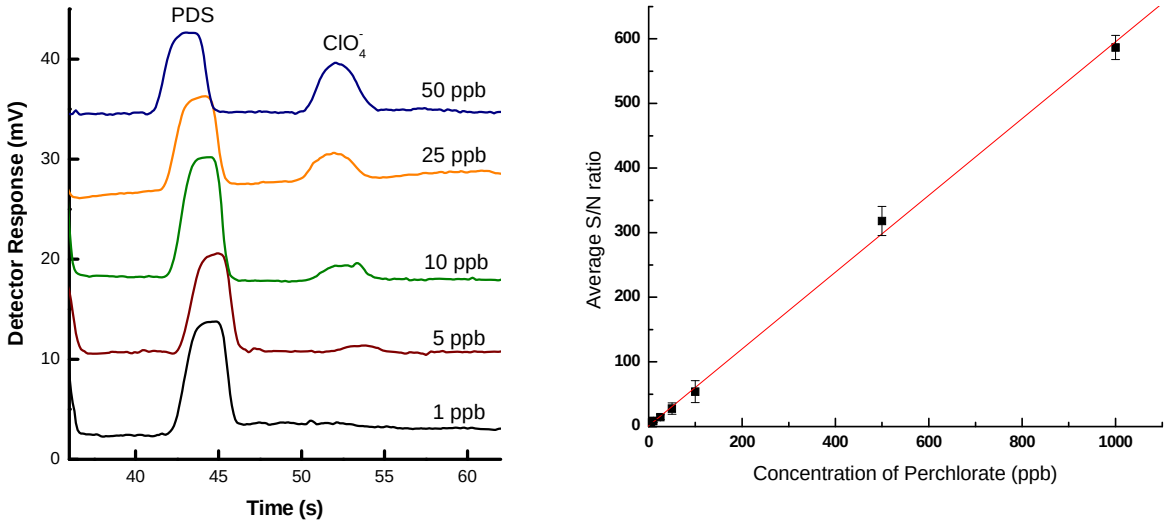

Figure 2.6. (A) Electropherograms showing the separation of perchlorate at concentrations between 1 ppb and 50 ppb. Electropherograms have been scaled to show internal standard and perchlorate peaks only. Sample contains 0.71 ppm chloride and 0.31 ppm nitrate, 0.12 ppm PDS, and 10% BGE (v/v) in 18.2 MΩ·cm water. Conditions: -350 V/cm, 3.0 s injections, BGE = 10 mM nicotinic acid, 1.0 mM TDAPS, pH 3.6. Detector range = 100 μS. **(B)** Calibration curve plotting the change in average signal to noise ratio with increasing perchlorate concentration in standards. Linear regression: $y = 0.53133x + 1.2026$, $R^2 = 0.9982$.

2.4.3 Interferences

Possible interference from anions in drinking water was also investigated. Anions of greatest concern include chloride, nitrate, sulfate and fluoride because of their ubiquity in drinking water. The separation of perchlorate from all interferences considered is shown in Figure 2.7. Early experiments proved the separation conditions capable of resolving perchlorate from sulfate, chloride, and nitrate, and under the described conditions, fluoride was not detected within a 120 s experimental window. Fluoride is not observed because the pK_a value of the fluoride ion (3.17) is near the pH of the buffer (3.6) causing a substantial fraction of fluoride ions to be protonated, thus, slowing its migration.[39]

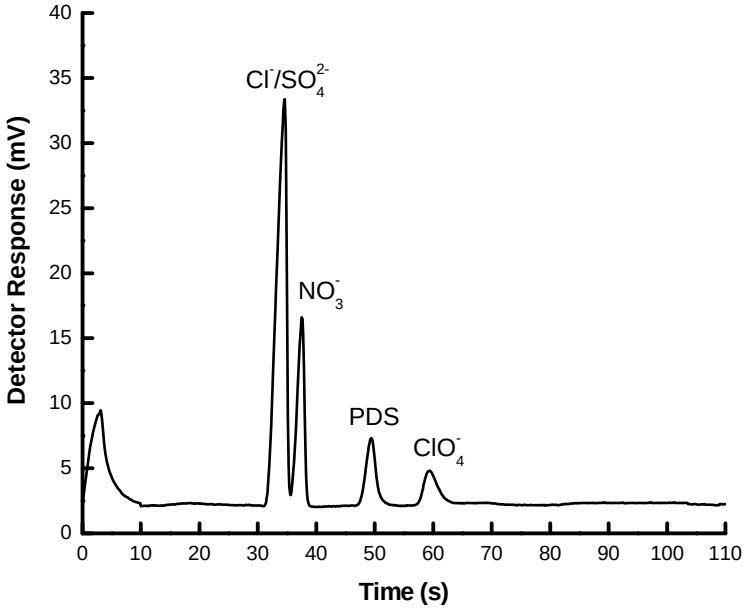

Figure 2.7. Separation of 1 μM analytes: 100 ppb perchlorate, 35.5 ppb chloride, 62.0 ppb nitrate, 135 ppb sulfate, 19.0 ppb fluoride, and 248 ppb PDS. Conditions: -350 V/cm, 3 s injection, BGE = 10 mM nicotinic acid, 1.0 mM TDAPS, pH 3.6. Detector range = 100 μS.

2.4.4 Analysis of Drinking Water

Drinking water collected from the Colorado State University Chemistry building was analyzed for the presence of perchlorate. Perchlorate was not detected in the native water sample, however, when spiked with 100 ppb perchlorate and 248 ppb PDS, both compounds were detected with 99% recovery for perchlorate, as calculated relative to PDS, rendering the microchip and separation conditions capable of analyzing perchlorate in this environmental matrix. Separations of drinking water samples spiked with perchlorate and PDS are shown in Figure 2.8. The limit of detection for perchlorate in drinking water was 5.6 ± 1.7 ppb (56 nM ± 17 nM), S/N = 3, with a linear range of 10 to 1000 ppb (R^2 = 0.9984). A calibration curve is also shown in Figure 2.8.

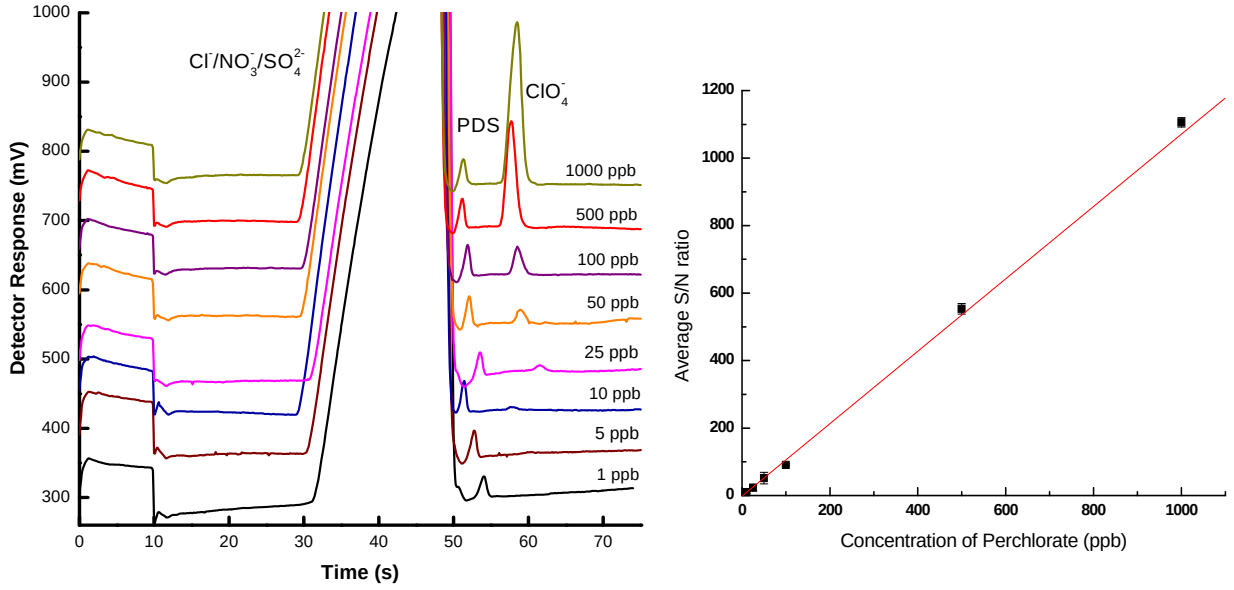

Figure 2.8. (A) Electropherograms showing separation of drinking water samples spiked with 0.12 ppm PDS and concentrations of perchlorate between 1 and 1000 ppb. Conditions: -350 V/cm, 10 s injection, BGE = 10 mM nicotinic acid, 1.0 mM TDAPS, pH 3.6. Detector range = 50 µS. **(B)** Calibration curve plotting the change in average signal to noise ratio with increasing perchlorate concentration in drinking water. Linear regression: y = 1.0645x – 3.0111, R^2 = 0.9984. Error bars are contained within the points.

2.5 CONCLUSIONS

A microchip capillary electrophoresis method has been developed for the detection of perchlorate in drinking water samples. Separation chemistry, including the comparison of two zwitterionic sulfobetaine surfactants, has been optimized. The device is capable of analyzing perchlorate over a relatively large linear range, with a detection limit of 5.6 ppb in drinking water which is below the USEPA regulatory requirement. Additionally, analysis times for the method are approximately 15 to 30 times shorter than current IC techniques. This is the first step towards development of a field-deployable platform for on-line, routine perchlorate monitoring in drinking water.

While the importance of monitoring perchlorate in drinking water is a viable application of this technology, the ability to determine perchlorate in other environmental matrices such as surface water, ground water, and military munitions waste water is also highly desired. The microchip CE method described in this work shows great promise for portable, high-throughput analysis; however, the high ionic strength of such environmental samples poses a great challenge for the microchip. In Chapter 3, a novel sample preparation method is investigated for the removal of high concentrations of competing anions from more complex samples. This method could be easily integrated into the microfluidic network for on-chip sample cleanup, enabling the analysis of a broader range of environmental samples.

2.6 REFERENCES

1. Gertsch, J. C.; Noblitt, S. D.; Cropek, D. M.; Henry, C. S. *Anal. Chem.* **2010**, *82* (9), 3426-3429.
2. Kirk, A. B. *Anal. Chim. Acta* **2006**, *567*, 4-12.
3. Dussault, J. H.; Ruel, J. *Ann. Rev. Physiol.* **1987**, *49*, 321-324.
4. Jacobsson, B.; Hagberg, G. *Best Practice & Research Clinical Obstetrics & Gynaecology* **2004**, *18*, 425-436.
5. Kirk, A. B.; Smith, E. E.; Tian, K.; Anderson, T. A.; Dasgupta, P. K. *Environ. Sci. Technol.* **2005**, *39*, 2011-2017.
6. Trumbo, P. R. *Nutrition Reviews,* **2010,** *68,* 62-66.
7. Dasgupta, P. K.; Martinelango, P. K.; Jackson, W. A.; Anderson, T. A.; Tian, K.; Tock, R. W.; Rajagopalan, S. *Environ. Sci. Technol.* **2005**, *39*, 1569-1575.
8. Urbansky, E. T.; Brown, S K.; Magnuson, M. L.; Kelty, C. A. *Environ. Pollut.* **2001,** *112,* 299-302.
9. Hogue, C. *Chem. Eng. News* **2003**, *81*, 11.
10. Urbansky, E. T.; Brown, S. K. *J. Environ. Monit.* **2003,** *5,* 455-462.
11. Jackson, A. W.; Joseph, P.; Laxman, P.; Tan, K.; Smith, P. N.; Yu, L.; Anderson, T. A. *J. Agric. Food Chem.* **2005**, *53*, 369-373.
12. El Aribi, H.; Le Blanc, Y. J. C.; Antonsen, S.; Sakuma, T. *Anal. Chim. Acta* **2006,** *567*, 39-47.
13. United States Environmental Protection Agency, *Interim Drinking Water Health Advisory for Perchlorate* **2008,** http://www.epa.gov/safewater/contaminants/unregulated/pdfs/healthadvisory_perchlorate_interim.pdf
14. Urbansky, E. T. *Crit. Rev. Anal. Chem.* **2000,** *30,* 311-343.
15. Anderson, T. A.; Wu, T. H. *Bull. Environ. Contam. Toxicol.* **2002,** *68,* 684-691.
16. Otero-Santos, S. M.; Delinsky, A. D.; Valentin-Blasini, L.; Schiffer, J.; Blount, B. C. *Anal. Chem.* **2009,** 81, 1931-1936.
17. Tian, K.; Dasgupta, P. K.; Anderson, T. A. *Anal.Chem.* **2003**, *75*, 701-706.
18. Noblitt, S. D.; Henry, C. S. *Anal. Chem.* **2008**, *80*, 7624-7630.
19. Duffy, D. C.; McDonald, J. C.; Schueller, O. J. A.; Whitesides, G. M. *Anal. Chem.* **1998,** *70,* 4974-4984.
20. Liu, Y.; Vickers, J. A.; Henry, C. S. *Anal. Chem.* **2004,** *76,* 1513-1517.
21. Noblitt, S. D.; Kraly, J. R.; VanBuren, J. M.; Hering, S. V.; Collett, J. L.; Henry, C. S. *Anal. Chem.* **2007,** *79,* 6249-6254.
22. Garcia, C. D.; Lui, Y.; Anderson, P.; Henry, C. S. *Lab Chip* **2003,** *3,* 324-328.
23. Yeung, K.; Lucy, C. A. *J. Chromatogr. A* **1998,** *804,* 319-325.
24. Lacher, N. A.; Garrison, K. E.; Martin, S. M.; Lunte, S. M. *Electrophoresis* **2001,** *22,* 2526-2536.
25. Jung, B.; Bharadwaj, R. Santiago, J. G. *Electrophoresis* **2003,** *24,* 3476-3483.
26. Yeung, K.; Lucy, C. A. *J. Chromatogr. A* **1998,** *804,* 319-325.
27. Okada, T. *J. Chromatogr. A* **1997,** *780,* 343-360.
28. Yokoyama, T.; Macka, M.; Haddad, P. R. *Anal. Chem.* **2001,** *371,* 502-506.
29. Mori, M.; Wenzhi, H.; Hasebe, K. *Anal. Bioanal. Chem.* **2002,** *374,* 75-79.
30. Lucy, C. A. *J. Chromatogr. A* **1999,** *850,* 319-337.
31. Haddad, P.R.; Yokoyama, T. *Anal. Chim. Acta* **2001,** *442,* 221-230.

32. Beckers, J. L.; Bocek, P. *Electrophoresis,* **2003,** *24,* 518-535.
33. Persat, A.; Chambers, R. D.; Santiago, J. G. *Lab Chip,* **2009,** *9,* 2437-2453.
34. Persat, A.; Suss, M. E.; Santiago, J. G. *Lab Chip,* **2009,** *9,* 2454-2469.
35. Landers, J. P. *Handbook of Capillary and Microchip Electrophoresis and Associated Microtechniques,* CRC Press, New York, 3rd edition, **2008.**
36. Garcia, C. D.; Dressen, B. M.; Henderson, A.; Henry, C. S. *Electrophoresis,* **2005,** *26,* 703-709.
37. Mora, M. F.; Giacomelli, C. E.; Garcia, C. D. *Anal. Chem.,* **2007,** *17,* 6675-6681.
38. Noblitt, S. D.; Schwandner, F. M.; Hering, S. V.; Collett, J. L., Henry, C. S. *J. Chromatogr. A* **2009,** *1216,* 1503-1510.
39. Harrison, C. R.; Sader, J. A.; Lucy, C. A. *J. Chromatogr. A* **2006,** *1113,* 123-129.

CHAPTER 3. ELECTROSTATIC ION CHROMATOGRAPHY AS A SAMPLE PREPARATION TECHNIQUE FOR THE ANALYSIS OF PERCHLORATE IN ENVIRONMENTAL WATERS

3.1 CHAPTER OVERVIEW

Previously, a microchip capillary electrophoresis (MCE) method was developed for the determination of perchlorate in drinking water, allowing for rapid analysis and low detection limits. While this achievement has great implications for water quality analysis and human health, the desire to monitor perchlorate contamination in the environment and in munitions waste generated at US Army facilities remains. In this capacity, the high ionic strength (reaching 1 mS/cm^2) of the sample matrix makes MCE analysis very challenging. One important advantage of MCE and a key factor in detecting ppb levels of perchlorate in drinking water is the ability to preconcentrate samples via field-amplified sample stacking (FASS). As discussed in Chapter 1, FASS is achieved in a scenario where a sample dissolved in a low-conductivity solution, such as DI water, is injected into a capillary containing a higher-conductivity BGE. Unfortunately, the FASS mechanism does not work for highly conductive samples such as surface water, ground water, or munitions waste water, making the determination of trace levels of perchlorate in these matrices very difficult.

One way to address this issue is through a sample cleanup step that would remove high concentrations of competing anions, therefore lowering the ionic strength, prior to

electrophoretic separation. The use of electrostatic ion chromatography (EIC) is an attractive solution to this problem because of its simplicity and ability to be incorporated directly into a microfluidic device. First reported in the early 1990's, EIC involves separations performed on a hydrophobic stationary phase dynamically coated with a zwitterionic surfactant. The amphoteric character of the surfactant provides both anion- and cation-exchange sites for selective interactions with polarizable ions, a phenomenon we observed with sulfobetaine surfactants and perchlorate. An important advantage of this technique is the use of simple eluents, such as pure water, to perform anion separations.

For analysis of perchlorate, incorporating a packed-bed, coated with zwitterionic surfactant, into the microfluidic network could provide a selective cleanup step, effectively retaining perchlorate and removing competing anions from the sample. The selective interaction between tetradecyl-N,N-dimethyl-3-ammonio-1-propanesulfonate (TDAPS) and perchlorate has been established and is discussed in Chapter 2. The work presented here evaluates the utility of a TDAPS-coated C18 stationary phase for sample preparation via conventional chromatography methods.

3.2 INTRODUCTION

A MCE method has been developed for analysis of ppb levels of perchlorate in drinking water. Further development of the microchip as a tool for monitoring perchlorate contamination in more complex environmental samples is hindered by the high ionic strength of these samples. As mentioned previously in Chapter 1, Field-amplified sample stacking (FASS) is a phenomenon first optimized by Mikkers and co-workers in the late 1970's.[1] FASS and related preconcentration techniques are instrumental to the low detection limits achieved by capillary

electrophoresis and more specifically, the detection of ppb levels of perchlorate in MCE. This method of preconcentration is based on the manipulation of the electrophoretic velocity of an analyte. Analytes dissolved in a low-conductivity matrix, such as water, will experience high electric field strength relative to a higher-conductivity BGE. Consequently, the velocity of analytes will be high in the sample zone until they reach the buffer interface. At the BGE boundary, the analytes slow down and stack into a narrow zone.[1,2] Under ideal conditions, stacking leads to the narrowing of analyte bands as well as the ability to inject larger sample volumes; both factors dramatically improve detection limits with 1000-fold increases in peak height reported.[3] A limitation of FASS, however, is that the ionic strength of the sample must be significantly lower than that of the BGE.[2,4,5] For analysis of some biological and environmental samples, where the sample matrix consists of salts in concentrations on the order of 100 mM or greater, this requirement causes a problem.[6-8] In this case, analytes migrate slowly through the high conductivity sample until they reach the BGE where they accelerate. This behavior leads to band broadening and decreased signal-to-noise ratio. The difficulty in using a BGE with lower resistance than the sample matrix is the generation of Joule heating as a result of high currents associated with high ionic strength buffers. In Figure 3.1, a surface water sample spiked with perchlorate was loaded on the MCE device, and the resulting electropherograms exemplify the challenge of detecting perchlorate in high ionic strength samples. One way of approaching this problem is to incorporate a sample cleanup step to reduce the ionic strength of the sample matrix prior to electrophoretic separation. The use of electrostatic ion chromatograph (EIC) for sample cleanup has great potential due to its simplicity, application of surfactants we have already studied, use of simple eluents, and ability to be integrated in a microfluidic device.

Electrostatic ion chromatography (EIC) was first introduced in the early 1990's by Hu and co-workers.[9] The method employs zwitterionic or amphoteric stationary phases for high-performance ion-exchange separations. These unique stationary phases have been realized via dynamically coating a hydrophobic, C18 chromatography column with a sulfobetaine-type surfactant, such as TDAPS, which has an inner positively charged quaternary ammonium group and an outer negatively charged sulfonate functional group separated by three methylene groups.[10-12] The bifunctional phases employed in EIC have been predominately used for anion separations; however, further development of the technique has encompassed analysis of cations and simultaneous anion/cation separations.[10,13] Another key advantage to the technique is the use of simple eluents, including pure water, which provides simplicity, eliminates the need for precise eluent composition, and facilitates method development. Also, detection techniques, such as conductivity and UV absorption, are enhanced by a reduction in background signal.[14]

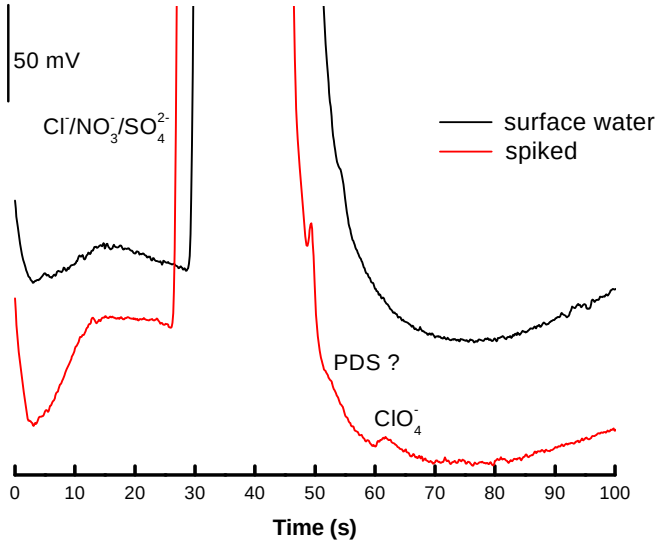

Figure 3.1 Direct analysis of surface water samples using MCE without a sample cleanup step. The electropherogram in the red trace shows a sample spiked with 10 µM perchlorate and 0.5 mM PDS.

Fundamentally, the partitioning mechanism of analyte ions in EIC is currently debated, and a number of mechanisms have been proposed; many of which are derived from the retention behavior of anions with sulfobetaine-type surfactants.[10,13,15-18] A schematic of a C18 phase dynamically coated with tetradecyl-N,N-dimethyl-3-ammonio-1-propanesulfonate (TDAPS) is shown in Figure 3.2. Also featured is a schematic of the retention mechanism proposed by Hu and co-workers, involving the formation of ion pairs between ions in solution and the bifunctional head group of the surfactant.[9] Okada and Patil presented a model describing retention behavior, reporting that small, well-hydrated anions interact with the zwitterionic surfactant via a partition mechanism while large, poorly-hydrated anions interact via the formation of ion pairs. However, the authors also found the retention behavior of anions was greatly influenced by the use of an electrolyte eluent, where the anions in the eluent had a greater affect than the cations.[16] Cook and co-workers presented experimental data showing separation selectivity of anions was correlated with increasing chaotropic character or the ability of an ion to disrupt the surrounding water structure, increasing the entropy of a system.[15] They found the more chaotropic the analyte anion, the greater its retention. Retention of anions increased across the series: $SO_4^{2-} < Cl^- < NO_2^- < Br^- < NO_3^- < ClO_3^- < I^- < ClO_4^-$. This trend generally follows the Hofmeister series and also increases with polarizability of the anions.

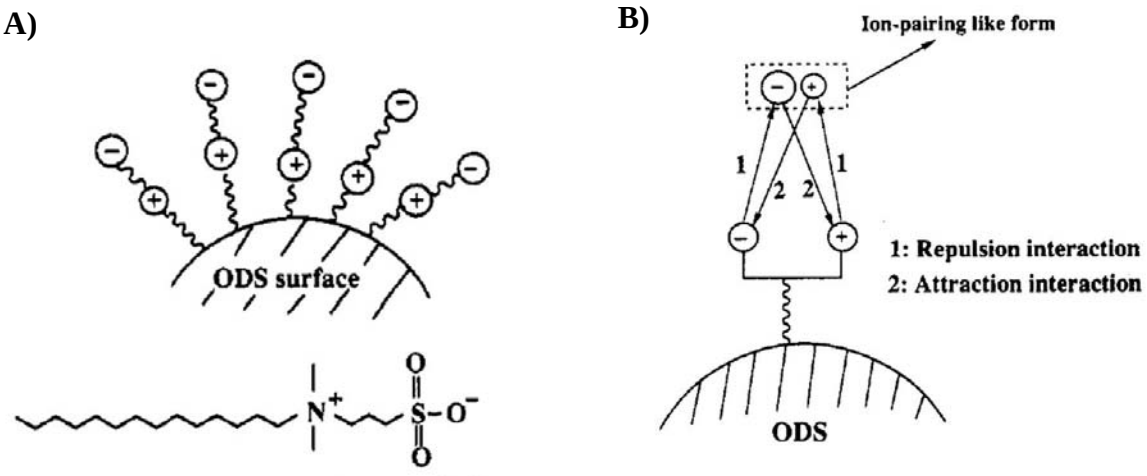

Figure 3.2. A) Structure of TDAPS and a schematic representation of coated C18 stationary phase. B) Proposed mechanism for the simultaneous electrostatic repulsion and attraction interactions between analyte ions and zwitterionic charged stationary phase. (Reprinted from Hu et al.)[9]

Utilizing the interaction between zwitterionic surfactant TDAPS and perchlorate, EIC was investigated as a sample preparation step in the analysis of perchlorate in environmental waters. Referring back to Chapter 2, the greatest challenge in further development of the MCE system for ground water, surface water, and munitions waste water is the high concentration of competing ions present in these sample matrices. While anion-exchange resins have proven successful in retaining perchlorate in high ionic strength samples, the eluents involved are either hydroxide based or contain organic modifiers such as methanol or *p*-cyanophenol.[19-22] In the investigation of an integrated sample cleanup step, introduction of organic solvents and high-conductivity eluents is not ideal for coupling to a capillary electrophoresis system. EIC is an attractive alternative due to the use of simple eluents that would be amendable and compatible with the MCE device. The ability to retain perchlorate on a solid support coated with TDAPS was evaluated on a conventional ion chromatograph with the goal of incorporating a surfactant-

coated, packed-bed into a microfluidic network for on-chip sample cleanup. A schematic of the proposed device is shown in Figure 3.3.

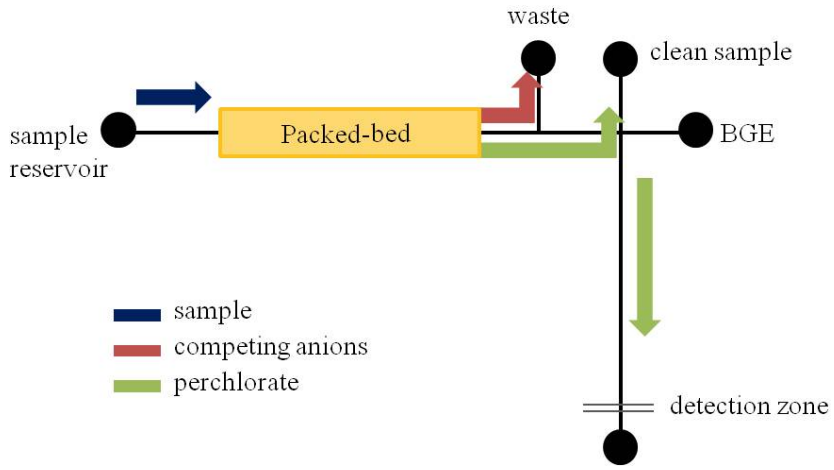

Figure 3.3. Schematic of a proposed microchip design incorporating a surfactant-coated, packed-bed for sample cleanup utilizing the principles of electrostatic ion chromatography.

3.3 EXPERIMENTAL

3.3.1 Materials and Instrumentation

Potassium salts of fluoride, chloride, bromide, nitrate, sulfate, perchlorate, and iodide were purchased from Sigma Aldrich (St. Louis, MO). Propane disulfonate, tetradecyl-N,N-dimethyl-3-ammonio-1-propanesulfonate (TDAPS), sodium carbonate, sulfuric acid, and methanol were also purchased from Sigma. The ion chromatograph used for this work was a Metrohm USA Inc. (Riverside, FL) IC System 800 series consisting of 818 serial dual piston pump, 833 peristaltic pump, 830 interface, and 819 conductivity detector. Separations were performed using Agilent Technologies (Santa Clara, CA) reverse-phase, Zorbax Eclipse XBD-C18 (3 x 250 mm), 5 µm particle diameter, analytical column. Electrophoretic separations were conducted with the microchip CE system described in Chapter 2.

3.3.2 Column Preparation

Prior to coating the C18 column with surfactant, a standard sample containing 1 mM perchlorate as well as a mixture of anions was injected onto the column to ensure none of the analytes were retained by the bare stationary phase. Next, the sulfobetaine-type zwitterionic surfactant, TDAPS, was used to dynamically coat the C18 stationary phase. TDAPS was chosen based on our previous success in effectively binding and separating perchlorate from competing anions in the microchip CE system. To condition the column, a previously published protocol was used in which 100 mL of a 10 mM aqueous TDAPS solution was passed through the column at a flow rate of 1.0 mL/min over a duration of at least 60 min.[23] Following the initial coating step, the column was conditioned with eluent until a steady baseline was achieved. It has been suggested that to enhance the stability of the column and maintain a constant amount of surfactant on the stationary phase surface, a low (below the critical micelle concentration) concentration of the surfactant can be added to the eluent.[23]

After a few days of use, an observed change in perchlorate retention would signify the need to regenerate the column. Regenerating the column to reestablish the surfactant coating involves passing a 50:50 (v/v) methanol:water mixture through the column at 1.0 mL/min for approximately 1 hr, followed by a pure water rinse for an additional 1 hr. Once regenerated, the column can be reconditioned with TDAPS using the protocol mentioned previously.

3.3.3 Characterization of EIC Column

After the preparation step, the column is equilibrated with eluent by passing the solution through the column at a 0.5 mL/min flow rate over a time period of 15 min. In the following studies, three eluents were investigated: pure DI water, a 0.1 mM TDAPS solution where the concentration of TDAPS is below the CMC, and a 1 mM TDAPS solution where the

concentration of TDAPS is above the CMC. Next, the retention/migration time of a selection of anions commonly found in environmental waters (chloride, nitrate, sulfate, perchlorate) was established individually. The retention time of iodide was also determined with each eluent type, since the polarizability and surfactant interaction is similar to that of perchlorate.

Next, calibration curves were generated for chloride, nitrate, iodide, and perchlorate in an effort to elucidate information about anion retention on the coated column. Standard solutions of these anions, with concentrations ranging from 10 μM to 1 mM, were made and injected onto the modified C18 column. Calibration curves were generated by plotting peak area versus analyte concentration.

3.3.4 Surface Water Sample Analysis

To demonstrate proof-of-concept for the EIC sample cleanup method, a surface water sample was analyzed via a two-dimensional separation: EIC in the first dimension and MCE in the second. The water sample was collected from the Cache La Poudre River in Fort Collins, CO, and the only sample preparation was to filter the sample prior to injection onto the IC column to remove large particulate matter. The sample was spiked with 100 μM perchlorate. Upon chromatographic separation from competing anions, perchlorate was collected as a fraction off the IC column by calculating the time to elution based on tubing dimensions and flow rate. The 1 mL fraction was spiked with an internal standard, 0.5 mM propane disulfonate, and the sample was immediately introduced to the MCE system. The protocol for MCE methods is discussed in Chapter 2.

3.4 RESULTS AND DISCUSSION

Three eluents were evaluated for the separation of perchlorate: pure water, 0.1 mM TDAPS solution, and 1.0 mM TDAPS solution. In Figure 3.4, consecutive injections of a standard anion solution can be seen for each eluent. The relative standard deviation (RSD) was calculated for the average retention time of perchlorate. For the pure water eluent, the average perchlorate retention was 9.28 ± 0.47 min with 5.1% RSD. Using the 0.1 mM TDAPS solution, the average perchlorate retention was 8.58 ± 0.12 min with 1.3% RSD. Finally, the 1.0 mM TDAPS solution gave an average perchlorate retention of 10.8 ± 1.7 min with 15.7% RSD. Notably, the retention of perchlorate decreases from injection to injection when the pure water mobile phase is used. This is likely due to degradation of the surfactant coating the C18 column and could also cause the high RSDs for this system. Over time, DI water could rinse the TDAPS from the C18 phase, and if less surfactant is present to retain perchlorate, the retention time will decrease. In Figure 3.4a, increasingly shorter retention times are observed for perchlorate with each consecutive injection. To prevent the degradation of the TDAPS coating, the literature suggests incorporating a small amount of surfactant in the mobile phase. When 0.1 mM TDAPS is used, the most consistent retention time for perchlorate was observed (Figure 3.4b), and this mobile phase was chosen for the remainder of the work presented here. An interesting trend is observed when 1.0 mM TDAPS is used, however. At a concentration above the CMC, the presence of surfactant micelles in the eluent is most likely causing the varied retention behavior. In this case, it is possible to have perchlorate interactions with surfactant micelles as well as interactions with immobilized surfactant monomers on the C18 column, leading to inconsistent retention patterns.

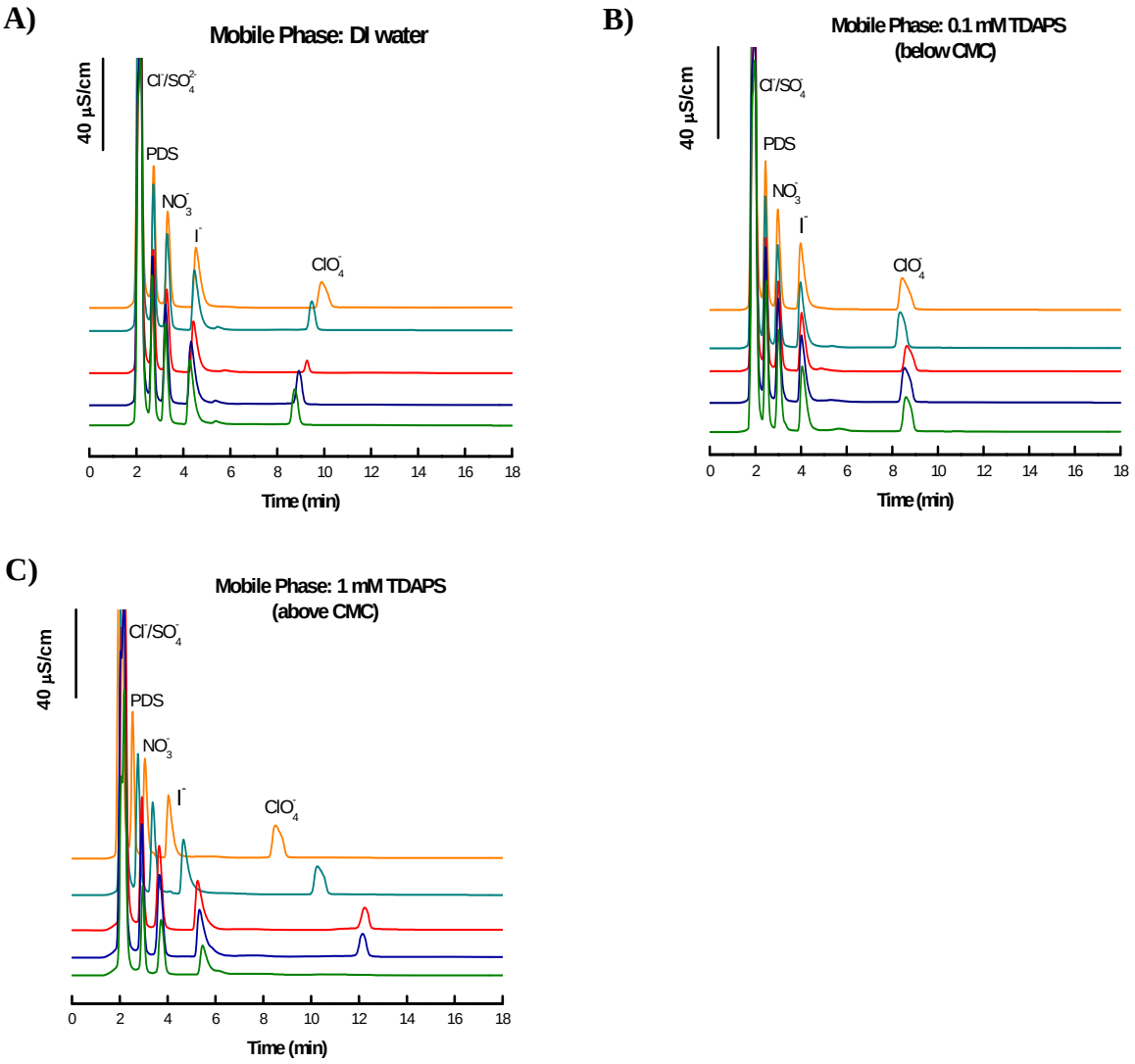

Figure 3.4. Chromatograms showing the retention of anions on a reverse-phase C18 column coated with TDAPS using mobile phases A) pure water, B) 0.1 mM TDAPS, and C) 1 mM TDAPS. Each set of chromatograms show consecutive injections of a standard sample containing 0.5 mM chloride, nitrate, sulfate, iodide, propane disulfonate (PDS), and 0.5 mM perchlorate. In early studies, PDS was added to standard samples as an internal standard. Conditions: 0.5 mL/min flow rate, 100 µL injection volume, 100 µS/cm detector range.

To characterize the EIC system, calibration curves were generated for chloride, nitrate, iodide, and perchlorate over a concentration range of 10 μM to 1 mM. Plots of peak area versus analyte concentration are shown in Figure 3.5. Curves for chloride and nitrate display good linearity with a correlation of 0.989 and 0.997, respectively. These anions have little to no interaction with the surfactant-coated stationary phase, while iodide and perchlorate are retained more strongly. The calibration of these polarizable anions gives a nonlinear trend over the chosen concentration range. The retention behavior described by the calibration curves suggests strong retention of both iodide and perchlorate, leading to saturation of the column. Furthermore, perchlorate is not detected at a concentration less than 100 μM (10,000 ppb), which could be due to an adsorbed concentration threshold of the column and/or poor sensitivity of the conductivity detector. The combination of these effects is highly undesirable for the application at hand. Additionally, studies employing a standard anion-exchange column for conventional ion chromatography suggest a notable limitation in the sensitivity of the Metrohm conductivity detector used in these experiments. Even while operating in a normal chromatography mode, perchlorate was never detected at relevant concentrations (< 1000 ppb).

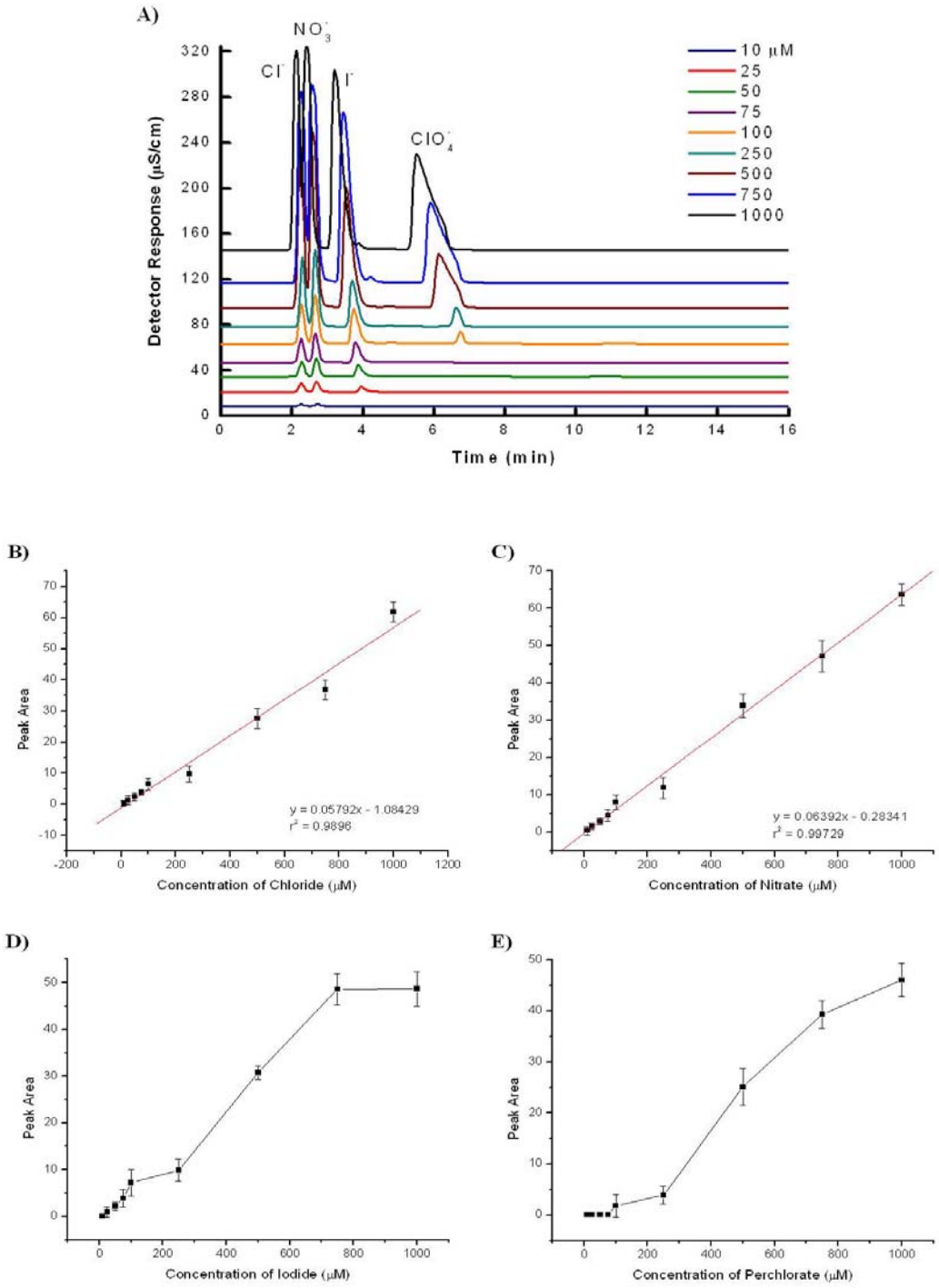

Figure 3.5. A) Chromatographs of standard solutions of anions ranging from 10 µM to 1 mM in concentration. Conditions: 0.1 mM TDAPS mobile phase, 0.5 mL/min flow rate, 100 µL injection loop, 100 µS/cm detector range. Calibration curves plotting peak area vs. analyte concentration for B) chloride, C) nitrate, D) iodide, and E) perchlorate, where each data point is the average peak area measured for n = 3 measurements and error bars represent the standard deviation from the mean.

Despite the limitations with the employed IC system, proof-of-concept for the EIC cleanup step was demonstrated with the direct analysis of a surface water sample. In this study, a surface water sample, collected from the Cache La Poudre River in Fort Collins, CO, undergoes a sample cleanup step via EIC, followed by separation on the MCE system. The water samples were spiked with 100 μM perchlorate and injected onto the EIC column. This concentration of perchlorate was chosen because it is the detection limit for the system, and in order to monitor the elution of perchlorate, the peak must be visible in the resulting chromatograph. The chromatographic separation of perchlorate in a real water sample is shown in Figure 3.6a. Next, perchlorate was collected from the eluent in a 1 mL fraction. The fraction was spiked with 0.5 mM PDS (internal standard) and injected onto the microchip CE device. The electropherogram for this separation is shown in Figure 3.6b. Comparing the initial chromatographic separation of the surface water sample to the subsequent electrophoretic separation, a dramatic reduction in the concentration of chloride, nitrate, and sulfate is observed. This study demonstrates the efficacy of using EIC to remove competing anions from sample matrices such as surface water, ground water, and munitions waste water, effectively 'cleaning' the sample and making it viable for MCE analysis. This study also marks for the first account of combining these two techniques in a two-dimensional separation. Unsuitably, the recovery for perchlorate was only 1.3%, but this low recovery could be associated with adsorbed perchlorate on the EIC column that was not collected in the eluent fraction.

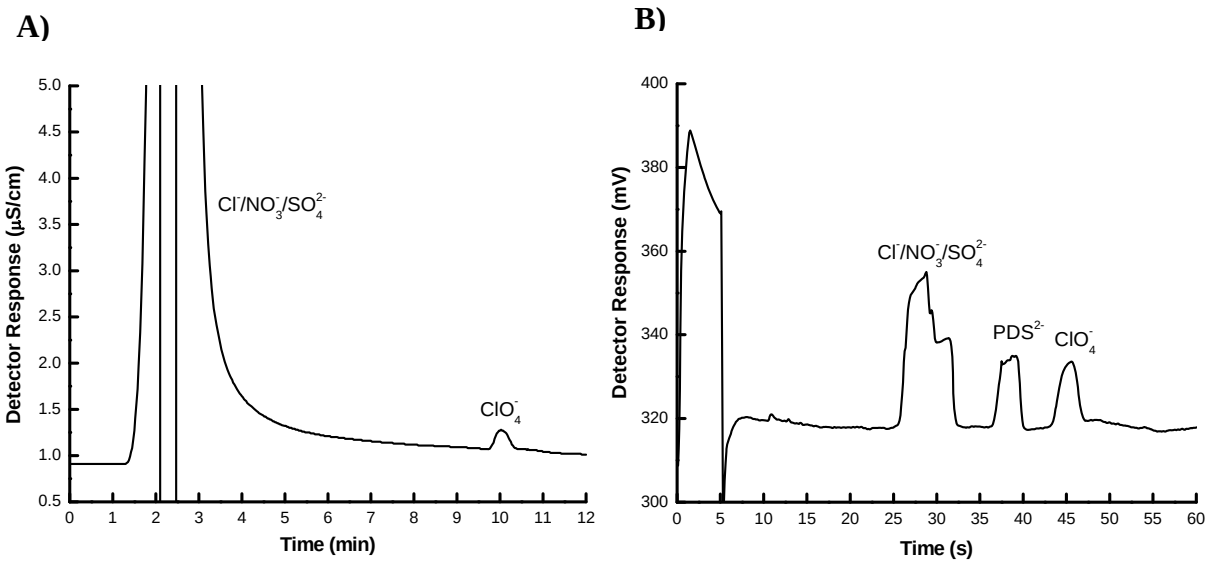

Figure 3.6. Progression of a spiked surface water sample analysis, demonstrating proof-of-concept for the utility of EIC cleanup. A) Chromatogram of the EIC separation of perchlorate in river water. Upon separation from high concentrations of competing anions, the perchlorate fraction was collected as it was eluted from the IC column, spiked with PDS, and immediately analyzed via MCE (B). The electropherogram in B shows the dramatic reduction in chloride, nitrate, and sulfate concentration, depicting the efficacy of sample clean-up via EIC.

3.5 CONCLUSIONS

In Chapter 2, the development of a MCE system for the analysis of perchlorate in drinking water was described. This method is highly effective for detecting low (ppb) levels of perchlorate in a rapid, electrophoretic separation. The biggest hurdle, however, is the ability to analyze more complex samples, containing higher concentrations of competing anions. A cardinal downfall of capillary electrophoresis is analysis of high conductivity samples, since stacking effects are hindered and Joule heating can decrease the signal-to-noise ratio. One solution to this problem is incorporating a sample cleanup step. Inherently, EIC offers a number of advantages as a sample cleanup technique that can be integrated into a MCE system, particularly the use of simple eluents. To investigate the effectiveness of EIC for perchlorate

analysis, a C18 column was dynamically coated with TDAPS surfactant, and the retention of perchlorate and other anions was studied using a conventional ion chromatograph. While the retention mechanism in this capacity is not fully understood and the system is hindered by fundamental limitations of the instrument, proof-of-concept was demonstrated via a two-dimensional analysis of surface water.

The ability to monitor perchlorate contamination in environmental samples as well as military munitions waste is a serious concern for public health. The work presented in this chapter shows great potential for the next phase of MCE analysis, laying a foundation for EIC as a sample preparation technique for high ionic strength samples. Although, further understanding of the retention mechanism between perchlorate and immobilized TDAPS surfactant must be attained. Perhaps this information could be gathered from a high-performance, IC instrument capable of detecting low and more relevant concentrations of perchlorate. Also, the transition from a conventional IC column to an integrated packed-bed will allow for further characterization of EIC in the microchip format. Our collaborators from the US Army Corps of Engineers in Champaign, IL continue to develop and characterize an integrated, sample preparation scheme in the microfluidic device. Future work in this area also includes the fabrication of a surface-modified, monolithic phase in a microchannel.

3.6 REFERENCES

1. Mikkers, F. E.; Everaerts, F. M.; Verheggen, T. P. *Journal of Chromatography A* **1979,** *169* (0), 11-20.
2. Osbourn, D. M.; Weiss, D. J.; Lunte, C. E. *Electrophoresis* **2000,** *21* (14), 2768-2779.
3. Zhang, C.-X.; Thormann, W. *Analytical Chemistry* **1996,** *68* (15), 2523-2532.
4. Ding, W.; Thornton, M. J.; Fritz, J. S. *Electrophoresis* **1998,** *19* (12), 2133-2139.
5. Zhao, Y.; Lunte, C. E. *Analytical Chemistry* **1999,** *71* (18), 3985-3991.
6. Zhang, C. X.; Aebi, Y.; Thormann, W. *Clinical Chemistry* **1996,** *42* (11), 1805-11.
7. Tagliaro, F.; Manetto, G.; Crivellente, F.; Smith, F. P. *Forensic Science International* **1998,** *92* (2–3), 75-88.
8. Ho, Y.-H.; Ko, W.-K.; Kou, H.-S.; Wu, H.-L.; Wu, S.-M. *Journal of Chromatography B* **2004,** *809* (1), 111-116.
9. Hu, W.; Takeuchi, T.; Haraguchi, H. *Analytical Chemistry* **1993,** *65* (17), 2204-2208.
10. Nesterenko, E. P.; Nesterenko, P. N.; Paull, B. *Analytica Chimica Acta* **2009,** *652* (1-2), 3-21.
11. Hu, W.; Haddad, P. R. *TrAC Trends in Analytical Chemistry* **1998,** *17* (2), 73-79.
12. Okada, T.; Patil, J. M. *Langmuir* **1998,** *14* (21), 6241-6248.
13. Cook, H. A.; Dicinoski, G. W.; Haddad, P. R. *Journal of Chromatography A* **2003,** *997* (1–2), 13-20.
14. Hu, W.; Tominaga, M.; Tao, H.; Itoh, A.; Umemura, T.; Haraguchi, H. *Analytical Chemistry* **1995,** *67* (20), 3713-3716.
15. Cook, H. A.; Hu, W.; Fritz, J. S.; Haddad, P. R. *Analytical Chemistry* **2001,** *73* (13), 3022-3027.
16. Okada, T. *Analytica Chimica Acta* **2005,** *540* (1), 139-145.
17. Hu, W.; Tao, H.; Haraguchi, H. *Analytical Chemistry* **1994,** *66* (15), 2514-2520.
18. Hu, W.; Haddad, P. R.; Tanaka, K.; Sato, S.; Mori, M.; Xu, Q.; Ikedo, M.; Tanaka, S. *Journal of Chromatography A* **2004,** *1039* (1-2), 59-62.
19. Jackson, P. E.; Laikhtman, M.; Rohrer, J. S. *Journal of Chromatography A* **1999,** *850* (1–2), 131-135.
20. Jackson, P. E.; Gokhale, S.; Streib, T.; Rohrer, J. S.; Pohl, C. A. *Journal of Chromatography A* **2000,** *888* (1–2), 151-158.
21. Lin, R.; De Borba, B.; Srinivasan, K.; Woodruff, A.; Pohl, C. *Analytica Chimica Acta* **2006,** *567* (1), 135-142.
22. Liu, Y.; Mou, S.; Heberling, S. *Journal of Chromatography A* **2002,** *956* (1–2), 85-91.
23. Ríordáin, C. Ó.; Nesterenko, P.; Paull, B. *Journal of Chromatography A* **2005,** *1070* (1–2), 71-78.

CHAPTER 4. INTRODUCTION TO PAPER-BASED ANALYTICAL DEVICES FOR THE DETECTION OF FOODBORNE, PATHOGENIC BACTERIA

4.1 INTRODUCTION

A great need exists for faster, simpler, on-site pathogen detection in foods. Foodborne illness is a serious public health concern in the US and across the world. Food processing companies and federal regulatory sectors, such as Food and Drug Administration (FDA) and Center for Disease Control (CDC), are faced with the challenge of monitoring food quality and tracing contamination outbreaks largely because of the difficulty in detecting as few as 1 pathogenic cell in contaminated food products. Culture methods continue to be the gold standard in microbial detection, identification, and enumeration for food contamination.[1,2] However, this technique is cumbersome and time-consuming, requiring large quantities of reagents, agar plates, and sample volumes, not to mention visual counting under a high resolution microscope. For confirmation of a microbial species, several days are needed to complete the multistep analysis which is very problematic for the shipment of contaminated foods that have a finite shelf-life.[3] Advances in molecular techniques such as polymerase chain reaction (PCR) have allowed for faster, more sensitive, and more selective results; however, PCR necessitates complex instrumentation as well as highly trained personnel for operation. Herein, a novel detection scheme is presented that utilizes a paper-based analytical device (μPAD) for the colorimetric determination of three pathogenic bacteria in ready-to-eat (RTE) meat, namely *Listeria*

monocytogenes, *Escherichia coli* O157:H7, and *Salmonella enterica*. This chapter discusses the disease characteristics, propensity for food contamination, and current detection methods for these three pathogens as well as an introduction to the development of the μPAD.

4.2 FOODBORNE BACTERIA

An estimated 48 million cases of foodborne illness occur in the US each year, resulting in several thousand deaths.[4] Pathogenic bacteria continue to encumber the food industry, federal regulatory agencies and public health laboratories with a staggering annual cost of $152 billion.[5] This economic burden is due to the time and cost of monitoring food contamination, product recalls for contamination, the difficulty in tracing outbreaks, as well as the severe illness and necessary hospitalization the affected individuals typically face. While a number of microbial pathogens are associated with food contamination, pathogenic *Escherichia coli* O157:H7, *Salmonella enterica*, and *Listeria monocytogenes* are three of the most common offenders.[6,7]

4.2.1 Listeria monocytogenes

L. monocytogenes (Figure 4.1) is a Gram-positive, rod-shaped bacterium, and is considered one of the most virulent foodborne pathogens.[8] *L. monocytogenes* has also been found in a large number of mammalian species, both domestic and feral, and has been isolated from environmental sources, such as soil, silage, and water.[6] The bacteria are responsible for listeriosis, a disease in humans, which manifests as gastroenteritis, encephalitis, meningitis, septicemia, and uterine infections in pregnant women that can lead to premature labor and even fetal mortality.[3] The severity and lethality of the infection is dependent on the susceptibility of the victim, making the elderly, immunocompromised persons, small children, as well as pregnant women and their fetuses the most vulnerable.[9] Listeriosis is contracted by ingesting

contaminated foods, and *L. monocytogenes* is most commonly associated with contaminated dairy products, specifically raw and pasteurized milk, soft cheeses, and ice cream, as well as ready-to-eat (RTE) meats, including deli meats, bologna, and hot dogs, because of its ability to grow at refrigeration temperatures and withstand high salt concentrations typically used in the preservation of these food products.[6,8,10] Other foodstuffs in which *L. monocytogenes* contamination has been reported include raw vegetables, raw and cooked poultry, as well as other raw meats. Recently, a multistate outbreak of *L. monocytogenes* in the US marked the first instance of listeriosis associated with cantaloupe. This outbreak is considered the third largest in US history with 84 cases reported in 19 states, resulting in 15 deaths.[3]

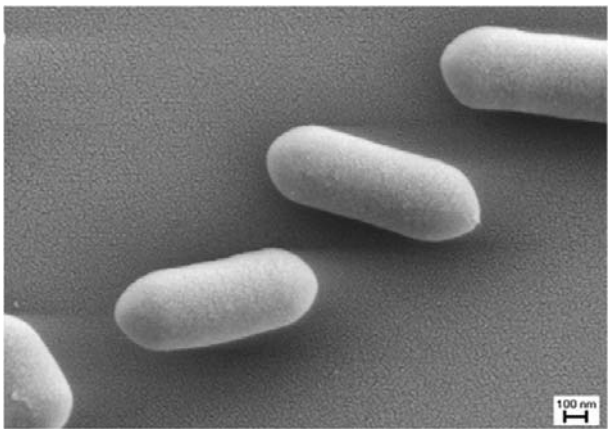

Figure 4.1 SEM image of *Listeria monocytogenes.*

4.2.2 Escherichia coli O157:H7

Escherichia coli species comprise multiple different strains that exhibit great genetic and phenotypic diversity. *E. coli*, shown in Figure 4.2, are Gram-negative, rod-shaped bacteria with a variety of serovar-dependent characteristics. While most strains are harmless, residing innocuously in the gastrointestinal tract of most mammals, some virulent serovars can be life-threatening.[11] Serovar O157:H7, in particular, is a rare but dangerous strain that produces potent

toxins, causing severe damage to the lining of the intestine. This strain of *E. coli* is considered enterohemorrhagic.[12-14] The illness it causes is characterized by abdominal pain and diarrhea which can lead to hemorrhaging of the intestine, hemolytic uremic syndrome, and even death if not treated.[3,9] Unlike listeriosis, anyone can be infected with *E. coli* O157:H7 by consuming contaminated foods. Food products such as raw meats, cheeses, raw vegetables, and unpasteurized fruit juices have been reported to be contaminated with *E. coli* O157:H7. In 2006, two children were hospitalized with hemolytic uremic syndrome, caused by a culture-confirmed *E. coli* O157:H7 infection, after consuming raw milk from a dairy in California.[3] This is just one of many examples of O157:H7 contamination and infection in the US.

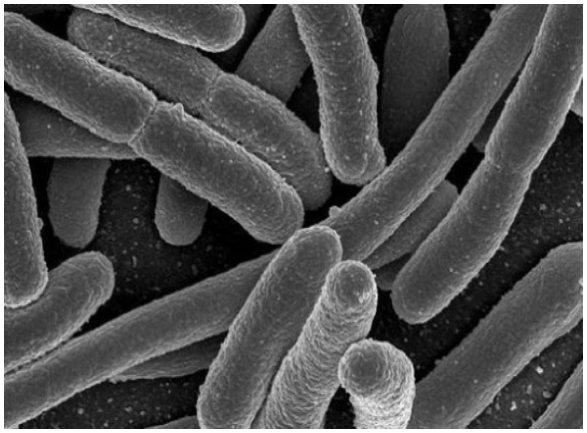

Figure 4.2 SEM image of *E. coli.*

4.2.3 Salmonella enterica

Salmonella spp. serovars are some of the most common causes of bacterial, gastrointestinal disease. Like pathogenic *E. coli,* the bacteria are Gram-negative, rod-shaped, and flagellated (Figure 4.3). More specifically, the species *S. enterica* is responsible for salmonellosis, a severe bacterial infection.[3] Salmonellosis is characterized by acute symptoms such as nausea, vomiting, abdominal cramps, headache and fever. All persons are susceptible to

infection; however, symptoms may escalate depending upon the age and health of the victim.[9] *S. enterica* have been known to contaminate poultry, eggs, raw meats, fish, sauces, salad dressings, dairy products, and peanut butter.[6,15,16] The wide variety of food types that have been associated with *S. enterica* contamination further exacerbate the challenges in monitoring food safety. In 2011, Cargill recalled 36 million pounds of ground turkey that was linked to *Salmonella* contamination. The multistate outbreak caused several hundred hospitalizations and one death.[3]

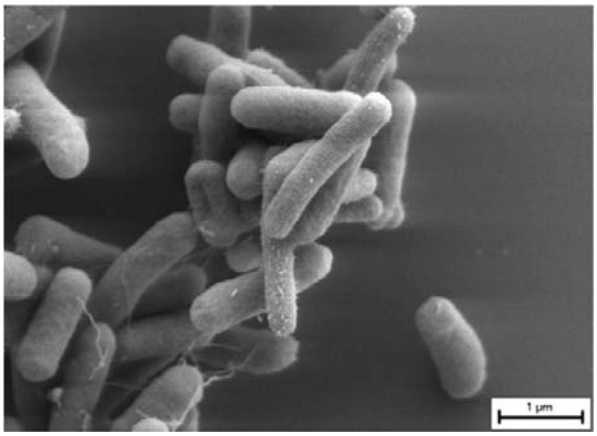

Figure 4.3 SEM image of *S.* Typhimurium.

4.3 CURRENT DETECTION METHODS

4.3.1 Culture Methods

Culture methods are the oldest bacterial detection technique and remain the standard. Selective media are used in an enrichment step to simultaneously enhance the growth of target species while inhibiting the growth of competing, background flora. Often this step may involve more than one type of media and require hours to days to complete. For confirmation and enumeration of target bacteria, species-specific agar plates are inoculated with enrichment medium. Agars contain particular nutrients and colorimetric substrates so that differentiation and identification of microbial species is achieved by detecting bacterial metabolites as a

function of available nutrients. An additional 24-48 hr is required to obtain a final plate count, and detection is typically performed by ocular inspection and manual counting. The culture method continues to be the regulatory method used in US Food and Drug Administration (USFDA) protocols, but is excessively time-consuming. A good example of the total analysis time necessitated is the detection of *Campylobacter* spp. In order to confirm a positive result, 14 to 16 days are required.[17] As a result, faster and simpler detection methods for on-site analysis are desired for food processing facilities.

4.3.2 Polymerase Chain Reaction

Polymerase chain reaction (PCR) is a widely accepted method of bacterial detection. First developed in the late 1980's, the technique involves the isolation, amplification, and quantification of short DNA sequences.[18] In a reaction chamber, the sample is combined with specific oligonucleotides, or primers, composed of the complementary base pairs to the target DNA sequence as well as DNA polymerase, the key enzyme in DNA replication. The sample undergoes thermal cycling, a controlled series of heating and cooling cycles, to effectively separate the two DNA strands of the sample and initiate DNA replication. This process generates thousands to millions of copies of the target DNA sequence, with the direction of specific primers, in a relatively short amount of time. Today, PCR is used extensively in nucleic acid-based assays to amplify specific segments from as little as a single copy of DNA to easily detectable quantities. In the case of pathogenic microbes, highly specific genetic material is targeted from a minimal number of cells, making this technique the most sensitive and selective detection method available. Another advantage of PCR for microbial detection is reduced analysis time when compared to culture methods. Results are typically obtained in 5 to 24 hours, depending on thermal cycles and whether or not an enrichment step is included. Historically,

PCR was limited by the inability to discriminate between viable and non-viable cells as target DNA sequences can originate from dead cells. However, recent developments have overcome this obstacle.[19] While PCR continues to evolve as a highly sophisticated method for pathogen detection, the technique is complex and the instrumentation is costly. Furthermore, a portable format has not yet been realized.

4.3.3 Immunoassay-based Methods

Biosensors utilizing immunological methods are emerging as an attractive alternative for pathogen detection due to reduced sample volumes, high specificity in complex matrices, and potential for portability, miniaturization, and automation.[1,7] Immunoassay-based methods for bacteria detection are considered powerful analytical tools. Gu and co-workers demonstrated enhanced pre-treatment or pre-concentration of target pathogens using immunomagnetic separation (IMS), where anti-body coated magnetic beads are used to capture and extract target bacteria in complex samples.[20] In addition to the high selectivity IMS provides, the ability to incorporate this technique with nearly any detection scheme is an added advantage.

Beyond pre-treatment strategies, immunological detection techniques are considered the fastest growing pathogen detection schemes, with enzyme-linked immunosorbent assay (ELISA) being the most established and most commonly used method.[1] In this strategy, specific anti-body/antigen interactions most often lead to detectable changes in fluorescence,[21,22] surface plasmon resonance,[23,24] or electrochemical signal.[25,26] Despite the good performance of ELISA, this technique remains a laboratory-based method, requiring complex instrumentation for signal transduction. In response to this drawback, colorimetric assays have been developed in both a well-plate and lateral flow paper strip platform, facilitating a simple, fast, and easily operable immunosensor.[27,28] While these devices are more amendable to on-site analysis, a fundamental

problem remains: immunoassays are hindered by the inability to distinguish between viable and non-viable cells, since target antigens may be present in dead cells. This drawback often leads to false-positive results.[29,30]

4.4 PAPER-BASED ANALYTICAL DEVICE FOR PATHOGEN DETECTION

Miniaturized, microfluidic devices offer a number of advantages suitable for food quality analysis, such as reduced reagent and sample consumption, ease of operation, portability, and rapid analysis. In particular, μPADs fabricated from patterned paper, have gained considerable attention over the past decade. The concept of fabricating a device from a paper substrate was conceived by Whitesides and co-workers in 2007.[31] Over the years, a number of fabrication techniques have been described to create well-defined channels in paper for fluid flow; wax printing is the simplest and most cost-effective reported to date.[32] As fabrication techniques become more efficient, μPAD designs become more complex. Two fundamental designs can be recognized: a simple zone or spot test and a fluidic network. The microzone design was introduced as an alternative to conventional multi-well plates. And while the paper-based plates function similarly to plastic well plates, they offer new capabilities such as reduced volumes and materials cost.[33] Paper-based fluidic devices use capillary wicking to distribute sample and reagent fluids through defined channels for multiplexed and even multidimenional analysis. These devices do not require external pumps, since the fibers act to transport fluids within the device, and offer low-cost when compared with their polymeric or glass counterparts.[34] Several μPAD designs are shown in Figure 4.4, demonstrating the diversity and capabilities of patterned paper.

A μPAD device has been developed for the colorimetric determination of *L. monocytogenes*, *E. coli* O157:H7, and *S.* Typhimurium, detecting enzymes that are specific to each bacterial species. As mentioned previously, μPADs show great promise for a wide variety of applications. The device presented in this dissertation marks the first application of a μPAD for bacterial detection in food. In the μPAD format, analysis of food samples can be more rapid, less costly, and easier to perform than current techniques. No sophisticated instrumentation is required since the paper-based devices are simple to operate and colorimetric results are easily interpreted. Furthermore, quantitative information can be gained by simply scanning the devices to generate a digital image and measuring color intensity with ImageJ software. The details of this quantitative analysis and the optimization of each enzymatic assay will be discussed in more detail in Chapter 5.

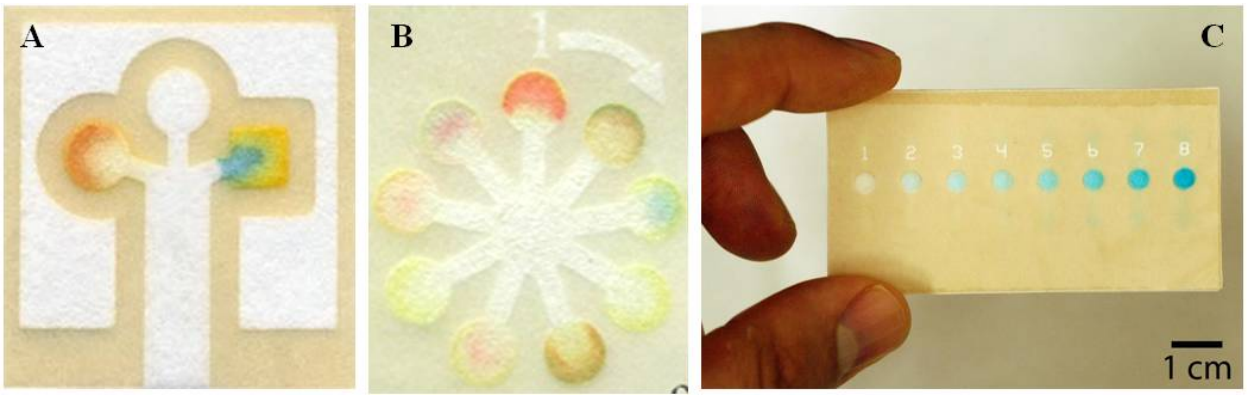

Figure 4.4. A) Chromatography paper patterned with SU-8 photoresist. Cured photoresist defines the central channel and three detection zones. The detection zones are prepared with reagents for glucose and protein detection. When the central channel is dipped in a urine sample, fluid is transported via capillary action to the detection zones where colorimetric assays take place. (Reprinted from Martinez et al.) B) A multiple indicator test for glucose, lactose, and uric acid in serum and urine. The dendritic structure of this paper device affords 9 detection zones used to increase the visual accuracy of each assay. In this design, sample is introduced as a 10 μL droplet in the center of the device. The sample is wicked out to the 9 detection zones. (Reprinted from Dungchai et al.) C) A paper-based microzone plate characterized with varying concentrations of coomassie blue dye. The microzone plate offer an inexpensive alternative to plastic well plates. Compared with their fluidic counterparts, all sample and reagent volumes are contained within a well on the paper. (Reprinted from Carrilho et al.)

4.5 ENZYMATIC ASSAYS FOR BACTERIA DETECTION

Enzymatic substrates are powerful tools in microbiology. In addition to providing valuable insight to metabolic pathways, enzymatic assays can be used to enumerate, identify, and detect microorganisms.[35] Synthetic substrates have been used to study microbial enzymatic activities since the early 20th century.[36,37] The detection schemes are typically based on a measurable change in absorbance or fluorescence upon enzyme-substrate interaction. Early use of chromogenic substrates incorporated nitrophenol or nitroaniline; however, these compounds produce a yellow color that is very difficult to distinguish from most microbial culture media. Furthermore, the yellow product lacks stability, degrading at low pH. More robust and discernable substrates have since been developed, producing black, purple, red, and blue precipitates. For example, indoxyl based substrates are ubiquitous in microbiology and were developed because of the indigo dye, formed upon oxidation of the liberated indoxyl, strongly contrasts from the color of microbial media.[38-40] Other commonly used synthetic, chromogenic substrates include *p*-naptholbenzein-, 8-hydroxyquinoline-, and aminophenyl acridine-based compounds.[35] The enzymatic assays used in this dissertation are presented below.

4.5.1 Assay for PI-PLC

Phosphatidylinositol-specific, phospholipase C (PI-PLC) is a known virulence factor of *L. monocytogenes*.[41] The enzyme functions to catalyze the hydrolysis of phosphoinositides to produce diacylglycerol and *myo*-inositol phosphates. A few chromogenic substrates have been synthesized for PI-PLC and are typically incorporated into culturing media, including 4-nitrophenyl *myo*-inositol phosphate[42] and 5-bromo-4-chloro-3-indolyl *myo*-inositol phosphate (X-InP).[43] A schematic of the enzymatic reaction and an image of the indigo product are shown in Figure 4.5. Other bacterial species that produce PI-PLCs include *Bacillus thuringiensis, B.*

anthracis, L. ivanovii, and *Clostridium novyi*;[41,42,44,45] however, their proclivity for food contamination is extremely rare, making this enzymatic assay highly specific for *L. monocytogenes* detection in its environmental niche.

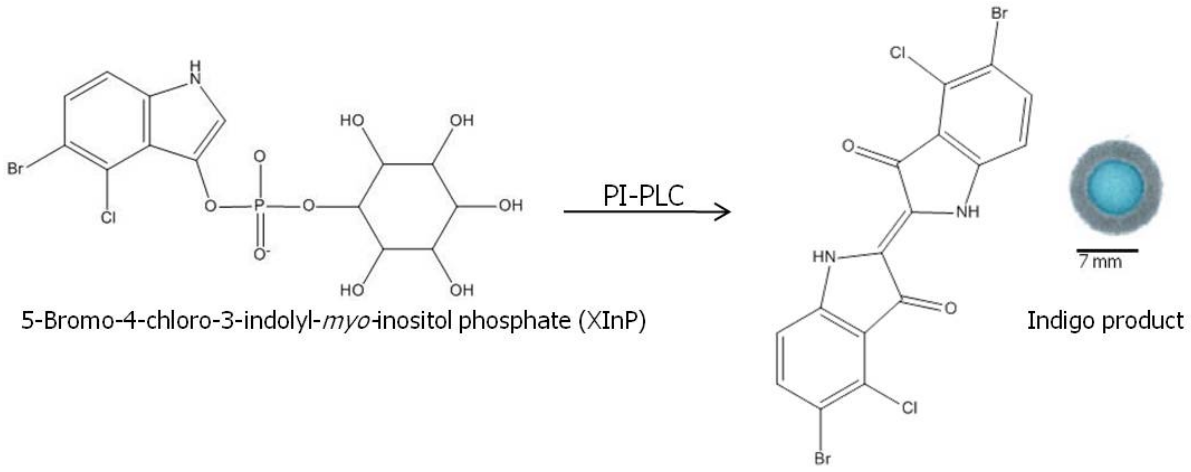

Figure 4.5. In the presence of PI-PLC, synthetic substrate 5-bromo-4-chloro-3-indolyl-*myo*-inositol phosphate (X-InP) is hydrolyzed, liberating the inositol phosphate and generating an indigo product. A digital image of the blue color change on paper-based spot test is also pictured.

4.5.2 Assay for C_8 esterase

Detection of esterase activity, specifically C_8 esterase, is a well accepted method of *Salmonella* spp. identification since the enzyme is not present in other non-lactose fermenting members of the family *Enterobacteriacaea* (which includes *Escherichia coli, Shigella,* and a number of other pathogens as well as several non-pathogenic species).[46-48] Tests for C_8 esterase first emerged as a fluorescent assay, using a 4-methylumbelliferone-conjugated substrate in media.[49,50] More recently, 5-bromo-6-chloro-3-indolyl octanoate (magenta caprylate) has been incorporated into chromogenic agars and culture media, producing magenta colored colonies

upon hydrolysis by C_8 esterase. A digital image of the magenta precipitate and a schematic of the enzymatic reaction are presented in Figure 4.6.

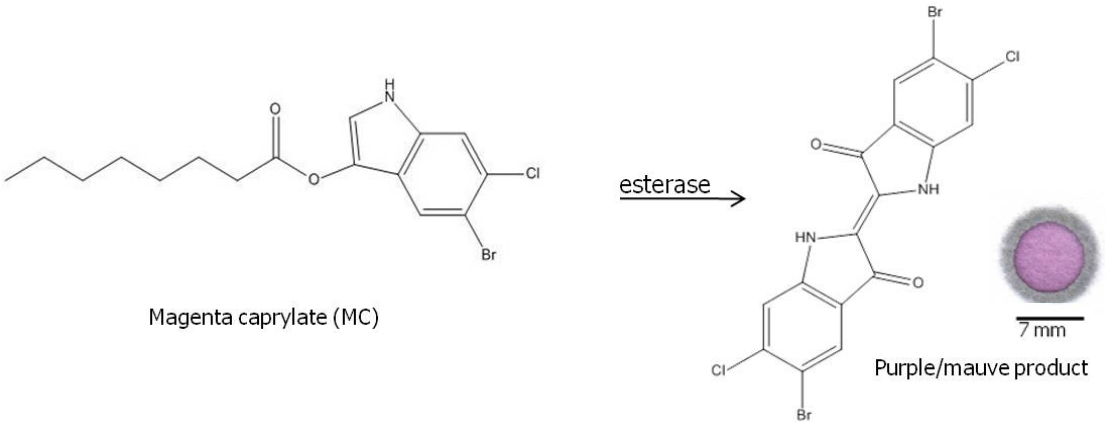

Figure 4.6. Magenta caprylate, also known as 5-bromo-6-chloro-3-indolyl octanoate, is cleaved by C_8 esterase to produce a purple product. A digital image of the purple color change on the paper-based spot test is pictured on the right.

4.5.3. Assay for β-galactosidase

The enzyme β-galactosidase is often referred to as lactase since it catalyzes the hydrolysis of lactose, producing glucose and galactose.[51] Playing a crucial role in a fundamental metabolic pathway, it is not surprising to consider the ubiquity of this enzyme in living organisms. Despite its prevalence, the detection of β-galactosidase is regarded as a standard method for the determination of total coliforms in water and food.[52,53] Assays for galactosidase have been developed for the detection of *E. coli* O157:H7 from food samples, often incorporating a synthetic, chromogenic substrate into selective agar media.[35,54] Chromogenic substrates for β-galactosidase include chlorophenol red-β-galactopyranoside (CPRG) and 5-bromo-4-chloro-3-indolyl-galactopyranoside (X-gal). The CPRG substrate was chosen for the work presented in this dissertation. A schematic of the enzymatic hydrolysis of CPRG as well as the yellow to red color change generated are shown in Figure 4.7.

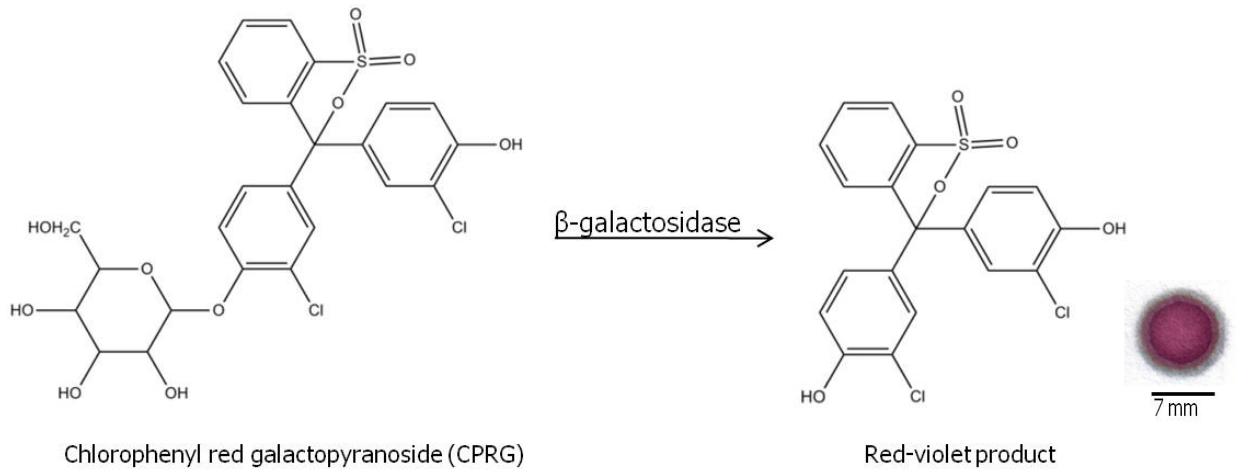

Figure 4.7. In the presence of β-galactosidase, chlorophenol red galactopyranoside (CPRG) is cleaved to produce a red-violet product and free galactopyranoside. The red-violet color change on the paper-based device is also pictured.

4.6 CONCLUSIONS

Foodborne, pathogenic bacteria are a continuing problem in the food industry. Bacteria such as *L. monocytogenes, S. enterica*, and *E. coli* O157:H7 can contaminate a wide variety of foods and if consumed, can cause severe illness that may even lead to death. The ability to monitor food contamination with microbial pathogens poses a great challenge due to the time and cost of analysis. In response to the need for faster, more cost-effective techniques for pathogen detection, a paper-based analytical device is proposed. The device provides a less expensive detection platform since it is fabricated from ordinary filter paper. Additionally, species-specific enzymes are targeted to generate a colorimetric result that is easily interpreted. The optimization of the paper device and colorimetric assays as well as the analysis of live bacteria in real food samples will be discussed in Chapter 5.

4.7 REFERENCES

1. Lazcka, O.; Campo, F. J. D.; Muñoz, F. X. *Biosensors and Bioelectronics* **2007**, *22* (7), 1205-1217.
2. Heo, J.; Hua, S. Z. *Sensors* **2009**, *9* (6), 4483-4502.
3. Bad Bug Book: Foodborne Pathogenic Microorganisms and Natural Toxins Handbook. http://www.fda.gov/Food/FoodSafety/FoodborneIllness/FoodborneIllnessFoodbornePathogensNaturalToxins/BadBugBook/default.htm.
4. Scallan, E. R. *Emerging Infectious Diseases* **2011**, *17* (1), 7.
5. Scharff, R. L. *Health-Related Costs From Foodborne Illness in the United States*; Georgetown University: Washington DC, **2010**.
6. Van Kessel, J. A. S.; Karns, J. S.; Lombard, J. E.; Kopral, C. A. *J. Food Prot.* **2011**, *74* (5), 759-768.
7. Chemburu, S.; Wilkins, E.; Abdel-Hamid, I. *Biosensors and Bioelectronics* **2005**, *21* (3), 491-499.
8. Farber, J. M. *Incidence and behavior of Listeria monocytogenes in meat products*. Marcel Dekker: New York, **1999**.
9. Foodborne Illness, Center for Diseases Control. http://www.cdc.gov/foodsafety/diseases/.
10. Amezquita, A.; Brashears, M. M. *J. Food Prot.* **2002**, *65* (2), 316-325.
11. Kaper, J. B.; Nataro, J. P.; Mobley, H. L. T. *Nat Rev Micro* **2004**, *2* (2), 123-140.
12. Gyles, C. L. *Journal of Animal Science* **2007**, *85* (13 suppl), E45-E62.
13. Boerlin, P.; McEwen, S. A.; Boerlin-Petzold, F.; Wilson, J. B.; Johnson, R. P.; Gyles, C. L. *Journal of Clinical Microbiology* **1999**, *37* (3), 497-503.
14. Abu-Ali, G. S.; Ouellette, L. M.; Henderson, S. T.; Whittam, T. S.; Manning, S. D., *Microbiology* **2010**, *156* (2), 408-419.
15. Kisluk, G.; Hoover, D. G.; Kneil, K. E.; Yaron, S. *Food Science and Technology* **2012**, *45* (1), 36-42.
16. Ruiz, J.; Varela, M. C.; Sempere, M. A.; Lopez, M. L.; Gomez, J.; Oliva, J. *European Journal of Clinical Microbiology & Infectious Diseases* **1991**, *10* (8), 649-651.
17. Brooks, B. W.; Devenish, J.; Lutze-Wallace, C. L.; Milnes, D.; Robertson, R. H.; Berlie-Surujballi, G. *Veterinary Microbiology* **2004**, *103* (1–2), 77-84.
18. Mullis, K.; Faloona, F.; Scharf, S.; Saiki, R.; Horn, G.; Erlich, H. *Cold Spring Harbor Symposia on Quantitative Biology* **1986**, *51*, 263-273.
19. Yaron, S.; Matthews, K. R., *Journal Of Applied Microbiology* **2002**, *92* (4), 633-640.
20. Gu, H.; Xu, K.; Xu, C.; Xu, B. *Chemical Communications* **2006**, (9).
21. Zhu, P.; Shelton, D. R.; Li, S.; Adams, D. L.; Karns, J. S.; Amstutz, P.; Tang, C.-M. *Biosensors and Bioelectronics* **2011**, *30* (1), 337-341.
22. Poltronieri, P. d. B., M. D.; D'Uros, O. F. *Plant Soil Environ.* **2009**, *55*, 363-369.
23. Oh, B.-K.; Lee, W.; Chun, B. S.; Bae, Y. M.; Lee, W. H.; Choi, J.-W. *Biosensors and Bioelectronics* **2005**, *20* (9), 1847-1850.
24. Taylor, A. D.; Yu, Q.; Chen, S.; Homola, J.; Jiang, S. *Sensors and Actuators B: Chemical* **2005**, *107* (1), 202-208.
25. Brewster, J. D.; Gehring, A. G.; Mazenko, R. S.; Van Houten, L. J.; Crawford, C. J., *Analytical Chemistry* **1996**, *68* (23), 4153-4159.
26. Croci, L.; Delibato, E.; Volpe, G.; Palleschi, G. *Anal. Lett.* **2001**, *34* (15), 2597-2607.
27. Park, S.; Kim, Y.; Kim, Y.-K. *BioChip Journal* **2010**, *4* (2), 110-116.

28. Pires, A. C.; Soares, N. F.; da Silva, L. H. M.; De Almeida, M. V.; Le Hyaric, M.; Andrade, N.; Soares, R. F.; Mageste, A. B.; Reis, S. G. *Sensors and Actuators B: Chemical* **2011**, *153* (1), 17-23.
29. Liu, Y.; Gilchrist, A.; Zhang, J.; Li, X.-F. *Applied and Environmental Microbiology* **2008**, *74* (5), 1502-1507.
30. Zhao, X.; Hilliard, L. R.; Mechery, S. J.; Wang, Y.; Bagwe, R. P.; Jin, S.; Tan, W. *P.N.A.S.* **2004**, *101* (42), 15027-15032.
31. Martinez, A. W.; Phillips, S. T.; Butte, M. J.; Whitesides, G. M. *Angewandte Chemie International Edition* **2007**, *46* (8), 1318-1320.
32. Carrilho, E.; Martinez, A. W.; Whitesides, G. M. *Analytical Chemistry* **2009**, *81* (16), 7091-7095.
33. Carrilho, E.; Phillips, S. T.; Vella, S. J.; Martinez, A. W. *Analytical Chemistry* **2009**, *81* (15), 5990-5998.
34. Martinez, A. W.; Phillips, S. T.; Whitesides, G. M. *P.N.A.S.* **2008**, 105, 19606-19611.
35. Orenga, S.; James, A. L.; Manafi, M.; Perry, J. D.; Pincus, D. H. *Journal of Microbiological Methods* **2009**, *79* (2), 139-155.
36. Aizawa, K. *Enzymologia* **1939**, *6*, 321–324.
37. Lederberg, J. *Journal of Bacteriology* **1950**, *60* (4), 381-392.
38. Barrnett, R. J.; Seligman, A. M. *Science* **1951**, *114* (2970), 579-582.
39. Kiernan, J. A. *Biotechnic & Histochemistry* **2007**, *82* (2), 73-103.
40. Sadler, P. W.; Warren, R. L. *Journal of the American Chemical Society* **1956**, *78* (6), 1251-1255.
41. Ryan, M.; Zaikova, T. O.; Keana, J. F. W.; Goldfine, H.; Griffith, O. H. *Biophysical Chemistry* **2002**, *101-102*, 347-358.
42. Shashidhar, M. S.; Volwerk, J. J.; Hayes Griffith, O.; Keana, J. F. W. *Chemistry and Physics of Lipids* **1991**, *60* (2), 101-110.
43. Schabert, G. G. S., U. P.; Humm, R. R. US patent # 06068988, **2000**.
44. Griffith, O. H. V., J. J.; Kuppe, A., *Methods in Enzymology* **1991**, *197*, 493-502.
45. Taguchi, R.; Ikezawa, H. *Archives of Biochemistry and Biophysics* **1978**, *186* (1), 196-201.
46. Aguirre, P. M.; Cacho, J. B.; Folgueira, L.; López, M.; García, J.; Velasco, A. C. *Journal of Clinical Microbiology* **1990**, *28* (1), 148-149.
47. Orden, B.; Franco, A.; Juárez, E.; González, A.; Caravaca, L. *European Journal of Clinical Microbiology & Infectious Diseases* **1993**, *12* (8), 630-633.
48. Ruiz, J.; Sempere, M. A.; Varela, M. C.; Gomez, J. *Journal of Clinical Microbiology* **1992**, *30* (2), 525-526.
49. Cooke, V. M.; Miles, R. J.; Price, R. G.; Richardson, A. C. *Appl. Environ. Microbiol.* **1999**, *65* (2), 807-812.
50. Gaillot, O.; Di Camillo, P.; Berche, P.; Courcol, R.; Savage, C. *Journal of Clinical Microbiology* **1999**, *37* (3), 762-765.
51. Manafi, M.; Kneifel, W.; Bascomb, S. *Microbiol. Mol. Biol. Rev.* **1991**, *55* (3), 335-348.
52. Torlak, E.; Akan, İ. M.; Gökmen, M. *Letters in Applied Microbiology* **2008**, *47* (6), 566-570.
53. Tryland, I.; Fiksdal, L. *Appl. Environ. Microbiol.* **1998**, *64* (3), 1018-1023.
54. Bettelheim, K. A. *Journal Of Applied Microbiology* **1998**, *85* (3), 425-428.

CHAPTER 5. DEVELOPMENT OF A PAPER-BASED ANALYTICAL DEVICE FOR COLORIMETRIC DETECTION OF SELECT PATHOGENIC BACTERIA IN FOOD

5.1 CHAPTER OVERVIEW

Foodborne pathogens are a major public health threat and financial burden for the food industry, individuals, and society, with an estimated 48 million cases of food related illness occurring in the United States alone each year.[1] Three of the most important causative bacterial agents of foodborne diseases are pathogenic strains of *Escherichia coli, Salmonella* spp*.,* and *Listeria monocytogenes*, due to the severity and frequency of illness and disproportionally high number of fatalities. Their continued persistence in food has dictated the ongoing need for faster, simpler, and less expensive analytical systems capable of live pathogen detection in complex samples. Current gold standard culture techniques for detection and identification of foodborne pathogens require 5-7 days to complete. Major improvements to the cultural detection techniques have been introduced in the recent years, including polymerase chain reaction (PCR). However, these methods can be tedious; require complex, expensive instrumentation; necessitate highly trained personnel; and are not easily amenable to routine screening of food due to cost. In response to the need for improved food quality methods, a paper-based analytical device (μPAD) has been developed for the rapid (8-12 hrs) detection of *E. coli* O157:H7*, Salmonella* Typhimurium*,* and *Listeria monocytogenes* in food samples as a 'first pass' screening system. Paper-based analytical devices encompass a new technology that provides a simple, portable, and

inexpensive platform for a variety of analytical applications. In this work, a paper-based microspot assay was created using wax printing on filter paper. The cost estimate of performing a single assay for all three pathogens is $1.35, including reagents. Detection is achieved by measuring the color change when an enzyme associated with the pathogen of interest reacts with a chromogenic substrate. When combined with standard enrichment procedures, the method allows for a reduced enrichment time of 12 hours or less and is capable of detecting bacteria in concentrations in inoculated ready-to-eat (RTE) meat as low as 10^1 CFU/cm^2. This work is publication in *Analytical Chemistry*.

5.2 INTRODUCTION

Bacterial contamination of food is a human health threat of global proportions. While the incidence of foodborne disease across the globe may be difficult to assess, the World Health Organization estimates 1.8 million die of enteric diseases every year.[2] In the US alone, the Center for Disease Control estimates 76 million cases of foodborne illness occur annually, resulting in approximately 325,000 hospitalizations and 5,000 deaths.[1,3] Several species of bacterial pathogens can be responsible for deadly food-related illness, with *Escherichia coli* O157:H7, *Listeria monocytogenes*, and *Salmonella* Typhimurium being three of the most prevalent.[4-6] Existing pathogen detection and identification methods and protocols employed by the food industry have not proved to be adequate in preventing foodborne illness. Currently, samples must be sent to a centralized laboratory for costly and time-consuming analysis. For an industry dealing with high consumer demand and limited shelf-life products, the current food quality and safety assessment process is a major hindrance. Rapid, easy to perform and cheap detection technologies are incrementally sought after and implemented by the food industry. The

need for faster, simpler and cheaper detection methods for pathogenic bacteria is not unique to food protection, but it may also find utility in other fields of public health, water safety, and quality in both developed and developing nations. In response to the need for such detection techniques, a simple detection system, involving a paper-based analytical device, has been developed for measuring the presence of live bacteria in food. The paper-based microspot device presented here has potential for use as a first level of screening for foodborne pathogens in food processing facilities, and could be used in conjunction with culture or molecular-based methods for final identification and confirmation.

The current gold standard for bacterial detection and enumeration remains the culture method. While continuous improvements in sensitivity and specificity have been slowly introduced over the years, including the incorporation of chromogenic agars, the culture approach still remains excessively time-consuming for routine analysis in the food industry. Culture methods require 5-7 days for preenrichment, enrichment, selective plating, identification and confirmation, at which point a contaminated product could have already reached the consumer.[7,8] A specific example includes the identification and differentiation of *L. monocytogenes* in food using the chromogenic agar, RAPID'L.Mono, a more selective agar base than what is used in standard culture methods. The procedure involves enriching a food sample for 24 hr, followed by 24 hr plate incubation.[9] Finally, the plate must be read, requiring a minimum of 48 hrs before a result is obtained. Moreover, the standard culture methods are neither simple nor portable making their use at the plant level cumbersome and limited. Molecular-based detection methods have been recently introduced to foodborne pathogen detection protocols as exemplified by polymerase chain reaction (PCR), which can be used to detect pathogens with high specificity and sensitivity. Commercially available systems capable

of detecting multiple pathogens are produced by multiple suppliers as a testament to the power of this technique. Despite the wide use of PCR and (real-time PCR), the method is still limited by the need for costly instrumentation and highly trained personnel.[10] Additional DNA purification and isolation are often necessary as well, further increasing the analysis time and expense. Furthermore, most PCR-based methods do not provide accurate microbial viability data as the amplified nucleic acids may originate from dead cells. As a result, biological enrichment is still needed to determine live versus dead cell counts, and overall analysis time ranges from 18-48 hrs depending on the bacterial species and the media used for enrichment.

Molecular-based detection methods may provide slightly faster results; however, the required instrumentation is still complex. Recent PCR-based lab-on-a-chip systems[11] and immunoassay-type biosensors[12,13] have been developed and are attractive platforms due to their compact size and the ability to use sensitive molecular detection. For example, Park et al. introduced a chemiluminescent immunoassay for selective detection of *S.* Typhimurium in environmental water samples.[12] The authors showed detection in the 10^3-10^6 CFU/mL range; however, analysis is performed on a lateral flow strip composed of four different membranes that must be functionalized individually for each step of analyte capture and detection. Sippy et al. developed a lateral flow immunoassay on nitrocellulose membranes for capture of *E. coli* O55, a model organism, with subsequent amperometric detection. Electrochemical detection relied on the consumption of hydrogen peroxide by bacterial catalase, providing 100 CFU/mL detection limits but also exhibiting low capture efficiencies (71%-25%).[13] In 2009, Beyor et al. developed an integrated device for on-chip PCR and subsequent capillary electrophoretic analysis for pathogen detection.[11] PCR in the microchip format is advantageous as it allows for reduced sample volumes and shorter thermal cycles. While the detection limits for *E. coli* O157:H7 were

as low as 200 CFU/mL, the device incorporates complex features fabricated through multilayered glass-PDMS stacking and requires an external power source for operation. While all of these approaches have merits for sensitivity and selectivity, they still require more complex instrumentation and analysis times that are limited by enrichment. A simple visual test that can provide direction for further testing is still needed.

In the past few years, paper-based analytical devices (μPADs) have become attractive alternatives to conventional microfluidics as patterned paper is an inexpensive assay platform.[14] In addition to cost, some of the advantages of μPADs include small (μL volumes and ng masses) sample and reagent consumption, simple operation and manufacturing, portability, disposability, an extensive application base, a high surface area for analyte capture and visualization, and potential for use in scenarios where minimal instrumentation is required.[15] A number of fabrication techniques have also been established for μPADs, including photolithography,[14,16] inkjet printing,[17] stamping,[18] cutting,[19] screen-printing,[20] and wax printing.[21] Wax printing is the fastest, simplest fabrication method established to date. A wax printer employs melted wax in the same way an ink jet printer uses ink cartridges. A hydrophobic barrier is created using the wax, enabling spatial control over fluid transport caused by the capillary flow in the paper. Generally, μPADs encompass two fundamental design schemes: fluidic networks and spot tests. Fluidic paper devices describe a fluidic network on paper where transport of sample and/or reagents is carried out through capillarity.[15,22,23] In recent years, this style of device has advanced from simple lateral flow types[24] to include more elaborate, three-dimensional designs.[25] The paper-based spot test provides utmost simplicity in which sample and regents are stationary within the device.[26-28]

The paper-based tool described here consists of a 7 mm-diameter spot array based on a simple well-plate design. Colorimetric assays are conducted in the paper "wells," utilizing the interaction between species-specific enzymes and chromogenic substrates.[29] The presence of pathogenic bacteria is indicated by a color change, a result that may be easily interpreted by the user without the need for complex instrumentation. Additionally, semi-quantitative analysis is performed by measuring the grey intensity of the colored spots using ImageJ software after capturing an image using an office scanner.[30] The use of synthetic substrates for the colorimetric or fluorogenic detection, identification, and enumeration of bacterial species is commonplace in microbiological techniques, particularly chromogenic agar media and real-time PCR; however, utilizing these chemistries in a paper-based assay has not been fully optimized.[31,32] In this format, we believe the paper-based microspot test provides simplicity, reduced analysis time, and a cost-effective means of pathogen detection as a tool to indicate the need for further testing. Carrilho et al. estimate the cost of printing a single 8.5 x 11 in sheet of Whatman #1 filter paper with a wax printer to be $\$0.001/cm^2$.[19,33] Using the 7 mm-diameter spot size, approximately 275 devices can be printed on a single 8.5 x 11 sheet for an approximate cost of $0.002/device. The total cost estimate of a single spot assay for all three pathogens is $1.35, where the bulk of the expense comes from the colorimetric substrate used for *L. monocytogenes* determination ($1.28/spot). Here, use of the microspot test system is optimized for detection of three common foodborne pathogens. Once optimized, the system is used to detect bacteria in concentrations as low as 10^1 CFU/cm^2 when sampled from ready-to-eat meat followed by standard enrichment procedures. The overall analysis time ranged from 8-12 hrs including enrichment and detection with the potential to achieve more rapid detection upon improvement of enrichment procedures.

5.3 EXPERIMENTAL

5.3.1 Materials

HEPES, bovine serum albumin, phosphatidylinositol-specific phospholipase C, β-galactosidase, esterase, 5-bromo-4-chloro-*myo*-inositol phosphate, chlorophenyl red β-galactopyranoside, and 5-bromo-6-chloro-3-indolyl-caprylate were purchased from Sigma (St. Louis, MO). Tryptic soy broth, yeast extract, and lambda buffer [100 mM NaCl, 8mM MgSO4·7H2O, 50 mM Tris-HCl (pH 7.5)] were purchased from Becton, Dickinson and Company (Franklin Lakes, NJ). Bacterial strains used here were: *Escherichia coli* O157:H7 SPM0000422 (Lawrence Goodridge Laboratory Strain Collection, obtained from USDA), *Salmonella enterica* subs. *entrica* serovar Typhimurium (ATCC 14028), and *Listeria monocytogenes* FSL C1-115 (1/2a, ILSI, human sporadic). MacConkey-sorbitol agar base, cefixime tellurite (CT) supplement, XLT-4 agar base, Tergitol-4 supplement, PALCAM agar base, and PALCAM supplement were purchased from Remel Inc (Lenexa, KS). Whatman #1 filter paper was purchased from Fisher Scientific (Pittsburgh, PA). A Xerox Phaser 8860 series wax printer was used for fabrication of μPAD devices.

5.3.2 Device Fabrication

Paper-based devices were fabricated using wax to define device features and control fluid flow using previously described methods.[33] The paper devices were developed using graphic software, CorelDRAW, and printed on Whatman #1 filter paper using the Xerox Phaser wax printer. Throughout this work, an array of 7 mm-diameter circles, with 4 pt line thickness, was employed. Since this configuration of circles conceptually resembles a well-plate, the 7 mm devices were termed well devices. Once printed, devices are placed on a 150˚C hot plate for 5 min in order to melt the wax through the paper, creating a three-dimensional

hydrophobic barrier. On the printed side of the paper, 2 in-wide clear packaging tape was placed to enhance control over fluid flow and prevent leaking during the assay, while the reverse side was used for application of reagents and sample.[34]

5.3.3 Characterization and Optimization of μPADs

To evaluate enzyme activity on paper and determine the optimal spot size, arrays of paper wells were fabricated with diameters ranging from 5 to 12 mm, with 5 mm being the smallest diameter capable of containing the 30 μL reaction volume. Using the β-galactosidase assay as a model system, a study was conducted to determine differences in the intensity of the enzymatic product on paper for various spot diameters. In this experiment, the same ratio of enzyme to substrate concentration was applied to each well and, once dry, the grey intensity of each well was measured. (Throughout this work, semi-quantitative information is gained by measuring the grey intensity of the wells from a digital image. The details of the data analysis are discussed below.) Next, the concentration of enzyme was varied across the range of well sizes to determine a saturation point for the assay as a function of available surface area. Again, the wells were allowed to dry and the grey intensities were measured for each spot.

5.3.4. Data Analysis

The μPAD devices provide a suitable platform for qualitative analysis by simply visualizing a color change on paper, providing an easily interpreted 'yes' or 'no' result. Furthermore, the paper substrate provides excellent contrast for observing the formation of chromogenic products. In addition to a simple, qualitative test, semi-quantitative information can be gained using graphic software. Digital images of the device arrays were acquired using a Xerox scanner after the spots had dried (approximately 2 hr for drying), and the maximum grey intensity of each well was measured using Image J software. Using Image J, the scale can be set,

defining the precise diameter of the wells. Next, the digital image is converted to 32-bit, grey scale and inverted so that grey intensity is measured in a normal mode (lowest to highest intensity). Using the circle tool, a circle is drawn that encompasses the interior of the well device, and the average grey intensity is measured over the circumscribed area which is normalized by the set scale. The circle can then be used to measure all wells in the array. A step-by-step explanation of the semi-quantitative analysis using Image J is presented in Figure 5.1.

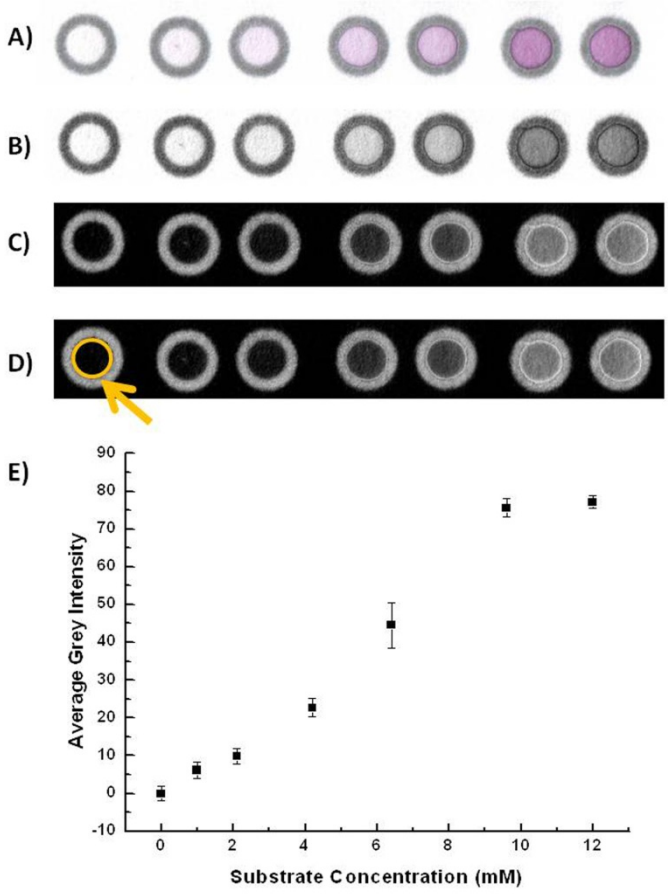

Figure 5.1. Protocol for ImageJ analysis. A) A digitial image of the paper device is generated using a flat-bed scanner. B) Using ImageJ, the image is converted to 32-bit grey scale. C) The image is then inverted. D) The spot area is selected individually, and the grey intensity is measured.

5.3.5 Characterization of Bacteria-Specific Enzymes

The three enzyme-substrate pairs used in this work were β-galactosidase with chlorophenyl red β-galactopyranoside (CPRG) for *E. coli* determination,[35,36] phosphatidylinositol-specific phospholipase C (PI-PLC) with 5-bromo-4-chloro-*myo*-inositol phosphate (X-InP) for *L. monocytogenes* determination,[37-39] esterase with 5-bromo-6-chloro-inositol caprylate (magenta caprylate) for *S. enterica* determination.[40] In the presence of the specific enzyme, CPRG changes from yellow to red-violet in color, X-InP changes from colorless to blue, and magenta caprylate changes from colorless to purple. Initial characterization of each assay involved optimization studies using the pure enzymes. (A schematic of each enzymatic reaction including the final colorimetric product is shown in Chapter 4.) Upon receipt of the enzymes, stock solutions containing 1 U/mL concentration were made and used throughout the remainder of this work. Aliquots were frozen until use and then warmed to room temperature. Optimization of substrate concentration and buffer pH was determined using an array of 7 mm diameter devices. In all studies, the paper devices were placed in petri dishes upon the application of sample and reagent solutions and kept in a 37˚C incubator, and due to the photosensitivity of magenta caprylate, petri dishes housing this particular assay were covered in foil to prevent exposure to light. It should be noted that covering the dish with foil did increase the drying time for the assay from 2 hr to approximately 3 hr.

5.3.6 Live Bacterial Assays

For the detection of β-galactosidase, esterase, and PI-PLC activity from live cultures, a number of factors were considered. For example, in order to free the enzyme from *E. coli* O157:H7 for subsequent colorimetric reaction with CPRG, equivalent 500 µL bacteria samples, grown overnight in broth, were lysed via probe sonicator. With the sonicator set to 5 W, 22 kHz,

various sonication durations were evaluated, ranging from 10 to 120 s. Immediately after sonication, each *E. coli* O157:H7 sample was tested on the paper device for β-galactosidase activity. Using this method, an optimal sonication time of 20s was determined.

In experiments involving pure cultures, a single colony was collected using a 10 μL sterile loop and transferred to a test tube containing growth media, tryptic soy broth with yeast extract (TSB-YE). In an effort to reduce analysis time, various enrichment volumes were studied. Previous studies have shown that conducting a low-volume enrichment (< 10 mL of media) aids in preconcentration of cells, and therefore, reduces the required incubation time.[41] A study was conducted to determine the preconcentration effects of various enrichment volumes for the determination of the species-specific enzymes. An *E. coli* O157:H7 culture, collected as a single colony, was transferred to 1 mL buffer and vortexed. Next, 100 μL aliquots were diluted in 10, 5, and 1 mL growth media and allowed to enrich for 5 hr with shaking. After enrichment, a 500 μL aliquot was collected from each sample, sonicated for 20 s, and tested on the paper device with CPRG. As expected, a more intense color change resulted from the smaller volume enrichments. Throughout the optimization studies of live bacterial assays, TSB-YE enrichment media was used in volumes as low as 0.5 mL.

For the optimization of the paper-based device with live *E. coli* O157:H7, *L. monocytogenes*, and *S.* Typhimurium, separate test tubes containing 2 mL of TSB-YE were inoculated with a single, isolated bacterial colony, placed in a 37˚C incubator, and allowed to enrich with shaking. At various time periods, a 500 μL sample of growth medium was collected from the tubes for each bacterium and analyzed using the paper device. Additionally, total plate counts, using tryptic soy agar with yeast extract (TSA-YE), were employed to obtain primary reference data for viable bacteria counts and for method validation. By analyzing each sample

over several hours at set time intervals, the shortest enrichment time necessary for the determination of a pure culture was estimated for each assay. Since the composition of one transferred bacterial colony may contain millions of viable cells, the shortest enrichment time can only be approximated and could fluctuate depending on the number of cells present initially as well as environmental factors that affect enzyme activity.

The limit of detection was also determined for each assay. Isolated colonies were enriched for overnight, to ensure a high concentration of cells, and serial dilutions were made in lambda buffer. A sample of each dilution was tested on the paper devices and plated for validation of bacterial cell concentration.

Finally, a cross-reactivity study was performed using pure cultures. Using an array of nine 7 mm wells on paper, each row was spotted with one of the three bacterial species in a concentration of approximately 10^9 CFU/mL and each column was spotted with one of the three colorimetric substrates so that cross-reactivity among the different enzyme-substrate pairs could be analyzed.

5.3.7 Food Sample Analysis

To demonstrate proof-of-concept, samples of bologna were inoculated with live bacteria and analyzed using the paper-based device. A 10 cm^2 area was marked with a permanent marker on each bologna sample. The samples were spot-inoculated with 10^3 CFU/cm^2, 10^2 CFU/cm^2, and 10^1 CFU/cm^2 concentrations of live *E. coli* O157:H7*, L. monoctyogenes,* and *S.* Typhimurium. The initial concentrations of the bacteria were confirmed via plating onto TSA-YE following serial 10-fold dilutions in lambda buffer. The food samples were then placed in a sterile biosafety cabinet and allowed to dry for 3 hrs. After the samples had dried, each 10 cm^2 area was swabbed thoroughly using the sampling swab from a Phast Swab device.[42] The swab

was placed directly into the Phast Swab reservoir containing 2 mL of TSB-YE. The tubes were placed in a 37˚C incubator and allowed to enrich with shaking. Aliquots of the media were tested on the μPAD at 0, 4, 8, 10, and 12 hr of enrichment for the presence of *E. coli, L. monocytogenes,* and *S.* Typhimurium and also plated using selective agar for method validation. Since these samples may contain a mixture of microorganisms, the use of selective and/or differential agars is necessary for satisfactory differentiation. Selective plating of *E. coli* O157:H7 was performed using MacConkey-sorbitol agar with CT supplement, PALCAM agar with supplement was used to selectively plate *L. monocytogenes*, and XLT-4 agar with Tergitol-4 supplement was used for plating *S.* Typhimurium. Both the enzymatic assay and plating results from spiked samples were compared with results from negative controls (bologna slices not inoculated with the target bacteria). All experiments involving live bacteria were carried out in a BSL-3 level biosafety cabinet using aseptic techniques to prevent infection.

5.4 RESULTS AND DISCUSSION

5.4.1 Device Optimization

The optimal well size was investigated for this work using the β-galactosidase assay as a model system. Similar to all enzymatic reactions discussed here, the hydrolysis of CPRG via β-galactosidase requires a certain reaction period and, therefore, a sufficient reaction volume in which to take place. If the paper well dries before the reaction is completed, enzyme activity is dramatically reduced or completely hindered. The reaction kinetics for this assay are relatively fast, with product formation within approximately 15 min; however, a total volume of 30 μL on the paper wells was deemed optimal for all three assays, with a drying time of approximately 2 hr. With a total reaction volume of 30 μL, well sizes ranging from 5 to 12 mm were tested.

First, a constant amount of β-galactosidase and CPRG was applied to each well to determine changes in intensity with well diameter. The results of this study are shown in Figure 5.2. A linear correlation is observed between grey intensity and well diameter (R^2 = 0.9864), and the greatest intensity is obtained from the smallest surface area (5 mm).

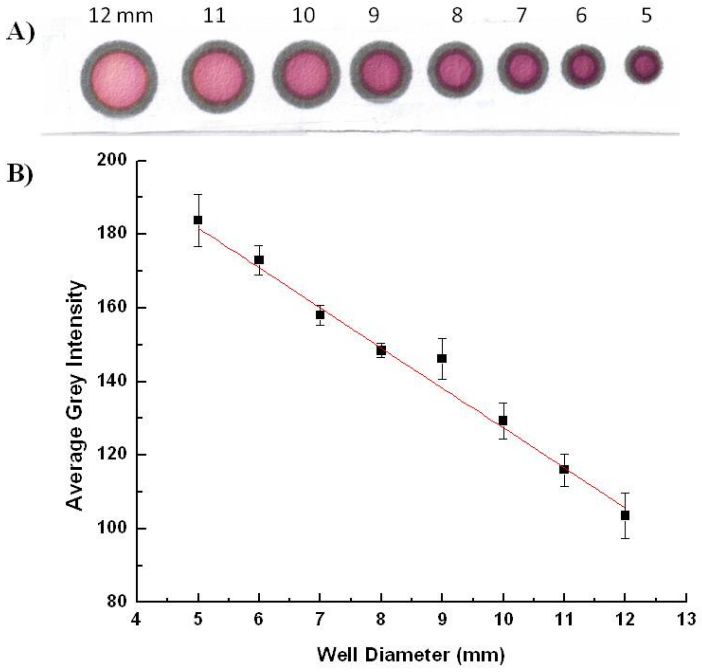

Figure 5.2. Characterization and optimization of spot size using the β-galactosidase assay as a model system. A) Digital image of β-galactosidase reaction with CPRG on paper spot tests with spot diameters from 12 to 5 mm. A darker, more intense color is observed for smaller well sizes since the reaction is confined to a smaller surface area. B) Average grey intensity measure (n = 4) for each well size versus the well diameter in mm. A linear relationship is observed for this system with R^2 = 0.9864.

Next, the concentration of β-galactosidase was varied from 0.05 to 0.8 μg/mL for each well size. In Figure 5.3 the varying color intensities for both spot size and enzyme concentration can be seen as well as a plot of grey intensity versus well diameter. According to the grey intensity analysis, surface saturation is observed for wells smaller than 7 mm in diameter causing

a plateau in grey intensity. Based on this information, the 7 mm well diameter was considered the optimal spot size for this work.

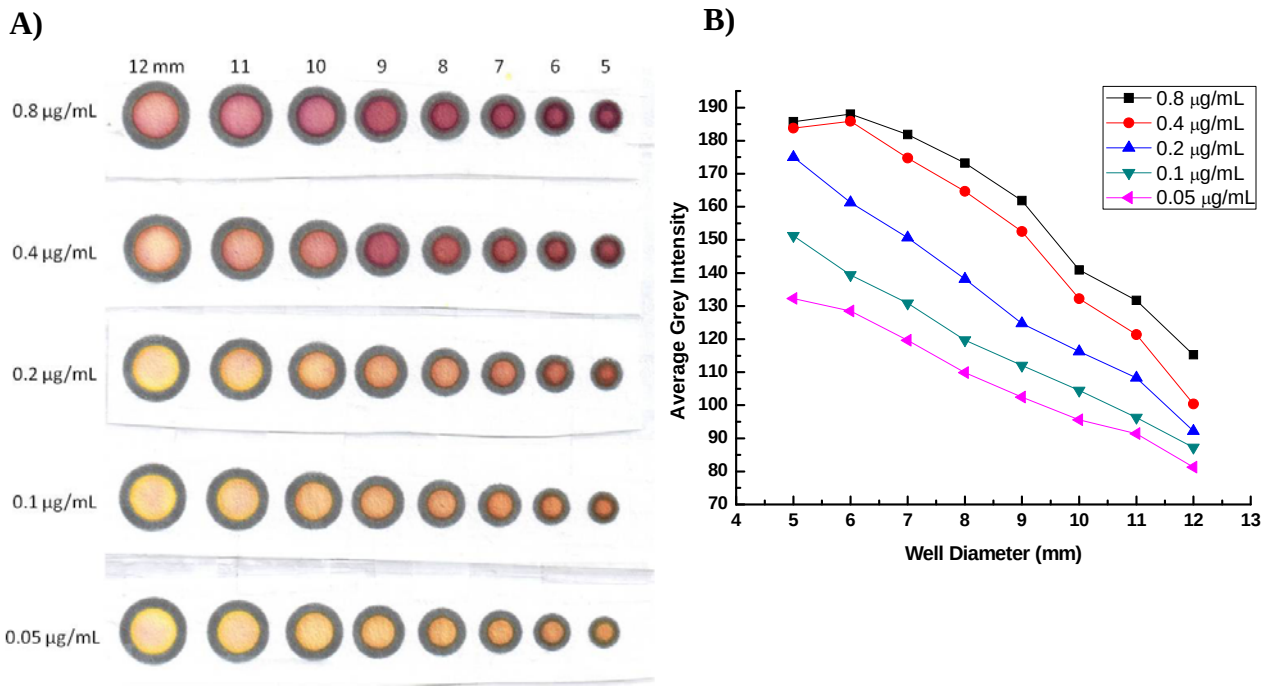

Figure 5.3. Characterization and optimization of spot size using β-galactosidase assay as a model system. A) Scanned image of wells ranging from 12 to 5 mm in diameter and enzyme concentrations ranging from 0.8 to 0.005 µg/mL. B) Plot of grey intensity versus well diameter for each enzyme concentration. Greatest intensity is acheieved for smaller well sizes, however, wells smaller than 7 mm in diameter display a surface satruation at the higher concentrations of β-galactosidase, and differences in intensity cannot be distinguished for varying concentrations of enzyme.

5.4.2 Assay Optimization

The optimal substrate concentration was established for each assay using only the enzyme. Various concentrations of substrate were added to the well device while the amount of enzyme and total volume of each well were held constant. The array of well devices was scanned after the enzymatic reactions were complete and wells had dried to generate a digital image and the grey intensity of each spot was measured. A plot of average grey intensity versus

substrate concentration was generated, and a point of saturation for each assay was identified (Figure 5.4). The concentration of substrate at this saturation point was considered the optimal concentration for the system.

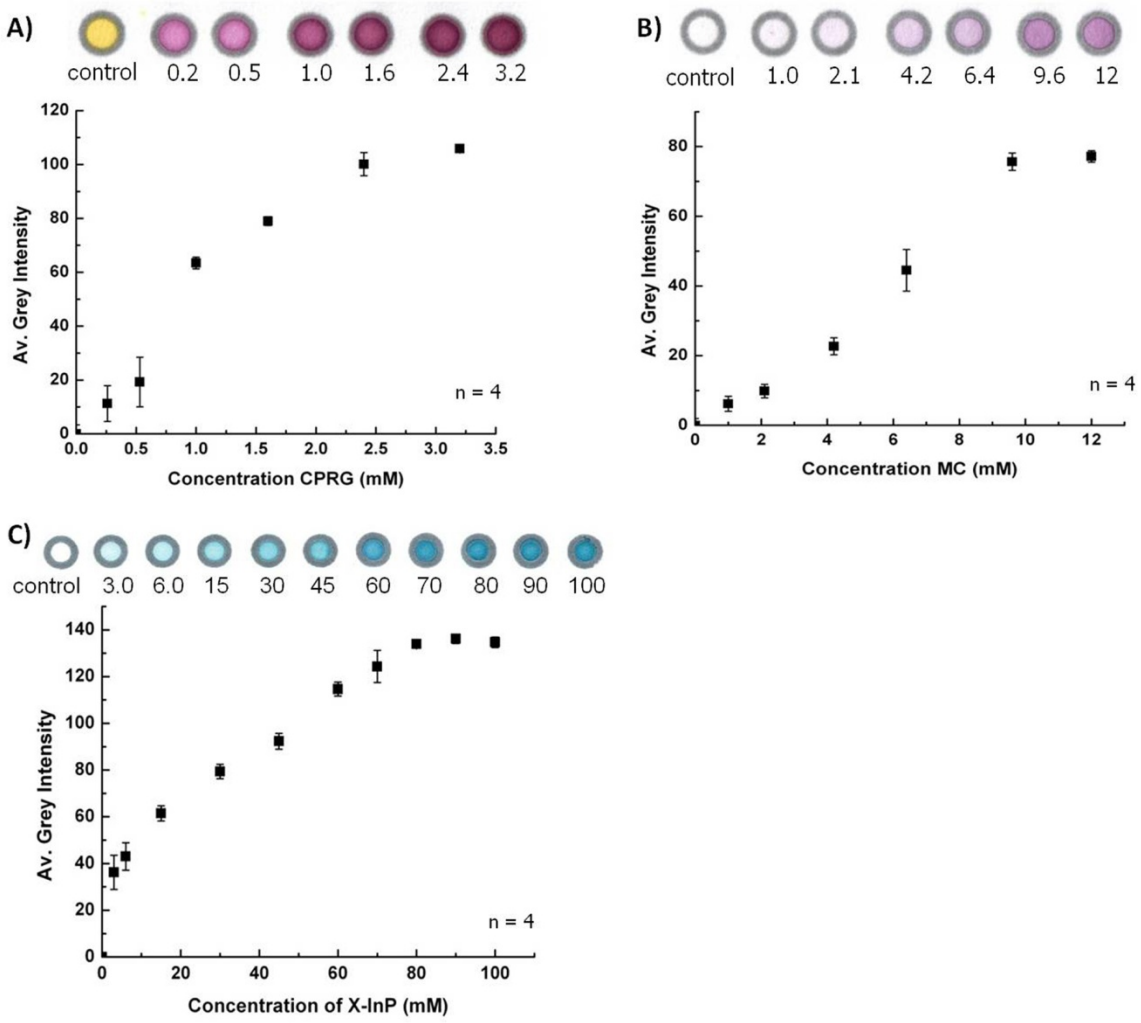

Figure 5.4. Determination of optimal substrate concentrations for A) CPRG B) MC and C) X-InP using the corresponding enzymes. In each paper device, a constant amount of the appropriate enzyme was used while the concentration of substrate (in mM) was increased. A negative control for each assay, in which no enzyme was present, is shown as the first well. The average grey intensity was measured and plotted versus substrate concentration, where each data point represents the average (± standard deviation) grey intensity of four measurements. The optimal concentration was determined from the maximum grey intensity generated for each assay.

Using the optimal substrate concentrations, a limit of detection was determined for each enzyme (Figure 5.5). The substrate concentration was held constant while the concentration of enzyme decreased until no color formation was measured. The limit of detection, defined as the lowest detectable amount of enzyme that can be distinguished from the control, for β-galactosidase, esterase, and PI-PLC were 0.01 ± 0.01 μg/mL, 0.23 ± 0.08 μg/mL, and 0.12 ± 0.08 μg/mL (n= 4) respectively. A logarithmic trend is exhibited for each assay which can be related to the measurement of reflectance from a limited surface area (7 mm diameter spot). Non-linear data correlations are common to colorimetric assays measured from digital images[43] and paper-based analytical devices and are the result of surface saturation at high concentrations of product.[44,45] Furthermore, in Michaelis-Menton enzyme kinetics, the reaction rate increases and asymptotically approaches the maximum velocity as the enzyme is saturated with substrate molecules.[46]

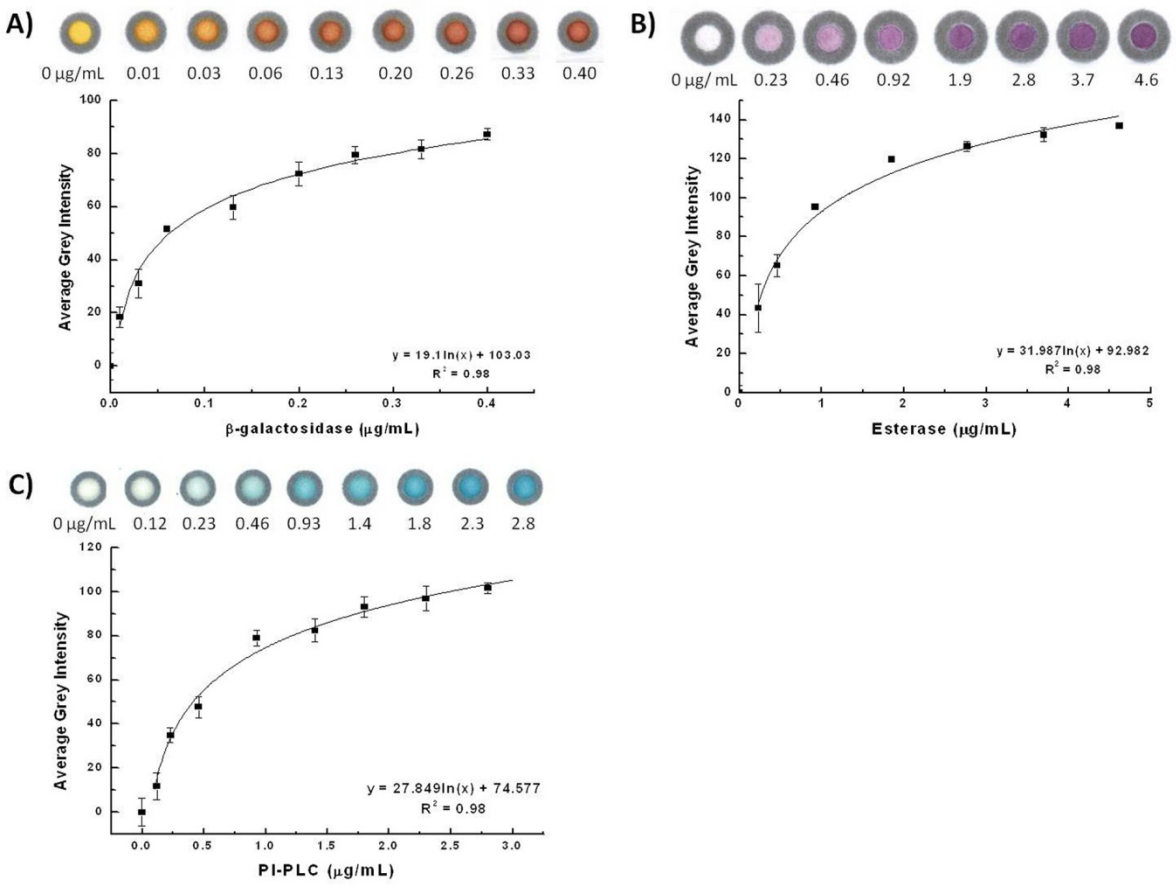

Figure 5.5. Determination of lowest detectable amount of A) β-galactosidase B) esterase and C) PI-PLC enzymes using optimal substrate concentrations. Average grey intensities are plotted vs the amount of enzyme in each spot (± standard deviation of n = 4 measurements), and in each assay data are fitted with a logarithmic regression.

5.4.3 Analysis of Live Bacteria

Using pure cultures, each assay was optimized for analysis of live bacteria, with particular consideration paid to reducing the enrichment duration and investigating the need for cell lysis. In the determination of PI-PLC and esterase from *L. monocytogenes* and *S.* Typhimurium, respectively, the enzymes are either produced on the exterior of the cell or secreted by the cell into the growth media, allowing the enzymatic reactions to occur without the need to lyse cells. However, in the determination of β-galactosidase from *E. coli* O157:H7, the

enzyme is generated inside the cell and is not secreted by the microorganism. Probe sonication was chosen as the lysis method since it provides fast, simple, non-chemical cell rupture without denaturation of the target enzyme and could easily be implemented in the field. Lysis of *E. coli* O157:H7 cells is relatively easy since the Gram-negative bacteria lack the rigid peptidoglycan layer in their cell wall.[47, 48] Samples of *E. coli* O157:H7 that were sonicated for 10 to 45 s produced the red-violet color change associated with the enzymatic hydrolysis of CPRG as shown in Figure 5.6a. Sonication durations longer than 45 s did not produce a color change, most likely due to denaturation of the enzyme from extended sonication periods and/or the heat generated from the process. A sonication duration of 20 s was chosen for the remainder of the work discussed here since this time period allows for sufficient lysing of cells and agrees with literature values.[48] Samples of *L. monocytogenes* and *S.* Typhimurium were also sonicated for 20 s and tested on the paper device to ensure sonication does not hinder the colorimetric detection of these species.

Figure 5.6. Optimization of the live *E. coli* assay on the well devices. A) Equivalent *E. coli* O157:H7 samples are lysed using various sonication durations (in s) with subsequent colorimetric detection on the paper device. B) Enrichment volume study with live *E. coli* O157:H7. Aliquots of *E. coli* cells were diluted in 10, 5, and 1 mL TSB growth media and enriched for 5 hr and then tested β-galactosidase activity. The bacteria grown in 1 mL growth media gave a more distinct and intense color change, indicating the enzyme was more concentrated.

In the determination and identification of live bacteria, current methods rely on a combination of cultural enrichment followed by biochemical and serological tests.[49] Enrichment media provides nutrients for bacteria, encouraging growth to the critical threshold concentration required for detection. Additionally, cultural enrichment can provide a level of selectivity when utilizing specific inhibiting and inducing supplements to allow for selective growth of a target species while simultaneously suppressing the growth of competing microorganisms. In an effort to reduce total assay time, a low-volume enrichment study was performed, evaluating the ability to preconcentrate target enzymes. As anticipated, a more intense color change was observed for the sample enriched in 1 mL growth media since this sample has a greater concentration of enzyme. The results of the colorimetric assay are shown in Figure 5.6b.

Using the low-volume enrichment strategy, inoculates of isolated bacterial cultures were tested on the paper devices at various enrichment time points to provide an estimate of the minimal enrichment time required for detection. The samples were also plated at each time point to confirm microbial numbers and validate the method. Pure culture of *L. monocytogenes* was detected after 5 hr of enrichment and the amount of PI-PLC enzyme detected was 0.18 ± 0.08 μg/mL. *E. coli* O157:H7 was detected after 4.5 hr of enrichment, with 0.016 ± 0.006 μg/mL β-galactosidase present. *S.* Typhimurium was detected after an enrichment period of only 3 hr, and the amount of esterase detected was 0.52 ± 0.06 μg/mL. The results of the enrichment time study are shown in Figure 5.7. While this study demonstrates relatively fast analysis times, longer enrichment periods will likely be required for real food samples due to lower concentrations of target cells and higher background flora.

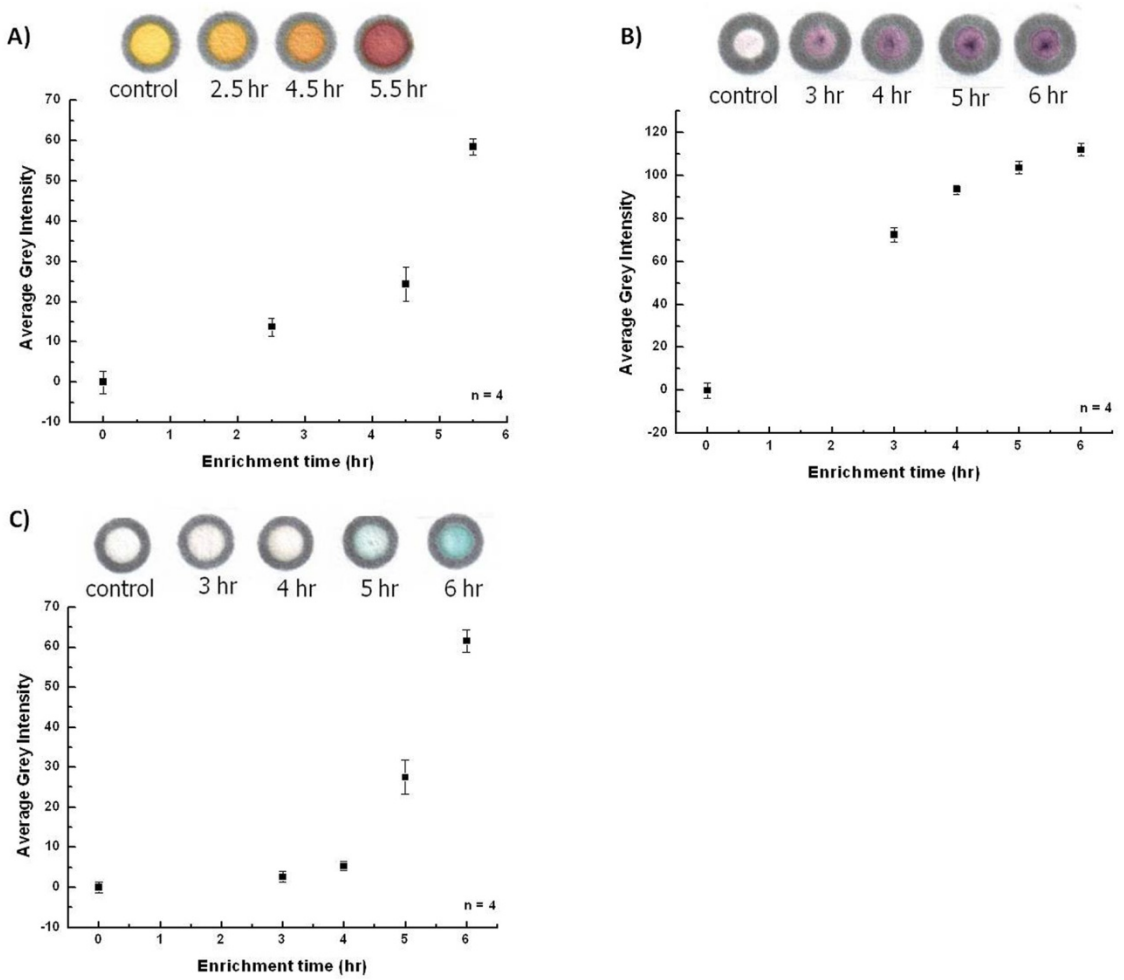

Figure 5.7. Enrichment time study for pure A) *E. coli* O157:H7, B) *L. monocytogenes*, and C) *S.* Typhimurium cultures, showing colorimetric results on the paper devices for each assay as well as measured grey intensities ± standard deviation for n = 4 spots.

5.4.4 Limits of Detection for Live Bacteria

The limit of detection for each assay in a live system was determined using pure bacterial cultures that were enriched overnight. The results of this study, including the grey intensity analysis, are shown in Figure 5.8. The limit of detection (LOD) for esterase occurs at 10^4 CFU/mL concentration of *S.* Typhimurium, while the LODs for β-galactosidase and PI-PLC occur at 10^6 and 10^8 CFU/mL, respectively. These studies provided a baseline for determining

the concentration of bacteria necessary in the enrichment media to allow detection of bacteria from food samples; however, because the bacteria were enriched overnight, an accumulation of the target enzymes can be expected, and the measured enzyme activity from these samples does not directly correlate with the concentration of cells present. Differences in LODs are most likely due to differences in the expressed enzyme levels as well as the molar absorbtivities of the dyes used in these experiments.

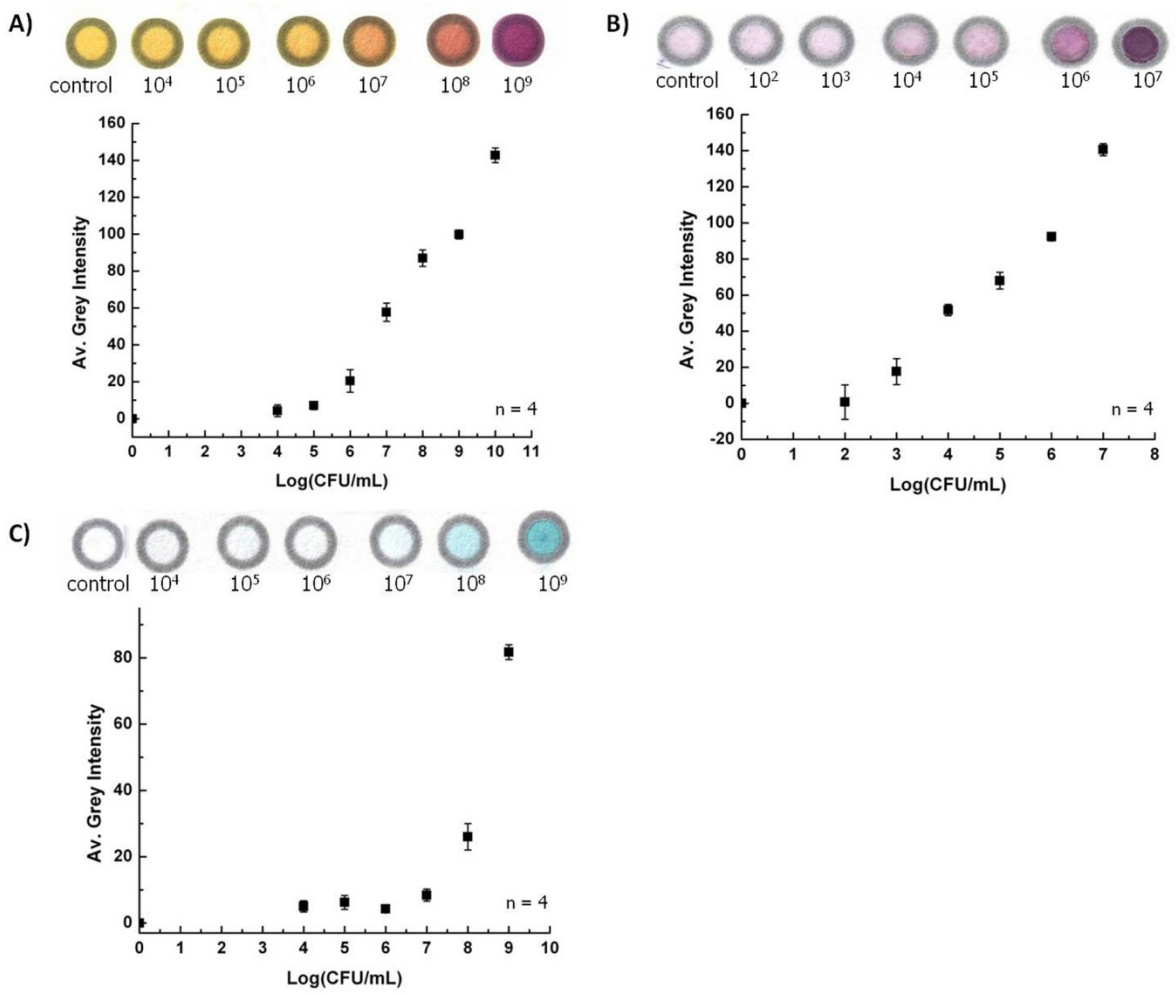

Figure 5.8. Determination of the limit of detection for each live bacterial assay. Pure cultures were enriched overnight with shaking. Serial dilutions were made in buffer from the bacterial samples, and each dilution was tested on the paper device for enzyme activity and average grey intensities were measured. The limit of detection for A) *E. coli* O157:H7 B) *S.* Typhimurium and C) *L. monocytogenes* was estimated to be 10^6, 10^4, and 10^8 CFU/mL, respectively. However, enzyme activity and concentration of cells do not directly correlate since target enzyme may accumulate over the long enrichment period.

5.4.5 Cross-Reactivity

The assays utilized in this work involve enzymes that may be produced by multiple species of bacteria, and therefore, the cross-reactivity between the three assays was studied. The PI-PLC enzyme produced by *L. monocytogenes* is highly selective to this particular species (the only other species of *Listeria* to demonstrate PI-PLC activity is *L. ivanovii*);[9,37,50] however, β-galactosidase is produced by many serotypes of *E. coli* in addition to O157:H7.[32] The selectivity of each assay was evaluated by performing a cross-reactivity study shown in Figure 5.9. For each assay, enzyme activity and color change were only observed when the correct enzyme-substrate pair is present, and none of the three bacterial species exhibited a false positive result. While this result is desirable for the analysis of the three target species, further reactivity studies will be conducted to evaluate the selectivity of each assay for particular serovars.

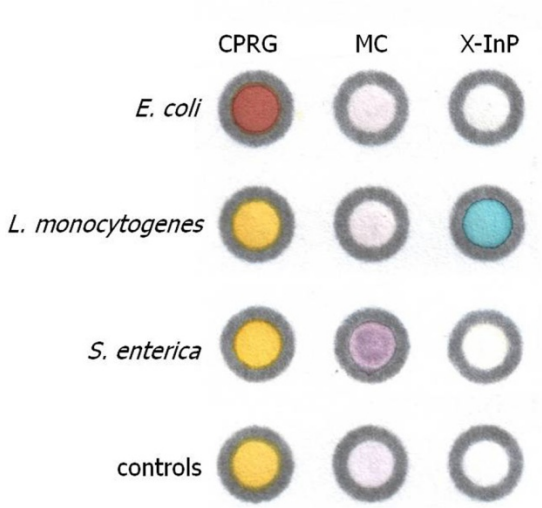

Figure 5.9. Cross-reactivity study testing the selectivity of each enzyme-substrate pair. Each row is spotted with a sample containing a single bacteria species and each column is spotted with a single chromogenic substrate. A color change is observed only when the correct enzyme-substrate pair is present.

5.4.6 Detection of Pathogens from Inoculated Food Samples

Individual ready-to-eat (RTE) meat samples were inoculated with 10^3 CFU/cm^2, 10^2 CFU/cm^2, and 10^1 CFU/cm^2 *E. coli* O157:H7, *L. monocytogenes*, and *S.* Typhimurium to demonstrate proof-of-concept for real samples and the ability of the devices to detect low concentrations of pathogenic bacteria in real samples. The surface of the bologna samples was swabbed to collect bacteria after a 3 hr drying period. The swab technique is less conventional than using a stomacher for sample preparation as it is strictly a surface sampling method; however, swabbing is fast, convenient, easy to perform, and pertinent to a RTE meat sample.[42,51] The 10^1 CFU/cm^2 concentration of the target bacterial species was detected within 8, 10, and 12 hr of enrichment for *S.* Typhimurium, *E. coli* O157:H7, and *L. monocytogenes*, respectively. The colorimetric results and corresponding grey intensity values for the three inoculated samples as well as controls are shown in Figure 5.10. Standard plating on selective agars was also performed to confirm the initial concentration of cells spiked onto RTE samples and to monitor the growth of target species throughout the enrichment process. Results from plating matched the results from the paper devices but required 48 hrs to complete.

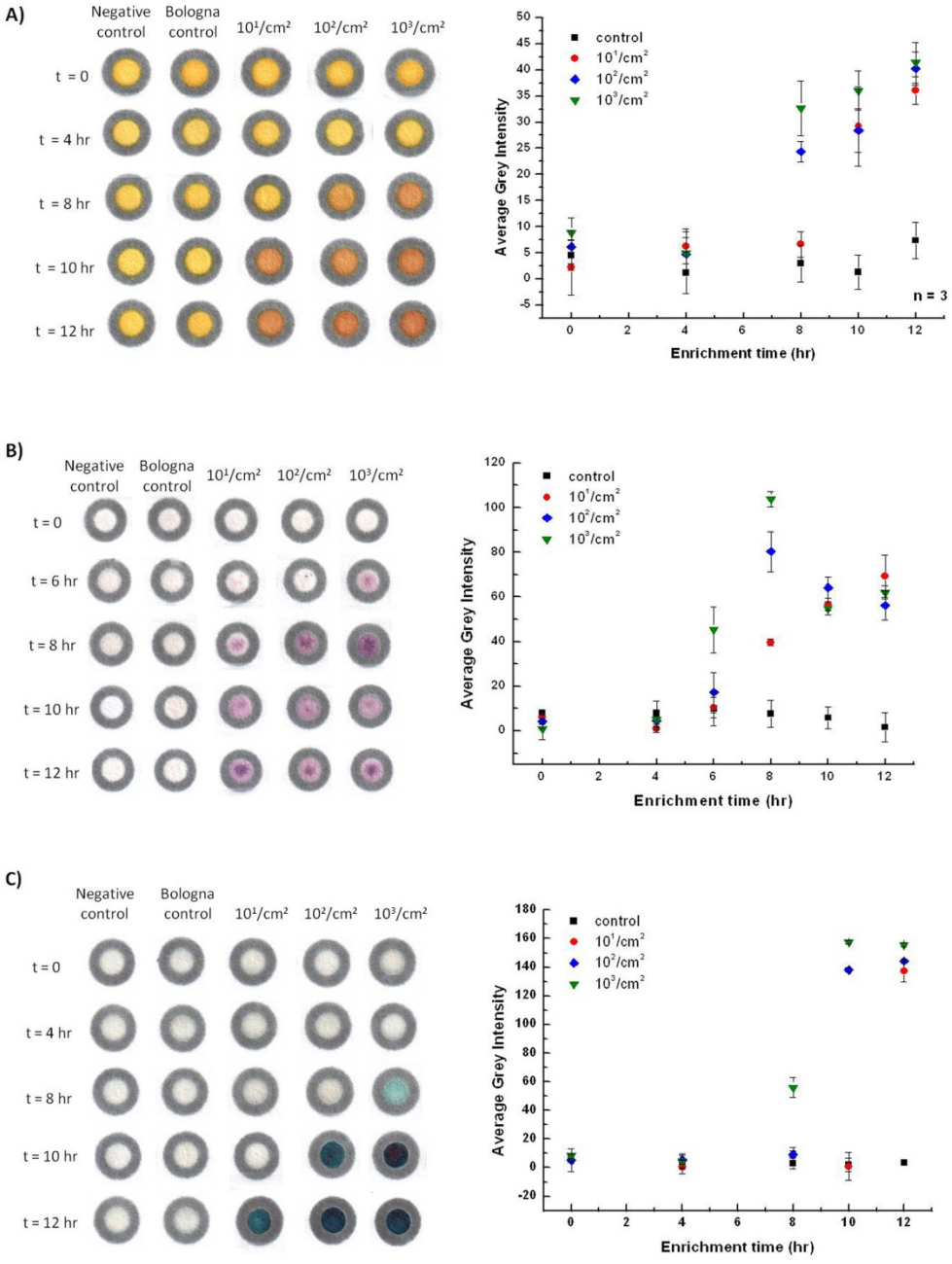

Figure 5.10. Analysis of RTE meat samples spiked with 10^1 CFU/cm^2, 10^2 CFU/cm^2, and 10^3 CFU/cm^2 A) *E. coli* O157:H7 B) *S.* Typhimurium and C) *L. monocytogenes*. Samples tested for enzyme activity after 0, 4, 8, 10, and 12 hr of enrichment.

5.5 CONCLUSIONS

A paper-based microspot assay for the colorimetric determination of pathogenic bacteria in food has been developed. Three enzymatic assays have been optimized for detection of *E. coli* O157:H7, *L. monocytogenes*, and *S.* Typhimurium with significantly reduced enrichment times relative to standard culture techniques. We have demonstrated proof-of-concept for this assay with the analysis of spiked bologna samples and validated our method via plating. The paper device is capable of detecting pathogenic bacteria at a concentration of 10^1 CFU/cm^2 within 8-12 hr of enrichment, depending on the target species. While this concentration range is comparable to that of standard methods, we aim to improve our detection limits by exploring the use of specific inducers to enhance enzyme production as well as utilizing selective enrichment media to inhibit the growth of competing microorganisms. Future development of the device will involve enhanced selectivity of each enzymatic assay, decreased limits of detection, and integration of all three assays for multiplexed analysis in a single sample. The method presented in this work implements a Phast Swab technique that is appropriate for rapid and easy sampling of a RTE meat, however, future work will include the conventional stomacher method for FDA compliance, aiming at 1 CFU/25 g sample.

At present, we believe the device serves as a cost-effective and simple detection method that could be utilized by the food industry as a first level of screening for the presence of pathogenic bacteria without the need for complicated instrumentation. Despite the current limitations with selectivity and sensitivity, we have demonstrated the ability of the paper-based biosensor to detect three pathogenic bacteria species in a real food sample within 8 hr of sampling with detection levels at the target of 10^1 CFU/cm^2, a total analysis time substantially less than currently available techniques rapid screening methods.

This work represents a significant achievement for the field of food quality analysis as well as a novel application of paper-based analytical devices. With a solid foundation established, future directions of this technology are both vast and varied. For example, the incorporation of multi-indicator tests, in which additional enzymatic assays are used concurrently, is one strategy for improving assay selectivity. As mentioned previously, selective enrichment processes can also be used to make the colorimetric tests more species selective. To address sensitivity, electrochemical detection on paper is a very promising future direction. In this format, the same species-specific enzymes can be targeted; however, speed and sensitivity are gained through the use of electrodes fabricated on paper. Also, the development of a paper device designed for multiplexing is under consideration, allowing for higher throughput analysis by performing the three assays simultaneously for a single sample.

5.6 REFERENCES

1. Scharff, R. L. *Health-Related Costs From Foodborne Illness in the United States*; Georgetown University: Washington DC, **2010**.
2. Food Safety and Foodborne Illness. World Health Organization, www.who.int/mediacentre.
3. Kannan, P.; Yong, H. Y.; Reiman, L.; Cleaver, C.; Patel, P.; Bhagwat, A. A. *Foodborne Pathogens and Disease* **2010,** *7* (12), 1551-1558.
4. Batt, C. A. *Science* **2007,** *316* (5831), 1579-1580.
5. Nugen, S.; Baeumner, A. *Analytical and Bioanalytical Chemistry* **2008,** *391* (2), 451-454.
6. Van Kessel, J. A. S.; Karns, J. S.; Lombard, J. E.; Kopral, C. A. *J. Food Prot.* **2011,** *74* (5), 759-768.
7. Brooks, B. W.; Devenish, J.; Lutze-Wallace, C. L.; Milnes, D.; Robertson, R. H.; Berlie-Surujballi, G. *Veterinary Microbiology* **2004,** *103* (1-2), 77-84.
8. Deisingh, A. K.; Thompson, M. *Analyst* **2002,** *127* (5), 567-581.
9. Lauer, W. F.; Facon, J.-P.; Patel, A. *Journal of AOAC International* **2005,** *88* (2), 511-517.
10. Heo, J.; Hua, S. Z. *Sensors* **2009,** *9* (6), 4483-4502.
11. Beyor, N.; Yi, L.; Seo, T. S.; Mathies, R. A. *Analytical Chemistry* **2009,** *81* (9), 3523-3528.
12. Park, S.; Kim, Y.; Kim, Y.-K. *BioChip Journal* **2010,** *4* (2), 110-116.
13. Sippy, N.; Luxton, R.; Lewis, R. J.; Cowell, D. C. *Biosensors and Bioelectronics* **2003,** *18* (5-6), 741-749.
14. Martinez, A. W.; Phillips, S. T.; Butte, M. J.; Whitesides, G. M. *Angewandte Chemie International Edition* **2007,** *46* (8), 1318-1320.
15. Martinez, A. W.; Phillips, S. T.; Whitesides, G. M.; Carrilho, E. *Analytical Chemistry* **2009,** *82* (1), 3-10.
16. Martinez, A. W.; Phillips, S. T.; Wiley, B. J.; Gupta, M.; Whitesides, G. M. *Lab on a Chip* **2008,** *8* (12), 2146-2150.
17. Abe, K.; Suzuki, K.; Citterio, D. *Analytical Chemistry* **2008,** *80* (18), 6928-6934.
18. Cheng, C.-M.; Mazzeo, A. D.; Gong, J.; Martinez, A. W.; Phillips, S. T.; Jain, N.; Whitesides, G. M. *Lab on a Chip* **2009,** *10* (23), 3201-3205.
19. Fenton, E. M.; Mascarenas, M. R.; López, G. P.; Sibbett, S. S. *ACS Applied Materials & Interfaces* **2008,** *1* (1), 124-129.
20. Nie, Z.; Nijhuis, C. A.; Gong, J.; Chen, X.; Kumachev, A.; Martinez, A. W.; Narovlyansky, M.; Whitesides, G. M. *Lab on a Chip* **2009,** *10* (4), 477-483.
21. Lu, Y.; Shi, W.; Jiang, L.; Qin, J.; Lin, B. *Electrophoresis* **2009,** *30* (9), 1497-1500.
22. Fu, E. L.; Ramsey, S.; Kauffman, P.; Lutz, B.; Yager, P. *Microfluid. Nanofluid.* **2011,** *10* (1), 29-35.
23. Osborn, J. L.; Lutz, B.; Fu, E.; Kauffman, P.; Stevens, D. Y.; Yager, P. *Lab on a Chip* **2010,** *10* (20), 2659-2665.
24. Struss, A.; Pasini, P.; Ensor, C. M.; Raut, N.; Daunert, S. *Analytical Chemistry* **2010,** *82* (11), 4457-4463.
25. Martinez, A. W.; Phillips, S. T.; Whitesides, G. M. *P.N.A.S.* **2008,** *150,* 19606-19611.
26. Carrilho, E.; Phillips, S. T.; Vella, S. J.; Martinez, A. W.; Whitesides, G. M. *Analytical Chemistry* **2009,** *81* (15), 5990-5998.
27. Clegg, D. L. *Analytical Chemistry* **1950,** *22* (1), 48-59.
28. Hossain, S. M. Z.; Luckham, R. E.; Smith, A. M.; Lebert, J. M.; Davies, L. M.; Pelton, R. H.; Filipe, C. D. M.; Brennan, J. D. *Analytical Chemistry* **2009,** *81* (13), 5474-5483.

29. Orenga, S.; James, A. L.; Manafi, M.; Perry, J. D.; Pincus, D. H. *Journal of Microbiological Methods* **2009,** *79* (2), 139-155.
30. Rasband, W. S. ImageJ. http://rsb.info.nih.gov/ij/.
31. Lazcka, O.; Campo, F. J. D.; Muñoz, F. X. *Biosensors and Bioelectronics* **2007,** *22* (7), 1205-1217.
32. Manafi, M.; Kneifel, W.; Bascomb, S. *Microbiol. Mol. Biol. Rev.* **1991,** *55* (3), 335-348.
33. Carrilho, E.; Martinez, A. W.; Whitesides, G. M. *Analytical Chemistry* **2009,** *81* (16), 7091-7095.
34. Martinez, A. W.; Phillips, S. T.; Nie, Z.; Cheng, C.-M.; Carrilho, E.; Wiley, B. J.; Whitesides, G. M. *Lab on a Chip* **2010,** *10* (19), 2499-2504.
35. Jacobson, R. H.; Zhang, X. J.; DuBose, R. F.; Matthews, B. W. *Nature* **1994,** *369* (6483), 761-766.
36. Tryland, I.; Fiksdal, L. *Appl. Environ. Microbiol.* **1998,** *64* (3), 1018-1023.
37. Notermans, S. H.; Dufrenne, J.; Leimeister-Wachter, M.; Domann, E.; Chakraborty, T. *Appl. Environ. Microbiol.* **1991,** *57* (9), 2666-2670.
38. Ryan, M.; Zaikova, T. O.; Keana, J. F. W.; Goldfine, H.; Griffith, O. H. *Biophysical Chemistry* **2002,** *101-102*, 347-358.
39. Wei, Z.; Zenewicz, L. A.; Goldfine, H.; Mekalanos, J. J. *P.N.A.S.***2005,** *102* (36), 12927-12931.
40. Goullett, P.; Picard, B. *Journal of General Microbiology* **1990,** *136* (3), 431-440.
41. Bisha, B.; Brehm-Stecher, B. F. *Appl. Environ. Microbiol.* **2009,** *75* (5), 1450-1455.
42. Willford, J. G., L. D. *Food Protection Trends* **2008,** *28* (7), 468-472.
43. Wang, S.; Zhao, X.; Khimji, I.; Akbas, R.; Qiu, W.; Edwards, D.; Cramer, D. W.; Ye, B.; Demirci, U. *Lab on a Chip* **2011,** *11* (20), 3411-3418.
44. Li, X.; Tian, J.; Shen, W. *Analytical and Bioanalytical Chemistry* **2010,** *396* (1), 495-501.
45. Steiner, M.-S.; Meier, R. J.; Duerkop, A.; Wolfbeis, O. S. *Analytical Chemistry* **2010,** *82* (20), 8402-8405.
46. Kisluk, G.; Hoover, D. G.; Kneil, K. E.; Yaron, S. *Food Science and Technology* **2012,** *45* (1), 36-42.
47. Gannon, V. P.; King, R. K.; Kim, J. Y.; Thomas, E. J. *Appl. Environ. Microbiol.* **1992,** *58* (12), 3809-3815.
48. Fykse, E. M.; Olsen, J. S.; Skogan, G. *Journal of Microbiological Methods* **2003,** *55* (1), 1-10.
49. Kim, H.; Bhunia, A. K. *Applied and Environmental Microbiology* **2008,** *74* (15), 4853-4866.
50. Vazquez-Boland, J. A.; Kuhn, M.; Berche, P.; Chakraborty, T.; Dominguez-Bernal, G.; Goebel, W.; Gonzalez-Zorn, B.; Wehland, J.; Kreft, J. *Clin. Microbiol. Rev.* **2001,** *14* (3), 584-640.
51. Saumya, B. *Molecular and Cellular Probes* **2003,** *17* (2-3), 99-105.

CHAPTER 6. CONCLUSIONS AND FUTURE DIRECTIONS

The field of microfluidics, encompassing micro-total analysis systems (μTAS) and other miniaturized technologies, shows great promise for the future. Early research in the field showed the ability to manipulate small volumes of liquids within a microfluidic network, affording valuable capabilities such as minimal sample and reagent consumption, short analysis times, and small footprints for the analytical devices. Over the years, miniaturized devices have extended utility to clinical, environmental, biological, and military defense applications, to name a few. With great potential as a practical technology that may be widely and inexpensively available for this extensive range of applications, research in microfluidics continues, and it is the combined and consorted efforts of engineers, chemists, and biologists that have made possible the achievements the date.

The advent of soft polymers, such as poly(dimethylsiloxane) or PDMS, as a microchip material instigated a rapid development in microfluidic devices. Plastics provided inexpensive, exploratory platforms, where valuable features like pneumatic valves, mixers, and pumps could be developed quickly. A variety of successful polymer-based chips have emerged, leaving their rigid and costly silicon counterparts behind. As we continue to work toward simple, cost-effective devices, the use of paper as a substrate for immunoassays, enzymatic assays, and metal complexation chemistries has reemerged. Today, paper-based analytical devices (μPADs) have far exceeded the capabilities of the traditional paper test strips and pH paper, with multiplexed

and multidimensional analyses that are characterized both qualitatively and quantitatively. Currently, μPADs are developed for numerous clinical tests that have utility in both developed and developing nations. Also, the determination of toxic metals from atmospheric aerosols has been developed on a μPAD device which enables faster air quality analysis for occupational exposure assessments.

The work presented in this dissertation comprises the development of two novel, miniaturized devices for food and water quality analysis. The first is a microchip capillary electrophoresis (MCE) device for the determination of perchlorate in drinking water. The MCE method described in Chapter 2 employs unique surfactant chemistry to selectively retain perchlorate, separating it from competing anions in the sample with detection limits as low as 5.6 ppb. This work was recognized as a noteworthy achievement and published in *Analytical Chemistry* as an accelerated article. The next phase of this project involved the development of an integrated, sample cleanup step to broaden the utility of the MCE system for more complex environmental samples. In Chapter 3, the use of electrostatic ion chromatography (EIC) was explored as a sample cleanup method. Using a conventional ion chromatograph, the migration/retention of a variety of inorganic anions on a surfactant-coated, C18 column was studied. While several obstacles were encountered, including non-linear calibration curves for perchlorate and unsuitably high detection limits of the conductivity detector, a solid foundation for the use of EIC as a sample preparation technique to reduce the ionic strength of complex samples has been established. Future work on this project includes fabrication of a packed-bed in the microchip to further study the retention mechanism in an integrated device. In addition, fabrication of a surfactant-coated monolithic stationary phase in a microchip channel will be investigated.

The second project presented herein describes a μPAD for the colorimetric detection of three foodborne, pathogenic bacteria: *Listeria monocytogenes*, *Escherichia coli* O157:H7, and *Salmonella enterica.* The paper-based spot test was developed for rapid screening of pathogenic bacteria in contaminated foods at the processing plant level. Current methodologies require samples to be analyzed at a centralized laboratory via time-consuming and costly culture methods. While more sophisticated techniques have been established, such as PCR, the instrumentation is complex and highly trained personnel are required. The μPAD described in Chapter 5, provides a simple platform for pathogen detection using species-specific enzymatic assays. The paper devices were tested with real food samples spiked with low concentrations of target bacteria, and results were obtained within 8-12 hr of enrichment. This device represents a significant accomplishment in the field of Analytical Chemistry as well as the food industry. Furthermore, this is the first application of a μPAD for bacterial detection. While further development of the paper device necessitates more selective enrichment and/or detection, the current device can serve as a rapid, cost-effective, and simple tool for first level screening.

The optimization and application of the μPAD for analysis of real food samples presented in Chapter 5 is published in *Analytical Chemistry*. Additionally, the culmination of this work resulted in the filing of a patent. Thus far, great strides have been made, launching the μPAD toward multifarious and promising future directions. Work continues in improving the selectivity of the enzymatic assays. Selective enrichment medium compositions will be investigated to reduce the growth of background microorganisms in complex food samples. Also, additional enzymatic assays will be included in the μPAD design. For example, a β-glucuronidase assay has been optimized for multi-indicator analysis of *E. coli* O157:H7. As mentioned in Chapters 4 and 5, many *E. coli* serovars produce β-galactosidase, which could

cause false positive results on the μPAD. The addition of the β-glucuronidase assay will improve selectivity by adding an elimination factor, since *E. coli* O157:H7 tests negatively for the enzyme. The results of a preliminary study, testing the β-galactosidase and β-glucuronidase activity in a select number of *E. coli* strains is shown in Figure 6.1. Also, this multi-indicator test for *E. coli* O157:H7 shows great potential for analysis of contaminated water samples. Testing for both β-galactosidase and β-glucuronidase activity is a very common technique for determining pathogenic *E. coil* and total fecal coliform counts in drinking and recreational water. We have demonstrated proof-of-concept for the multi-indicator test for *E. coli* as well as the optimized assay for *S. enterica* for analysis of spiked surface water samples (Figure 6.2). Furthermore, work is also being done to develop an electrochemical paper device (ePAD) with screen printed carbon ink and Ag/AgCl electrodes. Electrochemical detection may not only improve selectivity of the device but also reduce overall analysis time. The Henry group has developed ePAD devices for determination of glucose, lactose, and uric acid in human serum as well as detection of toxic metals in water using anodic stripping voltammetry on paper.

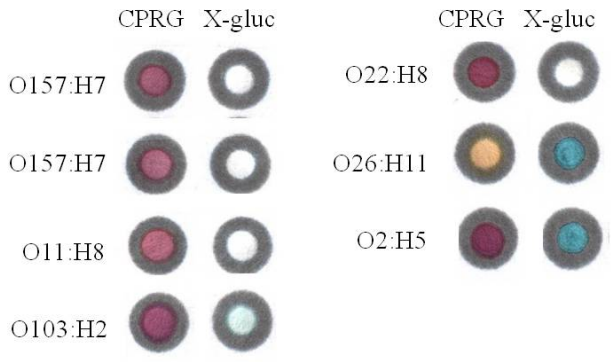

Figure 6.1 Preliminary study testing for β-galactosidase and β-glucuronidase activity from various *E. coli* strains (pathogenic and non-pathogenic). All strains but O26:H11 tested positively for β-galactosidase, as determined with CPRG substrate. A 5-bromo-4-chloro-3-indolyl-glucopyranoside (X-gluc) substrate was used in the determination of β-glucuronidase activity, and the enzyme was detected in strains O103:H2, O26:H11, and O2:H5. Notably, neither O157:H7 strain tested positively, as anticipated. Further optimization of this assay is underway.

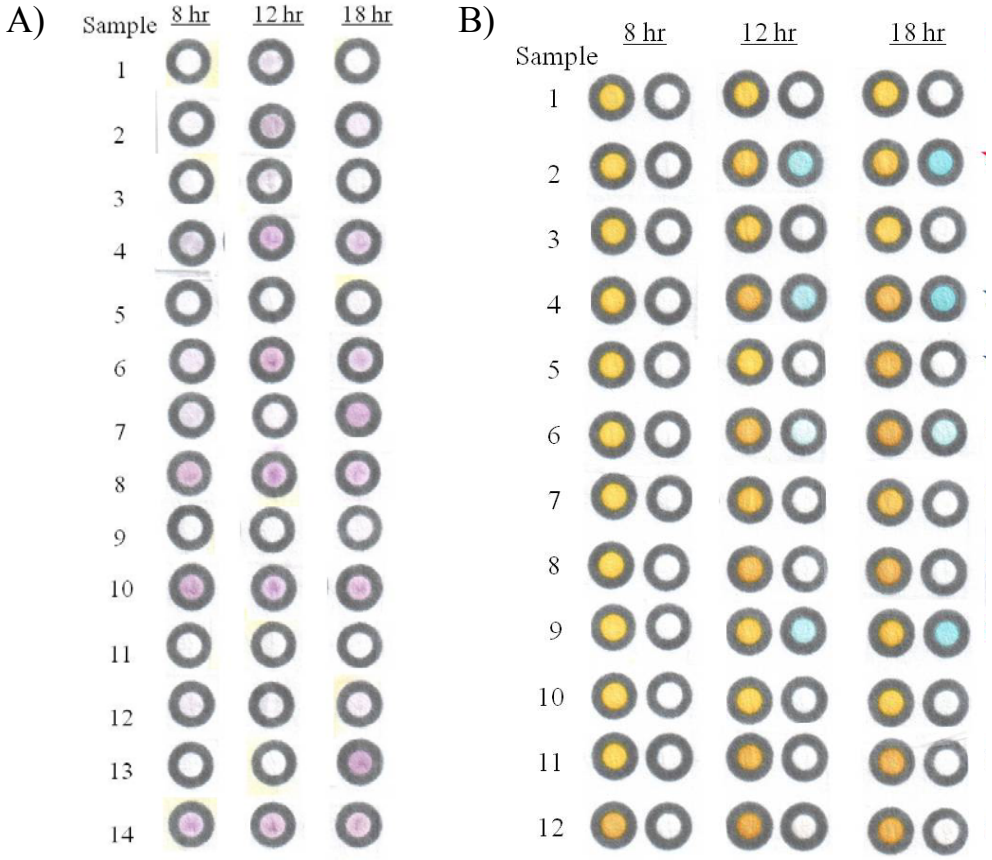

Figure 6.2 Analysis of surface water samples spiked with concentrations of (A) *S.* Typhiumurium and (B) *E. coli* O157:H7 ranging from 100 cfu/mL to 0.1 cfu/mL. Water sampling and enrichment was performed by our collaborators in the Department of Animal Sciences. Samples were tested on the μPAD after 8, 12, and 18 hours of enrichment. Samples 4, 6, 8, 10, 13, and 14 tested positively for *S.* Typhimurium. Samples 4, 5, 6, 7, 8, 9, 11, and 12 tested positively for *E. coli* O157:H7, and this was confirmed via changes in CPRG. The β-glucuronidase assay (second column) continues to be investigated. Some false positive results were reported for each assay. Despite this drawback, this preliminary study shows great potential for detecting low concentrations of pathogens in recreational water.

APPENDIX I. MINIREVIEW FOR *ANALYST:*

ADVANCES IN MICROFLUIDICS FOR ENVIRONMENTAL ANALYSIS

Jana C. Jokerst, Jason M. Emory, and Charles S. Henry

A1.1 APPENDIX I OVERVIEW

During the past few years, a growing number of groups have recognized the utility of microfluidic devices for environmental analysis. Microfluidic devices offer a number of advantages and in many respects are ideally suited to environmental analyses. Challenges faced in environmental monitoring, including the ability to handle complex and highly variable sample matrices lead to continued growth and research. Additionally, the need to operate for days to months in the field requires further development of robust, integrated microfluidic systems. This review examines recently published literature on the applications of microfluidic systems for environmental analysis and provides insight in the future direction of the field.

A1.2 INTRODUCTION

Over the past few decades, tremendous growth in the biochemical, industrial, pharmaceutical, and medical industries has led to a growing list of emerging contaminants and an increase in environmental regulations. As the number of regulated pollutants increases, greater demands are placed on environmental analysis. A number of powerful analytical techniques have been used for environmental monitoring; however, the instrumentation can be complex, leading to time-consuming and costly analysis resulting in incomplete assessment of

pollutant distribution. Some researchers have turned to microfluidic devices to realize improvements in environmental analysis. Microfluidic devices offer a number of advantages, including rapid detection and identification of compounds, low sample and reagent consumption, and the potential for field monitoring. While the capabilities of microfluidic systems have made great strides over the years, there remain important features for environmental analysis that are still lacking. For example, the ideal microfluidic device for environmental analysis would perform on-chip sample preparation from complex matrices such as ground water in a high-throughput manner with sensitive and selective detection while operating unattended in the field for days to months. Microfluidic devices for biological analysis can meet some but not all of these needs. Finally, the devices should be low-cost to allow broad distribution and portable to allow mobile sensing of pollution and/or identification of point source contamination. All of these requirements place a high demand on the microfluidic systems in a way that is very different from biological analysis.

The high demands on microfluidic ingenuity stem from the complexity and diversity of environmental sample matrices and the broad classifications of contaminants, including endocrine disrupting compounds, polyaromatic hydrocarbons, haloacetic acids and other disinfectant byproducts, pesticides and herbicides, inorganic ions, toxic metals, and microorganisms to name a few.[1, 2] We believe a review of the current advances in microfluidics for environmental analysis, discussing both the latest developments in the field and the fundamental unresolved issues, is pertinent to the future directions of microfluidic technology as it relates to environmental analysis. In recent years, similar articles have been published. Chen et al. focused on the broad environmental applications of microchip electrophoresis coupled with electrochemical detection.[3] Richardson published a comprehensive review of the most

commonly implemented analytical techniques (most of which are based on traditional methods), organized by pollutant type.[4] Li et al. discussed current progress in microchip electrophoresis and electrochromatography for environmental applications.[5] This review, while far from exhaustive, discusses literature published in the past three years on environmental analysis using microfluidics, highlighting the advances in sample preparation, novel separation methods, improvements in detection, and developments in integration across all areas of microfluidic analysis for environmental samples.

A1.3 SAMPLE PREPARATION

Preparative cleanup and preconcentration steps are required with most environmental analyses due to the complexity of sample matrix and the low relative abundance of pollutants (ppm-ppt levels are common).[4-6] Various preconcentration strategies have been developed off-line to improve sensitivity; conversely, these methods are time-consuming and run the risk of contamination and/or generation of artifacts. Performing the necessary preparation steps on-chip is ideal; however, integration of pretreatment into a microfluidic network for trace analysis is challenging. On-chip preconcentration methods can be broadly categorized as either static or dynamic.[6] Static mechanisms include extraction, surface adsorption, and membrane filtration, while dynamic mechanisms manipulate analyte velocities to achieve selective enrichment and include electrophoretic stacking, focusing, and sweeping. In static methods, the use of a functionalized solid support for sample pretreatment has shown great promise for isolation and concentration of target analytes in a complex sample matrix. The challenge of these methods lies in the difficulty of constructing frits, weirs and other physical features to trap sorbents. Nonetheless, advancements in the area of microfluidics continue in an effort to implement on-chip sample cleanup. Recently, Tennico and Remcho published a solid-phase extraction

technique using functionalized, magnetic iron oxide nanoparticles (NPs) as the solid support in a microchip device.[7] The particles are directed to an extraction zone in the microfluidic network and held there with the use of a magnet (Figure A1.1), making packing, removal and replenishment of the extraction bed straightforward. In addition to their magnetic properties, iron oxide NPs are stable, biocompatible, and easily modified. The authors synthesized silica-coated iron oxide NPs functionalized with octadecylsilane for extraction of parabens and nonsteroidal anti-inflammatory drugs (NSAIDs) in water and reported 90% analyte recovery.

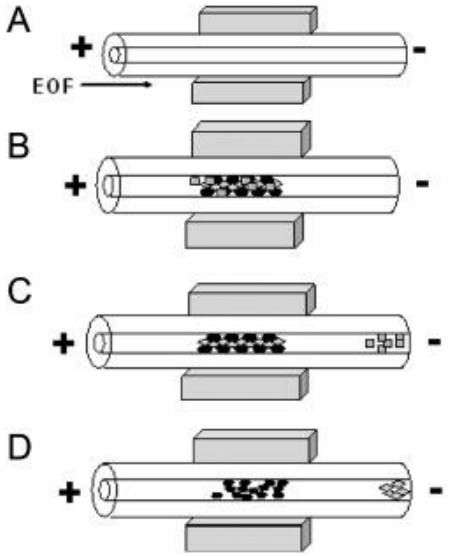

Figure A1.1. Schematic diagram of in-line magnetic extraction with CE. (A) Conditioning step: capillary is conditioned and NdFeB permanent magnets are placed around the capillary. (B) Sample loading: sample mixture containing magnetic particles is introduced into the capillary and retained by the magnets. (C) Washing step: analytes of interest interact with sorbents, whereas interfering components are eluted. (D) Elution step: retained analytes are eluted by applying a stronger eluent. Reprinted from Tennico and Remcho[5] with permission from Wiley InterScience (Copyright 2010 Wiley-VCH Verlag GmbH & Co. KGaA, Weinheim)

Monolithic phases have also been used for static preconcentration because they are generally easier to integrate than silica materials.[6] Xu et al. developed an *in-situ* polymerized butyl methacrylate monolithic column.[8] Polymerization of the monolithic material in poly(dimethyl siloxane) microchannels allows for controlled fabrication of an extraction bed

within the microfluidic network. The authors were able to achieve a 10-fold improvement in the detection limit of their model analyte, promethazine-luminal-potassium ferricyanide. Similarly, Faure et al. developed a lauryl methacrylate monolith polymerized in cyclic olefin copolymer (COC) chips for reverse-phase electrochromatography with the goal of generating a more portable and disposable analytical device.[9] Other recent reports on *in-situ* monolith fabrication in a microfluidic network include Landers,[10] Kang,[11] and Woolley[12] for biological and clinical analytes that have utility for environmental analysis. In electrophoresis, a number of electric field-based dynamic methods are available for preconcentration. Field-amplified sample stacking (FASS) and field-amplified sample injection (FASI) techniques have been studied for several decades and are commonly used in conventional CE systems as a single-step preconcentration method for achieving high sensitivity.[13] In FASS, a sample prepared in low conductivity solution is injected into a microchip channel filled with a higher conductivity background electrolyte. Because the electric field strength is higher in the sample solution, an increase in analyte mobility is observed. Analytes are then stacked at the interface between the sample solution and the buffer. Guan et al. presented a thorough characterization of sample stacking in a PDMS microchip, reporting a 16-fold decrease in the detection limit of a model analyte.[14] In the work of Noh et al., FASS and FASI methods are uniquely combined with a background electrolyte modified with gold nanoparticles to enhance preconcentration and separation performance.[15] The presence of nanoparticles in the background electrolyte provides additional site for solute interaction and has the ability to alter the apparent mobility of analytes as well as electroosmotic flow. The optimized microchip device showed a 200-fold increase in sensitivity in the cyclic voltammetric determination of phenolic endocrine disruptors when using FASS, FASI, and a nanoparticle-modified buffer. A schematic of the microfluidic device and

resulting electropherograms areshown in Figure A1.2, demonstrating the enhanced performance when using stacking. Drinking and surface water samples were tested for the presence of five endocrine disrupting species with detection limits in the fM range.

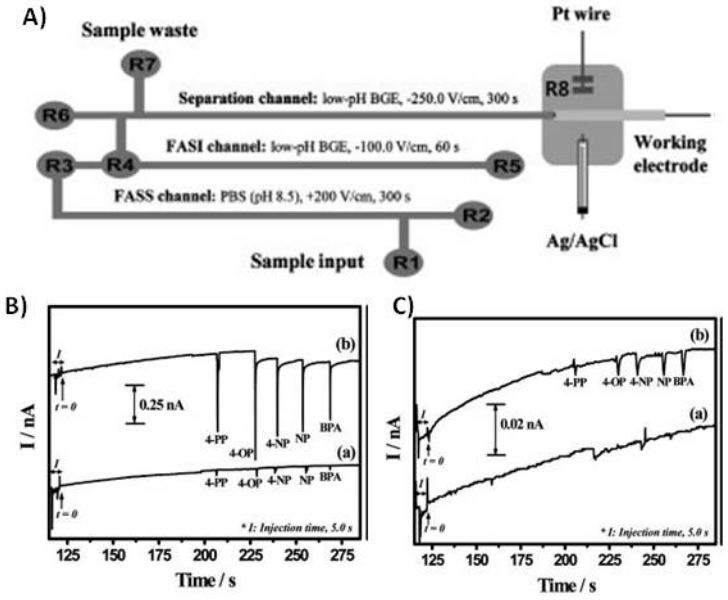

Figure A1.2. (A) Schematic of microfluidic device (B) Electropherograms for five endocrine disruptors obtained with (a) FASI and (b) both FASI and FASS. (C) Electrpherograms of (a) BGE without gold NPs and (b) BGE with gold NPs. Reprinted from Noh et al.[14] with permission from Wiley InterScience (Copyright 2010 Wiley-VCH Verlag GmbH & Co. KGaA, Weinheim)

In addition to chemical preconcentration, bacterial enrichment is necessary for selective enumeration of bacteria species and sensitive detection from environmental samples. Enrichment is a time-consuming process in which a species-selective growth medium is inoculated with a sample containing the target species allowing the bacteria to multiply over a period of 8 – 24 hours. The resulting culture then contains a population of the target bacteria large enough to be analyzed. The work of Dharmasiri et al. demonstrates an enrichment method that is integrated into the microchip device for improved sensitivity and decreased analysis time of *E. coli*. [16] The U.S. Environmental Protection Agency enforces a very stringent maximum

contaminant level for *E. coli* of 0 cfu/mL in drinking water since the minimum infectious dose can be as low as 10 cells.[17, 18] Recognizably, detecting *E. coli* at these very low levels requires - enrichment of cells as a preconcentration method. Dharmasiri et al. used selective antibodies to immobilize *E. coli* on the surface of a PMMA microchannel where enrichment takes place. The bacteria were then directed into a PCR microtube for off-chip detection. The authors reported a recovery of 72%, PCR detection limits between 6 -10 cfu/mL, and a total process time of 5 hr.

Similarly, Beyor et al. developed an immunomagnetic bead-based cell concentration microdevice for pathogen isolation from a dilute sample.[19] The device is constructed from PDMS and glass and incorporates on-chip pneumatic pumps for fluid flow. Superparamagnetic polystyrene beads were loaded into the chip and held in the microchannels using an external magnet (Figure A1.3), while isolation and preconcentration of *E. coli* cells is achieved through immunological interactions. Following this pre-concentration step, off-chip PCR and capillary electrophoresis (CE) were performed. The authors achieved capture efficiencies of 70% and a limit of detection of 2 cfu/μL.

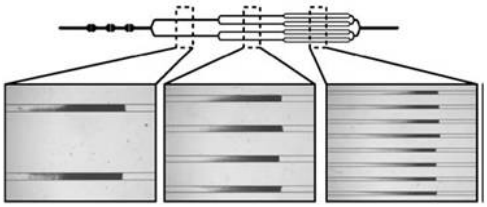

Figure A1.3. Images of beads loaded in the channels. A multi-step loading process using a sequentially bifurcated design enables equal distribution of bead beds in the multiple channels. Reprinted from Beyor et al.

A1.4 DETECTION METHODS

There are two general trends in detection methodologies for microfluidics: the development of a high-throughput interface coupling the microchip device with conventional instrumentation and development of stand-alone integrated detection systems.[5] Undoubtedly, the

latter of the two approaches better lends itself to more compact and less expensive platforms at the expense of performance. Furthermore, while techniques such as mass spectrometry, FTIR, and chemiluminescence are proven to be powerful detection methods for environmental analysis, many are not suitable as portable diagnostic tools. This section will focus on detection methods commonly used for environmental analysis.

A1.4.1 Electrochemical Detection. Electrochemistry is an attractive detection mode because the instrumentation is easily miniaturized and there is minimal loss of performance as size scales are reduced. Electrochemical detection techniques are capable of being universal detector (conductivity detection), semi-selective (amperometric detection by adjusting the potential) and highly selective by modification of the electrode surface such as electrochemical immunoassays.[20, 21] Furthermore, many techniques of electrochemistry for example amperometric and conductivity detection have been adapted to microfluidic devices and show high sensitivity.[3] As a result, incorporation of microelectrodes into microfluidic devices has become commonplace. Conductivity detection (CD), which can be used in either contact or contactless modes where contact refers to electrodes in galvanic contact with the working solution, is particularly promising for the analysis of small ions. Contactless detection is advantages because it can be used with a wide range of background electrolytes and can take place at any location along a channel. However, electrical shielding is critical in contactless CD and, therefore, requires an insulating layer between the electrodes and solution. On the other side, contact CD requires isolation of the electrodes from the high voltage and is subject to electrochemical reactions but utilizes mature conductivity detection instrumentation.[22] Gertsch et al. reported a microchip capillary electrophoresis device with contact conductivity detection for the determination of perchlorate in water at the ppb level.[23] Perchlorate competitively

inhibits the uptake of iodide into the thyroid, and long-term exposure has been linked to developmental and neurological disorders in infants and fetuses and also associated with thyroid cancer. Separation of perchlorate from competing anions in drinking water was achieved using a micellar pseudostationary phase containing a zwitterionic surfactant to selectively retain perchlorate. The method is capable of 5.6 ppb detection limits in drinking water with total analysis time of 60 s. A schematic of the microfluidic device as well as electropherograms of perchlorate separation in drinking water are shown in Figure A1.4.

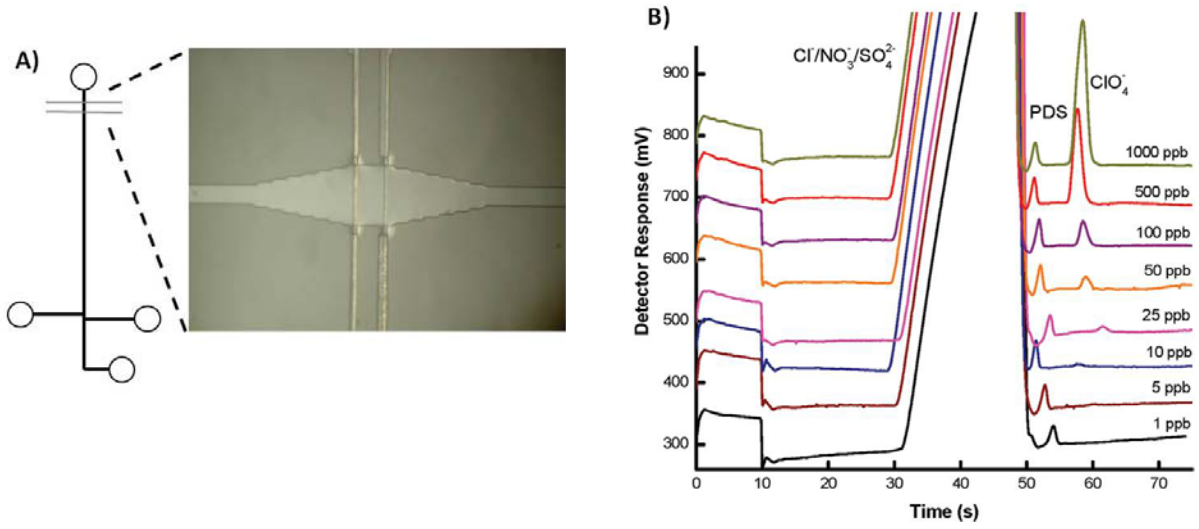

Figure A1.4. (A) Schematic of the microfluidid device, featuring a bubble cell (image) at the detection zone (B) Electropherograms showing separation of drinking water spiked with 0.12 ppm propane disulfonate (internal standard) and concentrations of perchlorate ranging from 1 to 1000 ppb. Reprinted from Gertsch et al.[18]

Recently, Liu et al. developed a microchip CE device with a contactless conductivity detector for separation and detection of inorganic ions and heavy metals.[24] The detection circuit is based on a lock-in amplifier and was designed on printed circuit boards for easy miniaturization and mergence within the microfluidic network. The device is capable of an average limit of detection of 0.4 μM for inorganic cations in water, a level below that of other

contactless detectors. Rogers and Ding reported a microchip CE method for the determination of haloacetic acids using contactless CD.[25] Haloacetic acids are a class of disinfectant byproducts generated during the water chlorination treatment process.[26,27] These compounds are a major health concern due to their known toxicity and carcinogenicity.[28] An off-chip solid-phase extraction step was implemented prior to microchip CE analysis, allowing determination of three HAAs in swimming pool water with limits of detection ranging from 38 – 500 ppb.

The work of Ha et al. describes a microchip electrophoresis device for monitoring endocrine disrupting species (EDCs) via amperometric detection.[29] Amperometric detection (and related pulsed amperometric detection modes) is attractive because it can provide selectivity relative to conductivity detection. Thin film electrodes fabricated from Prussian Blue-modified indium tin oxide were incorporated into a serpentine microchannel configuration. Separation of four endocrine disruptors was achieved in just over 2 min with detection limits as low as 59 nM. In 2010, Nie et al. reported a carbon disk electrode modified with mesoporous carbon material (CMK-3) for amperometric detection of nitroaromatic compounds (NACs) in water.[30] NACs are highly toxic, carcinogenic compounds used in explosives, fabric dyes, and agricultural products.[31, 32] NAC contamination of water and soil is a serious concern throughout the US as these compounds are considered dangerous to human health at low (ppb) levels. Chemically modified electrodes can greatly improve sensitivity and selectivity of electrochemical detection.[33] The CMK-3-modified working electrode exhibits chemical stability and good electrical properties as well as a highly ordered mesoporous structure with high surface area and large pore volume. Although the separation of four NACs was carried out using conventional CE instrument rather than the microchip format, using this novel electrode material, limits of

detection of 3.0 – 4.7 ppb were achieved in drinking water, wastewater, and river samples without complex sample pretreatment.

A1.4.2 Optical Detection. Optical detection techniques comprise some of the most inexpensive, simple, and universal detection modes. In microfluidic devices, however, the limited path length (generally 5 to 50 μm) associated with microchannels greatly hinders sensitivity and detection limits in absorbance measurements and decreases the overall intensity of fluorescent signals.[34] Despite this drawback, many groups are working to improve optical detection on microchips. Absorbance has been used for a number of analytes in microfluidic platforms including phenolic chemicals; air pollutants; benzene, toluene, and xylene (BTX) transition metal ions; as well as nitroaromatic and nitramine explosives.[35-38] Ohlsson et al. reported a microchip CE device with integrated waveguides for simultaneous absorbance and native UV-excited fluorescence detection.[39] Combining the two methods, a wide range of analytes may be analyzed. Additionally, enhanced sensitivity is achieved for compounds that exhibit native fluorescence, for example polycyclic aromatic hydrocarbons[40] and naphthalene sulfones.[41] This detection scheme could be particularly useful for the identification of analytes and quantification of co-eluting species. Gaspar et al. used a microphotometer coupled to a spectrometer to enhance the cross-sectional area of the irradiation zone, effectively increasing the optical path length in PDMS microchips, diminishing background noise, and improving detection limits.[42] Schulze and Belder summarized literature published in the last decade on fluorescence detection in CE and microchip CE.[34] The review discusses some of the challenges of fluorescence detection such as derivatization, which is often necessary, but the article also points out the unparalleled sensitivity and the potential for miniaturized optical components.

Fluorescence detection is a good choice for detection in microfluidics due to the inherent sensitivity and low detection limits achievable. These advantages overcome the normal short-comings associated with absorbance due to the short path length in a microfluidic device. However, fluorescence detection is not without its own drawbacks, including the lack of native fluorescence for a number of environmental analytes and the large size and complexity of optical instrumentation. The attachment of a fluorophore to environmental analytes requires additional sample preparation steps and increases the cost of the assay. Despite these disadvantages, fluorescence has been used successfully for environmental analysis with microfluidic devices. Walworth et al. demonstrated the analysis of multi-component mixtures representing three different classes of compounds in real sample matrices (Tennessee River and Second Creek).[43] They used a high performance extraction disk cartridge (HPEDC) to preconcentrate analyte mixtures containing several classes of compounds (toxin, pharmaceutical, and endocrine disrupting compounds) in aqueous samples. The HPEDC extracts were analyzed using CD-modified MEKC (CD-MEKC) with a confocal laser induce fluorescence (LIF) detection setup.

Shen et al. developed a microfluidic analytical system for characterization of dissolved organic carbon (DOC) in environmental waters.[44] The design was based on a capillary gel electrophoresis (CGE) device with a LIF detector using microchips made from polymethylmethacrylate. The authors demonstrated reproducible peaks for standard organic solutions with analysis times less than 70 s. Additionally, DOC in environmental water from the Biwa Lake and the Hino River was analyzed, showing the content of DOC in the Biwa Lake changed seasonally.[45]

The major drawback of fluorescence detection is the need to derivatize most analytes with a fluorophore prior to analysis. An alternative to derivatization is the use of native

fluorescence. Tolba et al. demonstrated native fluorescence utilizing deep-UV excitation in microchannel electrophoresis. Different analytes such as pollutants, neurotransmitters, and proteins have been successfully detected in more or less complex matrices.[46] Organic pollutants can be separated and detected on microfluidic devices with LIF detection. An example is a μCEC device with LIF detection which was applied to the separation and detection of polyaromatic hydrocarbons (PAHs) of anthracene, pyrene, 1,2-benzofluorene, and benzo[a]pyrene. The PAHs were excited at 325 nm by a He-Cd laser, and the fluorescence emitted was detected at 350 nm.[47] Benhabib et al. used microchip capillary electrophoresis to identify nine PAH components. They demonstrated that benzo[a]pyrene and perylene were distinguishable from a coeluting peak of anthanthrene by spectral analysis.[48] One of the disadvantages of deep UV native fluorescence, however, is the high background signal arising from Rayleigh scattering. Another approach to avoid derivatization was presented by Wallenborg and Bailey in which they employed indirect LIF detection with MEKC to determine 14 explosives with a limit of detection of 1 μg/mL in natural water.[49]

Fluorescently labeled antibodies are commonly used in immunoassay platforms, providing sensitive detection of a captured analyte. Ramon-Azcon et al. used microparticles as solid supports to improve immunological detection of herbicides in a microchip device.[50] Microparticles increase the surface area and allow faster assay kinetics. Microparticles were used in combination with dielectrophoresis (n-DEP) for the sorting and separating particles and cells of interest using simple electrode components without any moving actuators. The microparticles were functionalized with bovine serum albumin conjugated with atrazine (atrazine-BSA) and were incubated with anti-atrazine IgG antibody and atrazine. The immunocomplex was then injected into the microfluidic device that was comprised of two caged

areas surrounded by n-DEP-generated electric barriers in order to trap the microparticles. The anti-atrazine IgG antibody immobilized on the atrazine-BSA microparticles was retained in the caged area created by n-DEP, whereas antibodies that reacted with free atrazines were flowed downstream. A solution containing FITC-labeled anti-rabbit IgG antibody (FITC-anti-IgG) was used to detect the immunocomplex. Detection limits as low as 0.11 ppb were determined for the immunosensing microchip device. The authors proposed simultaneous measurements using a device with different caged areas for multiple analytes.

Som-Aum et al. developed chemiluminescence (CL) detection for the determination of arsenate in water samples based on luminol CL with a heteropoly acid complex.[51] Their method was based on the complex between luminol and vanadomolybdoarsenate heteropoly acid (VMoAs-HPA) in basic solution. CL was performed by the reaction between the adsorbed ion-pair complex and alkaline luminol. The CL detection was easy to integrate into a microchip and has potential for on-site detection of low levels of contaminants. Advantages of this technique include improved sensitivity, high specificity due to the VMoAs-HPA complex, and the elimination of interference [Co(II), Cu(II) and Fe(II)]. However, an anion exchange resin was necessary to remove interfering ions such as chromate and phosphate. A detection limit of 8.9 mM was achieved for As(V) and a linear calibration range from 1.0×10^{-7} to 5.0×10^{-5} M, which spans the USEPA's maximum contaminant level (MCL) in drinking water.

Recently, surface-enhanced Raman scattering (SERS) techniques have been used for highly sensitive detection in a microfluidic chip.[52] The observed enhancement factor of SERS provides a sensitivity that is comparable to fluorescence detection. Additionally, molecular structural information can be obtained, and the detection and identification of non-fluorescent samples is possible using this technique. Raman spectroscopy has been integrated into

microfluidics to quantitatively analyze p-aminobenzoic acid (PABA), benzene, toluene, ethylbenzene, o-,m-, p-xylene, pyridine, nicotinic acid, and several pesticides such as carbendazim and metazachlorine.[53] Ashok et al. reported a directly embedded split-fiber-probe based on a Raman detection system in a microfluidic chip.[54] Using the embedded split-fiber-probe offered flexibility to modify the collection geometry, minimizing the background signal and allowing an alignment free system. The development of this device affirms the feasibility of using Raman spectroscopy with portable, lab-on-a-chip devices for environmental analytes.

A1.4.3 Mass Spectrometry. Mass spectrometry has been widely applied to many different fields of chemical analysis, including environmental analysis. The complex sample pretreatment, large solvent consumption, and complexity of maintenance, however, has restricted the application of on-line environmental sample analysis using mass spectrometry. Wei et al. developed a microfluidic-based device which combined ESI-Q-TOF mass spectrum with a single particle analysis for the determination of herbicides in water.[55] The authors demonstrated a simplified pretreatment process in which analytes are retained on a silicone polymer-coated silica gel modified with C_{30} alkyl chains within a microfluidic channel. The microchip is coupled to an ESI-Q-TOF mass spectrum for direct detection of herbicides upon desorption from the single particle. In principle, single particle analysis on microfluidic devices coupled with on-line MS detection could be applied to a variety of environmental samples.

A1.5 MICROCHIP INTEGRATION

Microfluidic devices offer the possibility of environmental analysis systems with far-reaching advantages such as autonomous on-site monitoring using an instrument that possesses a small footprint, relative to conventional systems.[56] Unfortunately, many existing microfluidic systems fail to fully realize this goal because of the peripheral equipment used for signal

acquisition and processing, such as the electronics and optics. The peripheral equipment size typically over-shadows the small footprint of the microfluidic chip and can prevent its use for in-field monitoring applications. Thus, continued miniaturization of not only the microfluidic chip but also the peripheral equipment is paramount to the delivery of true point-of-use microfluidic systems.

Ramirez-Garcia et al. presented work towards a fully integrated microanalytical instrument with focus on the development of a pump and detector.[57] Their pump design was based on conducting polypyrrole (ppy). Ppy was synthesized electrochemically by oxidizing the monomer in the presence of large anions which become trapped in the structure of the polymer. The polymer swells and shrinks with repeated reduction and oxidation due to the hydration and dehydration of the charged backbone, producing mechanical work such as pumping. The swelling of the polypyrrole was used to deform thin walled polyurethane tubes, generating liquid movement in microfluidic channels with very low power consumption. Further integration was achieved by using Light Emitting Diodes (LEDs), which provided low-power consumption, long lifetime and extremely low detection limits.

Alves-Segundo et al. demonstrated the fabrication of miniaturized, continuous flow, analytical microsystems based on photometric detection with optical elements such as light emitting diodes and photodiodes.[58] Figure A1.5 shows the integrated continuous flow microfluidic system. The integration of a glass window eliminates the transparency problem of ceramic material and allows for the bubble-shaped flow cell to increase the area of the light beam. The microsystem was used for the colorimetric determination of Cr(VI) ion in waters based on the diphenylcarbazide reagent. The authors demonstrated a limit of detection of 50 ppb and a linear response range of 0.1 to 20 ppm. The sensitivity was enhanced by the use of the

bubble-configuration flow cell coupled to an LED and photodiode. A fully integrated microsystem with the capability of automation, robustness or portability to field applications is still being developed; while the integration of an LED and photodiode for nitrite detection off-chip was shown.

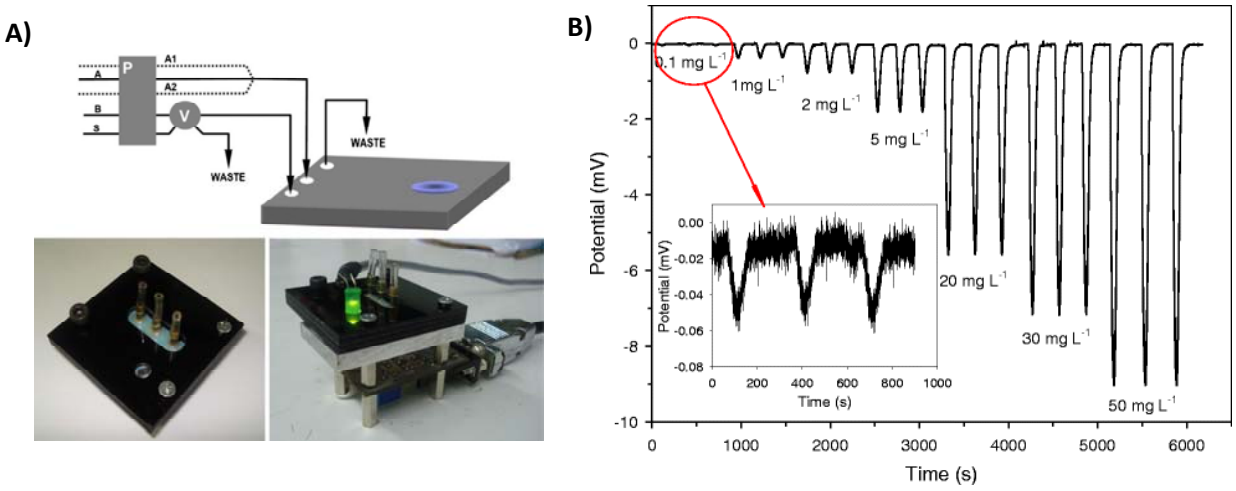

Figure A1.5. A) Continuous flow microsystem set-up. a) Experimental manifold: A, acidified DPC reagent solution; A1 H_2SO_4 solution; A2, DPC reagent solution; B, deionized water; S, sample; P, peristaltic pump; V, six-port injection valve. b) Protective PMMA black support for the external optical components. c) Optical detection set-up: (1) LED; (2) PMMA support; (3) Photodetector and associated electronics; (4) DB9 (RS232) computer connector. B) Response signal obtained, by injecting Cr (VI) from 0.1 to 50 mg L–1, using the optimal experimental conditions Reprinted from Alves-Segundo et al.

Sieben et al. demonstrated the use of microfluidic devices which integrate fluid processing and optical detection, enabling the development of a low-cost, miniature, portable and sensitive nitrite sensor based on the Griess assay.[59] The sample was mixed with the Griess reagents, forming a colored Azo dye which can be measured by absorbance to determine the nitrite concentration. The design incorporated four separate absorbance cells (2.5 cm path length) separated by three serpentine mixers to monitor the reaction kinetics and mixing efficiency. The

on-chip integration of the LED, photodiode, and the absorbance cell are shown in Figure A1.6. The detection system had integrated LEDs and photodiodes which yielded a limit of detection of 14 nM and a linear range between 50 nM and 10 mM. The tinted PMMA was used to adsorb non-directional and background light, substantially reducing the background signal. The authors hope to implement an integrated and miniaturized system to continuously measure nitrite concentrations in the environment, generating a profile of the temporal and spatial distribution of chemistry in the oceans.

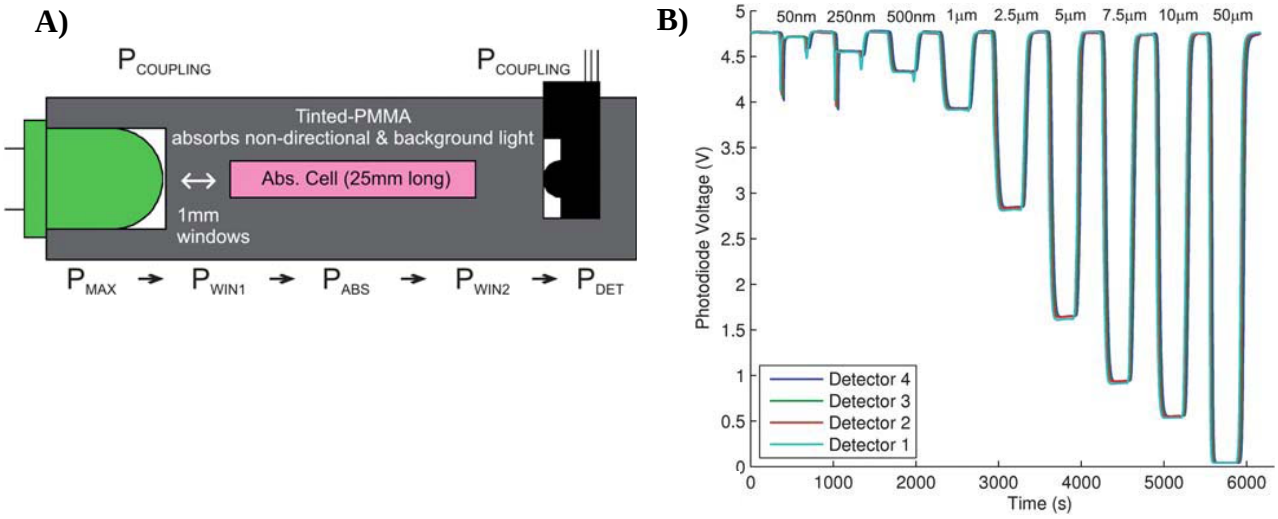

Figure A1.6. A) Cross-sectional view of the microfluidic absorption cell with optical power budget (see text for details). P_{MAX} is the maximum power that will reach the detector from the LED (determined by the solid angle), $P_{COUPLING}$ is the power remaining after the lumped losses from coupling the LED and photodetector to the microfluidic device, P_{WIN1} is the power remaining after the first window, P_{ABS} is the power remaining after the adsorption of the Azo dye formed in the presence of nitrite (desired measurement), P_{WIN2} is the power remaining after the detection window and P_{DET} is the optical power that is detected. B) The photodiode output voltage for all four detectors for a sequence of nitrite samples of varying concentrations from 50 nM to 50 mM, flowing through the microfluidic device. Reprinted from Sieben et al.

Barat et al. designed an integrated optical system for particle analysis on-chip using a combination of scattered light and fluorescence.[60] Scattered light is collected at two different

angles using optical fibers inserted into microfabricated grooves. The optical fibers are used for both excitation and emission detection, eliminating bulky off-chip optics and the need for a complex, integrated lens. Within the microfluidic device, the fibers act as waveguides to deliver excitation light to a defined location of the device in a well controlled volume, producing high photon irradiances. The illumination volume is controlled by the core diameter of the fiber optics as well as the acceptance angle of the fiber. In working toward a low-cost, disposable platform suitable for environmental applications, simple optical components that may be incorporated into a microfluidic device during the fabrication process are highly advantageous.

In 2009, Beyor et al. further advanced their lab-on-a-chip system for pathogen detection that integrates cell preconcentration, purification, PCR and CE analysis.[61] The device is constructed from a four-layer design using glass-glass-PDMS-glass. Micropumps and valves are employed for fluid direction and control throughout the system. Superparamagentic beads are functionalized for immunological cell capture of *E. coli* O157 and K12 serotypes, and an external magnet is used for retaining beads in capture channels. After this preconcentration step, bead-cell duplexes are hydrodynamically transferred to an on-chip PCR reactor for amplification of the target microorganisms. Finally, the PCR products are injected onto a 5 cm CE column and detected using laser-induced fluorescence. A schematic of the integrated system is shown in Figure A1.7. The authors achieved a detection limit of 0.2 cfu/μL for *E. coli* O157 and confirmed no false positive results even in the presence of a high background (10^4 cfu/μL) of *E. coli* K12 cells.

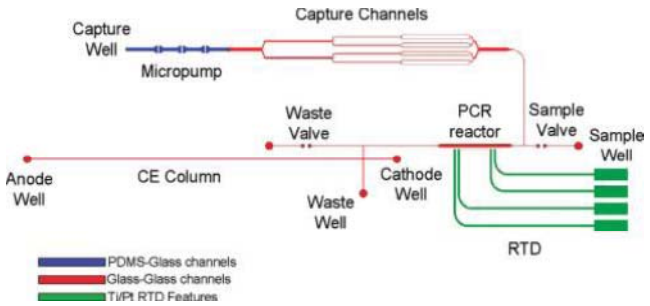

Figure A1.7. Cell capture-PCR-CE microdevice that integrates a capture structure with PCR and capillary electrophoresis. Immunomagnetic beads are immobilized by an external magnet in the capture channels as sample solution is driven through the bead bed. After capture and washing, the bead-cell duplexes are pumped into the 100 nL PCR reactor, where an external heater drives the reaction. Finally, the PCR amplicons are injected onto the CE column, separated, and detected near the anode using LIF. Channels in blue are enclosed using a PDMS-glass sandwich. Channels in red are enclosed by thermally bonding the etched glass wafer to the RTD wafer. Green features delineate the Ti/Pt resistance temperature detector features. Reprinted from Beyor et al.

A1.6 EMERGING APPLICATIONS AND TECHNOLOGIES

Lab-on-a-chip technology offers many advantages to environmental analysis by reducing analysis time, improving detection limits, and allowing on-line, real time monitoring. Although the literature discussed thus far focuses primarily on water quality analysis, the field of microfluidics is certainly growing to include air quality and aerosol monitoring. Many of the challenges associated with air quality assessment are common to those of water quality, such as the difficulty in determining low levels of pollutants in a complex sample. Dossi et al. reported a microchip electrophoresis method for the determination of aldehydes in the atmosphere.[62] The method involves forcing air samples through a silica gel cartridge coated with 2, 4-dinitrophenylhydrazine for derivatization of aldehydes followed by elution onto the microchip device.

Noblitt et al. recently demonstrated an integrated microfluidic device for analysis of ambient aerosol composition.[63] The instrumentation involves a water condensation particle collector coupled with an electrophoresis microchip using contact conductivity detection. As aerosol particles were collected onto the microchip, the concentration of inorganic anions was measured every 60 s using the electrophoresis system. In preliminary results, the system ran continuously for 28 hr, demonstrating the ability to perform long-term field work in this new area of research.

Low-cost, paper-based diagnostic and analytical devices are another emerging technology for environmental analysis. Paper-based analytical devices have several advantages including light-weight, portability, disposability, and cost-effective fabrication. Electrochemical sensing provides a versatile and quantitative methodology as demonstrated by the use of microfluidic paper-based electrochemical devices (μPEDs) in the selective analysis of Pb(II) in an aqueous solution containing a mixture of Pb(II) and Zn(II).[64] The schematic of the paper-based electrochemical detection device is shown in Figure A1.8. The measurement of Pb(II) showed a limit of detection of 1.0 ppb. Apilux et al. presented a novel lab-on-paper device combining electrochemical and colorimetric detection for the rapid screening of Au(III) in the presence of a common interference, Fe(III), in industrial waste solutions. [65] They used a colorimetric method to simultaneously detect Fe(III) as a screening tool for the determination of Au(III). According to the authors, Fe(III) is the only metal that affects the electrochemical determination of Au(III) when present above a 2.5-fold excess concentration of that of the Au(III). The calibration curve showed good linearity in the concentration range of 1-200 ppm of Au(III) and a limit of detection of 1 ppm.

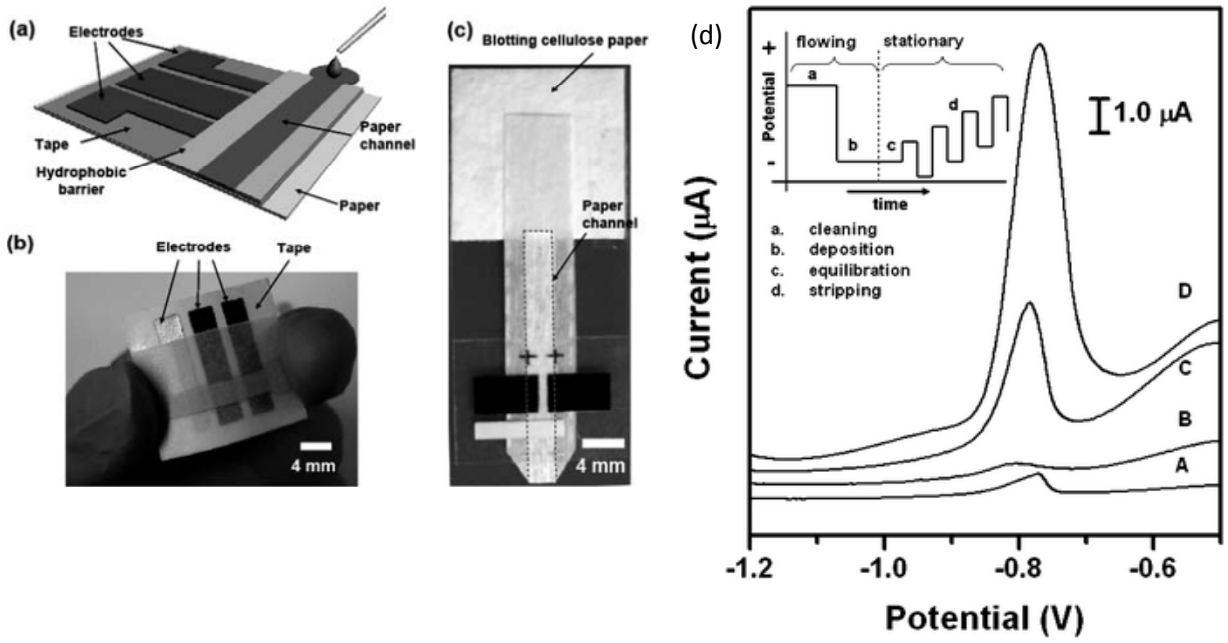

Figure A1.8. (a) Schematic of a paper-based electrochemical sensing device. The sensor comprises three electrodes printed on a piece of paper substrate (or plastic) and a paper channel. The paper channel was in conformal contact with the electrodes, and was held in place by double sided adhesive tape surrounding the electrodes. A photograph of a paper-based electrochemical sensing device for the analysis of glucose (b), and a hydrodynamic paper-based electrochemical sensing device for the measurement of heavy-metal ions (c). The device consists of two printed carbon d) Square-wave anodic stripping voltammograms for 25 ppb solution of Pb(II) in 0.1 M acetate buffer (pH 4.5) in the presence of 25 ppb Zn(II) : (A) a 100 μL solution placed directly on the electrodes; (B) a 100 μL solution added to the stagnant μPEDs (without a pad of blotting paper as sink); (C and D) a solution of analytes continuously wicking the paper channel of the hydrodynamic μPEDs. The deposition time was 120 s (A, B, C) or 360 s (D). The SWASV was performed in the potential range of −1.2 to −0.5 V under optimized conditions: frequency, 20 Hz; amplitude, 25 mV; potential increment, 5 mV; equilibration time, 30 s. Deposition was performed at −1.2 V; 'cleaning' was performed at +0.5 V for 60 s. A bismuth(III) concentration of 500 μg L^{-1} was chosen for the co-deposition of heavy-metal ions. Inset shows the schematic of the four steps of the square-wave anodic stripping voltammetry. Reprinted from Nie et al.

A1.7 CONCLUSION

The field of microfluidics has made tremendous strides in recent years with the majority of the effort focused on biological analysis. A growing number of groups, however, have recognized the utility of microfluidic devices for environmental analysis particularly in light of the increasing need to understand the impacts of human activity on the world around us

(Summary of recent research work is detailed in Table A1.1). Microfluidic devices are in many respects ideally suited to this task because they can be made at low costs relative to traditional instrumentation and are small and thus potentially quite portable. We believe the future growth of environmental analysis with microfluidics will be focused on two key elements: 1) Production of non-technical instrumentation either through fully integrated systems or elegantly simple paper-based type devices. This would allow for greater application of devices by minimally trained technicians. 2) Portability remains as one of the major selling points of microfluidics over the more conventional techniques. The ability to perform analysis in the field allows for more complete understanding of the complex dynamics of environmental sites with rapid quantitative and qualitative results. As research in this field continues to grow, significant challenges will be faced including the ability to handle complex and highly variable sample matrices, the need to operate for days to months in the field, and the generation of systems that require little to no power. To address these challenges, great strides have been made in on-chip sample preparation and preconcentration techniques such as solid-phase extraction, stacking methods for electrophoretic separations, and integrated bacterial enrichment. Groups have advanced electrochemical, optical, and spectroscopic detection methods on-chip in order to analyze low abundance contaminants in complex environmental samples. Finally, the advent of new device materials, like paper-based analytical devices, allows for simpler fabrication and operation, greater cost efficiency, and enhanced portability.

Table A1.1 Summary of Recent Work on Microfluidic Devices for Environmental Analysis

Authors	Core Technological Component	Class of Pollutant Tested	Limit of Detection	Sample Matrix
Tennico et al.	Functionalized magnetic iron oxide nanoparticles as the solid support	Parabens and NSAIDs	N.R.	Standards
Xu et al.	Monolithic phase by in-situ polymerized butyl methacrylate	Promethazine	1.6 ng/mL	Standards
Noh et al.	FASS and FASI	Phenolic endocrine disruptors	7.1-11.1 fM	Drinking and surface water
Dharmasiri et al.	Bacterial cell capture	*E. coli*	6-10 cfu/mL	Recreational water
Beyor et al.	Bacterial cell capture	*E. coli*	0.2 cfu/μL	Standards
Gertsch et al.	Contact conductivity	Perchlorate	5.6 ppb	Drinking water
Liu et al.	Contactless conductivity using a lock-in amplifier	Inorganic ions and heavy metals	0.4 μM	Standards
Rogers and Ding	Capacitively coupled contactless conductivity (C^4D)	Haloacetic acids	38-500 ppb	Recreational water
Ha et al.	Amperometric detection with thin film electrodes fabricated from Prussian blue	EDC	59 nM	Water in Styrofoam containers
Nie et al.	Carbon disk electrode modified with mesoporous carbon material	Nitroaromatic compounds	3.0-4.7 ppb	Drinking, ground, cooking waste water
Ohlsson et al.	Integrated waveguides for simultaneous absorbance and native UV fluorescence	Polycyclic aromatic hydrocarbons and naphthalene sulfones	2-4 μM native fluorescence 14-31 μM absorbance	Reference standard
Gaspar et al.	Microphotometer coupled to a spectrometer to enhance the cross sectional area of the irradiation zone	Inorganic anions	0.78 μM	Standards
Walworth et al.	High performance extraction disk cartridge	Toxin, pharmaceutical and EDC	N.R.	Surface water
Shen et al.	CGE-LIF	Dissolved organic carbon	N.R.	Surface water

Tolba et al.	Native fluorescence utilizing deep-UV excitation	pharmaceutical	250-900 ng/mL	Reference standard
Banhabib et al.	Used spectral analysis to distinguish coeluting peaks	PAH's	1 ppb- 400 ppm	Reference standard
Wallenborg et al.	Indirect-LIF with MEKC separation	14 explosive compounds	1 μg/mL	Soil extracts
Ramon-Azcon et al.	Microparticle as solid supports in combination with dielectrophoresis	Herbicides	0.11 ppb	Wine
Som-Aum et al.	Chemilumninescence	arsenated	89 nM	Drinking and mineral water
Wei et al.	Combined ESI-Q-TOF mass spectrum with a single particle analysis using a silicone polymer-coated silica gel modified with C_{30}	Herbicides	0.11 ppm	Tuber vegetables
Ramirez-Garcia et al.	Integrated pump and detector based on polypyrrole	Nitrites	0.05 ppm	Standards
Alves-Segundo et al.	Integration of light emitting diodes an photodiodes for a colorimetric analysis	Cr(VI)	50 ppb	Surface water
Sieben et al.	Integrated fluid processing and optical detection elements with tinted PMMA	Nitrite	14 nM	Standards
Dossi et al.	Forcing air sample through a silica gel cartridge to determine aldehydes in the atmosphere	Aldehydes	7.2 -9.2 μM	Urban air samples
Noblitt et al.	Water condensation particle collector coupled to MCE	Inorganic anions	19 nM	Aerosol extracts
Nie et al.	Electrochemical sensor on a paper-based microfluidic device	Pb(II)	1.0 ppb1.0 ppb	Standards
Apilux et al.	Paper-based electrochemical device for electrochemical and colorimetric detection	Au(III), Fe(III)	1 ppm AU(III)	Gold-refining waste water
*N.R. not reported				

A1.8 REFERENCES

1. Z. Y. Xie and R. Ebinghaus, *Analytica Chimica Acta*, **2008**, *610*, 156-178.
2. J. M. Wu, L. F. Zhang and Z. G. Yang, *Crit Rev Anal Chem*, **2010**, *40*, 234-245.
3. G. Chen, Y. Lin and J. Wang, *Talanta*, **2006**, *68*, 497-503.
4. S. D. Richardson, *Analytical Chemistry*, **2009**, *81*, 4645-4677.
5. H. F. Li and J. M. Lin, *Analytical and Bioanalytical Chemistry*, **2009**, *393*, 555-567.
6. C. C. Lin, J. L. Hsu and G. B. Lee, *Microfluid. Nanofluid.*, **2011**, *10*, 481-511.
7. Y. H. Tennico and V. T. Remcho, *Electrophoresis*, **2010**, *31*, 2548-2557.
8. Y. Xu, W. Zhang, P. Zeng and Q. Cao, *Sensors*, **2009**, *9*, 3437-3446.
9. Y. Ladner, G. Cretier and K. Faure, *Journal of Chromatography A*, **2010**, *1217*, 8001-8008.
10. C. Cakal, J. P. Ferrance, J. P. Landers and P. Caglar, *Analytical and Bioanalytical Chemistry*, **2010**, *398*, 1909-1917.
11. Q. S. Kang, Y. Li, J. Q. Xu, L. J. Su, Y. T. Li and W. H. Huang, *Electrophoresis*, **2010**, *31*, 3028-3034.
12. W. C. Yang, M. Yu, X. H. Sun and A. T. Woolley, *Lab on a Chip*, **2010**, *10,* 2527-2533.
13. M. C. Breadmore, M. Dawod and J. P. Quirino, *Electrophoresis*, **2011**, *32*, 127-148.
14. Q. Guan and C. S. Henry, *Electrophoresis*, **2009**, *30*, 3339-3346.
15. H. B. Noh, K. S. Lee, B. S. Lim, S. J. Kim and Y. B. Shim, *Electrophoresis*, **2008**, *31*, 3053-3060.
16. U. Dharmasiri, M. A. Witek, A. A. Adams, J. K. Osiri, M. L. Hupert, T. S. Bianchi, D. L. Roelke and S. A. Soper, *Analytical Chemistry*, **2010**, *82*, 2844-2849.
17. W. E. Keene, J. M. McAnulty, F. C. Hoesly, L. P. Williams, Jr., K. Hedberg, G. L. Oxman, T. J. Barrett, M. A. Pfaller and D. W. Fleming, *The New England Journal Of Medicine*, **1994**, *331*, 579-584.
18. S. O. Van Poucke and H. J. Nelis, *Journal Of Applied Microbiology*, **2000**, *89*, 390-396.
19. N. Beyor, T. Seo, P. Liu and R. Mathies, *Biomedical Microdevices*, **2008**, *10*, 909-917.
20. H. Dong, C.-M. Li, Y.-F. Zhang, X.-D. Cao and Y. Gan, *Lab on a Chip*, **2007**, *7*, 1752-1758.
21. J.-J. Xu, A.-J. Wang and H.-Y. Chen, *TrAC Trends in Analytical Chemistry*, **2007**, *26*, 125-132.
22. S. D. Noblitt and C. S. Henry, *Anal Chem*, **2008**, *80*, 7624-7630.
23. J. C. Gertsch, S. D. Noblitt, D. M. Cropek and C. S. Henry, *Analytical Chemistry*, **2010**, *82*, 3426-3429.
24. B. Liu, Y. Zhang, D. Mayer, H.-J. Krause, Q. Jin, J. Zhao and A. Offenhäusser, *Electrophoresis*, **2011**, ***32***, 699-704.
25. Y. S. Ding and K. Rogers, *Electrophoresis*, **2010**, *31*, 2602-2607.
26. Y. Qi, C. Shang and I. M. C. Lo, *Water Research*, **2004**, ***38***, 2375-2383.
27. V. Kanokkantapong, T. F. Marhaba, B. Panyapinyophol and P. Pavasant, *J. Hazard. Mater.*, **2006**, *136*, 188-196.
28. M. L. Hanson and K. R. Solomon, *Environ. Pollut.*, **2004**, *130*, 371-383.
29. K. Ha, G. S. Joo, S. K. Jha and Y. S. Kim, *Microelectron. Eng.*, **2009**, *86*, 1407-1410.
30. D. X. Nie, P. Li, D. Zhang, T. S. Zhou, Y. Liang and G. Y. Shi, *Electrophoresis*, **2010,** *31*, 2981-2988.
31. Y. Bhattacharjee, *Science*, **2008**, *320*, 1416-1417.
32. J. D. Rodgers and N. J. Bunce, *Water Research*, **2001**, *35*, 2101-2111.

33. S. Hrapovic, E. Majid, Y. Liu, K. Male and J. H. T. Luong, *Analytical Chemistry*, **2006**, *78*, 5504-5512.
34. P. Schulze and D. Belder, *Analytical and Bioanalytical Chemistry*, **2009**, *393*, 515-525.
35. S. Wakida, K. Fujimoto, H. Nagai, T. Miyado, Y. Shibutani and S. Takeda, *Journal of Chromatography A*, **2006**, *1109*, 179-182.
36. B. C. Giordano, A. Terray and G. E. Collins, *Electrophoresis*, **2006**, *27*, 4295-4302.
37. Y. Ueno, T. Horiuchi, O. Niwa, H. S. Zhou, T. Yamada and I. Honma, *Sensors and Actuators B-Chemical*, **2003**, *95*, 282-286.
38. Q. Lu and G. E. Collins, *Analyst*, 2001, **126**, 429-432.
39. P. D. Ohlsson, O. Ordeig, K. B. Mogensen and J. P. Kutter, *Electrophoresis*, **2009**, *30*, 4172-4178.
40. J. Kuijt, C. García-Ruiz, G. J. Stroomberg, M. L. Marina, F. Ariese, U. A. T. Brinkman and C. Gooijer, *Journal of Chromatography A*, **2001**, *907*, 291-299.
41. S. J. Kok, G. P. Hoornweg, T. de Ridder, U. A. T. Brinkman, N. H. Velthorst and C. Gooijer, *Journal of Chromatography A*, **1998**, *806*, 355-360.
42. A. Gáspár, I. Bácsi, E. Garcia, M. Braun and F. Gomez, *Analytical and Bioanalytical Chemistry*, **2009**, *395*, 473-478.
43. M. J. Walworth, R. M. Connatser and M. J. Sepaniak, *Journal of Separation Science*, **2009**, *32*, 2985-2992.
44. N. Hudson, A. Baker and D. Reynolds, *River Research and Applications*, **2007**, *23*, 631-649.
45. S. L. Shen, Y. Li and S. Wakida, *Environmental Monitoring and Assessment*, **2010**, *166*, 573-580.
46. K. Tolba and D. Belder, *Electrophoresis*, **2007**, *28*, 2934-2941.
47. B. S. Broyles, S. C. Jacobson and J. M. Ramsey, *Analytical Chemistry*, **2003**, *75*, 2761-2767.
48. M. Benhabib, T. N. Chiesl, A. M. Stockton, J. R. Scherer and R. A. Mathies, *Analytical Chemistry*, **2010**, *82*, 2372-2379.
49. S. R. Wallenborg and C. G. Bailey, *Analytical Chemistry*, **2000**, *72*, 1872-1878.
50. J. Ramon-Azcon, R. Kunikata, F. J. Sanchez, M. P. Marco, H. Shiku, T. Yasukawa and T. Matsue, *Biosensors & Bioelectronics*, **2009**, *24*, 1592-1597.
51. W. Som-Aum, H. Li, J. J. Liu and J. M. Lin, *Analyst*, **2008**, *133*, 1169-1175.
52. Y. S. Ding, C. D. Garcia and K. R. Rogers, *Analytical Letters*, **2008**, *41*, 335-350.
53. L. X. Chen and J. B. Choo, *Electrophoresis*, **2008**, *29*, 1815-1828.
54. P. C. Ashok, G. P. Singh, K. M. Tan and K. Dholakia, *Optics Express*, **2009**, *18*, 7642-7649.
55. H. B. Wei, H. F. Li and J. M. Lin, *Journal of Chromatography A*, **2009**, *1216*, 9134-9142.
56. P. S. Dittrich and A. Manz, *Anal. Bioanal. Chem.*, **2005**, *382*, 1771-1782.
57. S. Ramirez-Garcia, M. Baeza, M. O'Toole, Y. Z. Wu, J. Lalor, G. G. Wallace and D. Diamond, *Talanta*, **2008**, *77*, 463-467.
58. R. Alves-Segundo, N. Ibanez-Garcia, M. Baeza, M. Puyol and J. Alonso-Chamarro, *Microchimica Acta*, **172**, 225-232.
59. V. J. Sieben, C. F. A. Floquet, I. R. G. Ogilvie, M. C. Mowlem and H. Morgan, *Analytical Methods*, **2**, 484-491.
60. D. Barat, G. Benazzi, M. C. Mowlem, J. M. Ruano and H. Morgan, *Optics Communications*, **2009,** *283*, 1987-1992.

61. N. Beyor, L. N. Yi, T. S. Seo and R. A. Mathies, *Analytical Chemistry*, **2009**, *81*, 3523-3528.
62. N. Dossi, S. Susmel, R. Toniolo, A. Pizzariello and G. Bontempelli, *Electrophoresis*, **2009**, *30*, 3465-3471.
63. S. D. Noblitt, F. M. Schwandner, S. V. Hering, J. L. Collett and C. S. Henry, *Journal of Chromatography A*, **2009**, *1216*, 1503-1510.
64. Z. H. Nie, C. A. Nijhuis, J. L. Gong, X. Chen, A. Kumachev, A. W. Martinez, M. Narovlyansky and G. M. Whitesides, *Lab on a Chip*, **2009,** *10*, 477-483.
65. A. Apilux, W. Dungchai, W. Siangproh, N. Praphairaksit, C. S. Henry and O. Chailapakul, *Analytical Chemistry*, **2010,** *82*, 1727-1732.

APPENDIX II. ORIGINAL RESEARCH PROPOSAL:

A MICROFLUIDIC DEVICE FOR EARLY-PREGNANCY, FETAL SEX DETERMINATION USING A GOLD NANOPARTICLE-BASED ASSAY

A2.1 APPENDIX II OVERVIEW

A non-invasive method for the determination of fetal sex in the first trimester of pregnancy is desired for the management of congenital diseases and could aid in further screening for X-linked genetic disorders. Currently, fetal sex is determined via ultrasonic examination with 68-78% accuracy at 11 weeks and 83-100% accuracy at 13 weeks gestation. However, for pregnant women at risk for chromosomal abnormalities, chorionic villus sampling (CVS) is offered for fetal sex determination and diagnosis in the first trimester. CVS is an invasive procedure that is known to increase the risk of miscarriage, birth defects and even death. The development of a non-invasive, point-of-care method for fetal sex determination in the first trimester would eliminate the need for CVS in many cases. The discovery of fetal DNA in maternal circulation provides great potential for non-invasive, prenatal diagnostics. Detection of Y-chromosome specific sequences via sensitive polymerase chain reaction (PCR) methods confirms a male fetus while the absence of these genes is associated with a female fetus. Some research has been conducted in this area and typically involves detection of PCR products with either fluorescence or mass spectrometry detection. While these methods are highly selective and sensitive, the high cost of analysis and need for well-trained technicians are major hindrances.

The method proposed here involves a microfluidic device for detection of three Y-chromosome specific sequences: SRY, DBY, and TTTY2, for enhanced specificity. A plasma sample is collected from the mother and undergoes on-chip PCR in parallel within designated chambers of the device. After the amplification step, the PCR products are directed to three detection zones containing gold nanoparticles functionalized with both the 3'- and 5'- terminus of the complementary bases for each of the three sequences. Upon hybridization of the target DNA, the gold nanoparticles undergo cross-linking aggregation to generate a color change visible to the naked eye. A positive result for all three Y-chromosome sequences confirms a male fetus. Initial optimization of the device would involve analysis of plasma samples from pregnant women at various time points within the first trimester of pregnancy as well as testing the same patients in the second or third trimester, when the fetus sex can be confirmed with ultrasound for method validation. Ultimately, this device could provide a fast and inexpensive means of fetal sex determination in the early weeks of pregnancy, relative to available technologies.

A2.2 BACKGROUND AND SIGNIFICANCE

The development of prenatal diagnostic techniques has allowed for a tremendous increase in the understanding of genetic disorders and the advent of new treatment options. For example, congenital adrenal hyperplasia (CAH) is a class of hormonal disorders in which the adrenal gland does not produce normal levels of steroid hormones required for healthy endocrine function. For families at high risk for CAH, the ability to distinguish a fetus sex and subsequently administer the appropriate hormones to the mother prior to 9 weeks gestation is crucial for the prevention of birth defects. Additionally, early diagnosis of X-linked genetic disorders, such as Duchenne muscular dystrophy, can prove helpful in establishing treatment options. X-linked disorders are

genetic abnormalities associated with the X chromosome. The disorders and diseases that arise from such chromosomal deviations are almost always expressed in male fetuses, who inherit the X chromosome from the mother. While the incidence of X-linked diseases is estimated at only 0.5% of pregnancies; the resulting complications are severe and often fatal.[1]

Currently, chorionic villus sampling (CVS) is offered as a first step for fetal sex determination in conjunction with the diagnosis of X-linked genetic disorders at 11-13 weeks of gestation.[2] CVS is an invasive technique that has become standard practice in obstetric care for prenatal karyotyping and is offered to pregnant women with indications of chromosomal abnormalities in the fetus.[3] These risk indicators include abnormalities in a previous pregnancy, genetic disposition or family history, as well as the age of the mother. The extent to which this invasive technique jeopardizes the health of the fetus or infant continues to be examined; however, this procedure has been linked to increased risk of major orthopaedic deformities, respiratory disorders, premature birth, and even fetal mortality.[3-6] The development of a non-invasive, cost-effective technique for determining fetal sex within the first trimester would lead to a substantial reduction in the use of unnecessary diagnostic tests, such as karyotyping and molecular analysis, in the case of female fetuses. The number of time-consuming, costly, and risky CVS procedures would also dramatically decrease.[6]

In the late 1990's, fetal DNA was discovered in the maternal circulation, offering new alternatives for non-invasive prenatal diagnosis.[7] Reports by Lo and co-workers have shown that fetal DNA exists in maternal circulation not only as intact fetal cells but also cell-free DNA (cff-DNA).[7] Lo also determined a surprisingly high fetal DNA concentration in maternal plasma, estimated at 3.4% of the total plasma DNA at gestational periods as early as 5 weeks and 6.2% of the total plasma DNA in late-stage pregnancy.[8,9] While the biological mechanism by

which fetal DNA is liberated into maternal plamsa is still under investigation, researchers have recognized the powerful impact of this discovery for prenatal diagnostics. The most sensitive molecular technique that allows for detection and quantification of low concentrations of specific DNA sequences is polymerase chain reaction (PCR).[10] Since the discovery of fetal DNA in maternal circulation, PCR amplification and detection of cff-DNA has been used in the diagnosis of X-linked disorders such as Hunter's syndrome, adrenoleukodystrophy, hemophilia, Menke's syndrome, X-linked mental retardation, Duchenne muscular dystrophy, and Alport's syndrome, to name a few.[9]

Polymerase chain reaction is an extremely valuable technique for the analysis of low-abundance, molecular analytes in biological samples. The technique was developed in the early 1980's and involves the duplication or amplification of specific DNA sequences.[11] Specific oligonucleotides, or primers, with the complementary base pairs of the target DNA sequence are introduced along with DNA polymerase, the key enzyme in DNA replication. The sample undergoes thermal cycling, a controlled series of heating and cooling cycles, to effectively separate the two DNA strands of the sample and allow replication of target sequences, directed by selective primers. Upon completion of several thermal cycles, thousands to millions of copies of the target DNA sequence are generated. Today, nearly all assays for DNA sequences use PCR to amplify specific segments from as little as a single copy of DNA to easily detectable quantities.

One specific example of detecting fetal DNA in maternal circulation includes the work of Miura and co-workers.[2] The authors developed a PCR method for the detection of cff-DNA from maternal plasma. The goal of this study was to determine fetal sex for prenatal diagnosis in carriers of Duchenne muscular dystrophy using a non-invasive, conventional PCR technique at

9-12 weeks of gestation. If the fetus is confirmed male, follow-up CVS could be performed at 12 weeks of gestation. If the fetus is female, however, CVS and the associated risks can be avoided. Using PCR to amplify the X-specific FMR1 gene and the Y-specific SRY gene from plasma samples collected from pregnant women, Miura and co-workers determined the fetal sex in 100 trials with 100% accuracy, including three pregnant carriers of Duchenne muscular dystrophy. In plasma samples for women pregnant with a male fetus, both X- and Y-specific PCR products were detected via gel electrophoresis; while for women pregnant with a female fetus, only X-specific products were detected.

The advent of functional integration of PCR in a microchip has made great contributions in the field of micro total analysis systems (μTAS), leading to major advancements in clinical applications.[12] Miniaturized and integrated microfluidic devices are attractive alternatives to conventional instrumentation because of their ability to perform the necessary complex processes for high-throughput analysis with reduced reagent and sample consumption, smaller footprint, and shorter analysis times. Conventional PCR, in particular, suffers from high analysis cost due to microliter reaction volumes and long assay times because of slow thermal transition rates. On-chip PCR addresses these problems by allowing rapid thermal cycling of low (nanoliter) reaction volumes for high-speed analysis and low-volume amplification. Additionally, high-throughput analysis is gained from the ability to multiplex in a parallel format. A number of microchip PCR devices have been developed with fabrication in silicon, glass, and silicon-glass hybrids as the most commonly used substrates. These materials, specifically, are advantageous as they are easily chemically modified for assay compatibility, fabricated from well-established wet etching techniques, provide good thermal stability compared to plastic microdevices, and posses ideal optical properties for fluorescence and UV/vis detection.

Recently, Liu and co-workers developed a multichannel, PCR-CE device that contains four independent reactor-separations systems for parallel analysis. The device is constructed from multiple layers of glass and poly(dimethylsiloxane) (PDMS). A glass pneumatic manifold acutates a PDMS microvalve for fluid control, while resistance temperature detectors (RTDs) and heaters are integrated and employed for rapid, simultaneous thermal cycling. Schematics of the various device components are shown in Figure A2.1. PCR chamber valves are opened and closed by applying a vacuum or pressure using tubing connected to the glass manifold, and thermal cycling is controlled via a LabVIEW program and an external power supply.

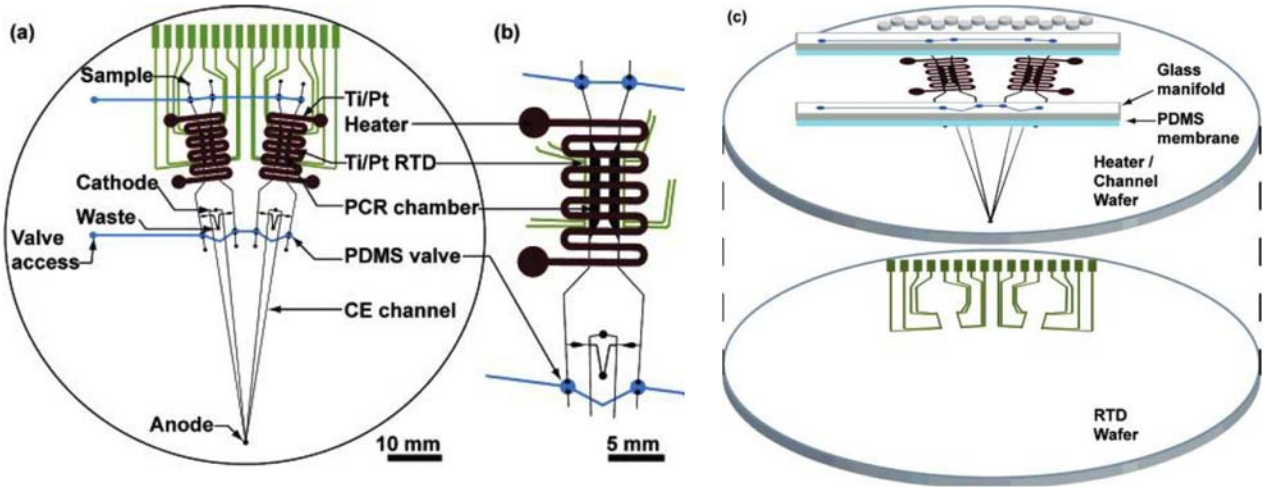

Figure A2.1. A) Schematic of the microfluidic PCR-CE device designed by Liu and co-workers. B) Detailed view of the PCR chambers with overlaid heater and resistive temperature detector for thermal cycle control. C) Assembly of the microchip PCR-CE device from multiple layers of glass and PDMS.

Commonly implemented techniques for the analysis of PCR products include gel electrophoresis, fluorescence, and mass spectrometry. However, DNA hybridization using functionalized nanoparticles for simple, colorimetric analysis is gaining momentum in the realm of genetic diagnostic schemes. This strategy has several advantages including simplicity, cost-effectiveness, and the ability to be integrated into a microfluidic network.[13] Commercially

available gold nanoparticles (AuNPs), generally 10 to 50 nm in diameter, have proven to be very sensitive colorimetric labels in miniaturized biosensor platforms. AuNPs display an intense red color, with an extinction coefficient significantly higher than that of organic dyes, in aqueous environments due to the localized surface plasmon resonance. Characteristically, the interpartical distance of AuNPs has a direct effect on the color of the particles in solution. Therefore, when individual spherical AuNPs are in close proximity, which is generally defined as a center-to-center distance smaller than 2.5 times the particle diameter, a color change from red to blue is observed, resulting from the combined surface plasmon of the particles (Figure A2.2).[14-16] The application of this interparticle plasmon coupling of AuNPs has been used extensively for solution-phase, colorimetric biodetection.[17] Specifically, aggregation of AuNPs, with controlled interparticle distances, has been conducted with the molecular recognition properties of DNA. DNA-functionalized nanoparticles have been successfully implemented in sandwich-type assays in which target DNA cross-links two AuNPs through sequence specific hybridization, generating a qualitative, spectral shift visible to the naked eye. For a colorimetric assay, a solution containing a mixture of modified AuNPs is used. In order for controlled aggregation to occur via selective DNA hybridization, two types of modified AuNPs must exist in solution: those functionalized with 3'-terminus and 5'-terminus DNA sequences.

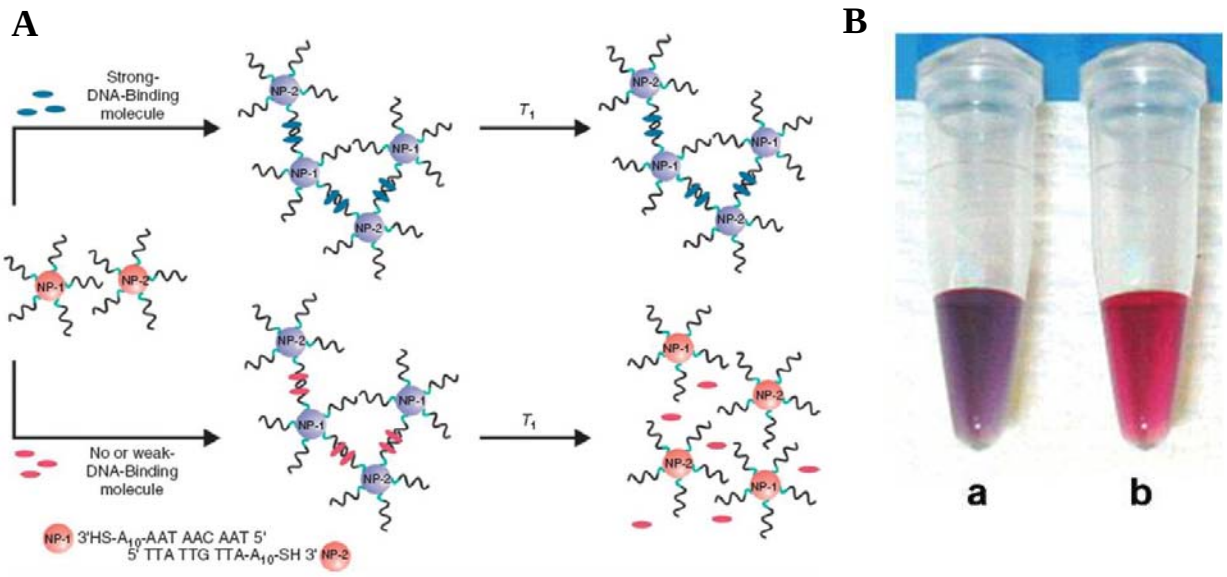

Figure A2.2. A) Illustration showing DNA-functionalized Au nanoparticles aggregating upon hybridization with complementary strands. B) Two AuNP solutions containing (a) complementary DNA sequences and (b) noncomplementary.

A2.3 RESEARCH DESIGN AND METHODS

A2.3.1 Specific Aims.

A microfluidic device will be constructed to include four on-chip PCR chambers for DNA amplification of three Y-chromosome specific genes (SRY, DBY, and TTTY2) and one X-chromosome specific gene (FRM1) to be used as a control, with subsequent hybridization on gold nanoparticles to generate a colorimetric effect in designated detection zones. This device will be developed for the purpose of providing non-invasive, disposable, cost-effective, and point-of-care analysis for fetal sex determination in the first trimester of pregnancy. The ability to determine fetal sex in the earliest weeks of pregnancy would aid in the diagnosis of X-linked genetic disorders, allowing for more treatment options and potentially eliminating the need for CVS. And while the utility of the proposed device holds great significance for the advancement of clinical diagnostics, commercial appeal is also a major selling point. A device for early fetal

sex determination could prove informative and desirable for many pregnant women, not just those at risk for chromosomal abnormalities.

A2.3.2 Optimization of Assays for SRY, DBY, TTY2, and FRM1 Sequences

The first task in this specific aim involves the optimization of each nucleic-acid based assay. Initially, optimization will be performed off-chip with conventional PCR, including thermal cycling sequences and determination of detection limits for each gene. In the work of Akolekar and co-workers, a single PCR method was developed for the simultaneous amplification of SRY, DBY, and TTTY2, the three Y-chromosome specific sequences.[19] This protocol will be investigated for the application presented here, where each of the four target genes will be amplified in separate PCR chambers containing the necessary primers and using a single resistive thermal detector to control temperature cycles. If simultaneous amplification is not sufficient for any of the four sequences, alternative methods will be developed for individual assays and these modifications will be considered in the final chip design.

The second task is to optimize the gold nanoparticle assembly scheme, using commercially available nanoparticles and well established thiol adsorption chemistry.[20,21] For a single assay, one set of AuNPs will be modified with oligonucleotides of specific sequence and length, which are functionalized with alkane thiols at their 3' terminus. The other set of AuNPs will undergo the same modification; however, the specific oligonucleotides are functionalized at their 5' terminus. The two AuNP solutions are combined and the previously amplified, complementary DNA sequence is added to induce aggregation and a visible color change. Optimal buffer conditions and annealing temperatures will be determined for each of the four assays. Successful colorimetric detection of all three Y-chromosome specific sequences and one X-chromosome specific sequence will demonstrate proof-of-concept for the device.

A2.3.3 Design and Fabrication of the Microfluidic Device

The microfluidic device will be constructed, modeling much of the design after the device presented by Liu and co-workers. Identical to Liu's device, two resistive temperature detectors and heaters are fabricated side-by-side, each used to control thermal cycles for two PCR chambers. The resistive temperature detectors and heaters will be fabricated on a glass wafer, sputter-coating the wafer with Ti and Pt. Photolithography is used to define and etch temperature detector elements and electrical leads. Four PCR chambers, microfluidic channels, and detection zones will be patterned with photoresist and etched in glass.[12,22] Fluid control is achieved using an etched glass manifold wafer that actuates PDMS microvalves, as described by Grover et al.[23] Using these valves, amplified samples from the four PCR chambers may be directed to designated detection zones, housing the DNA-labeled gold nanoparticles, where hybridization takes place. Each detection zone will be designated for one of the three Y-chromosome specific sequences and a fourth zone for the X-chromosome specific sequence. To complete fabrication, all of the layers of the chip are aligned and thermally bonded. Figure A2.3 presents images of Lui's device; the footprint of the chip, power supply, and laptop; as well as a schematic of the proposed microfluidic design.

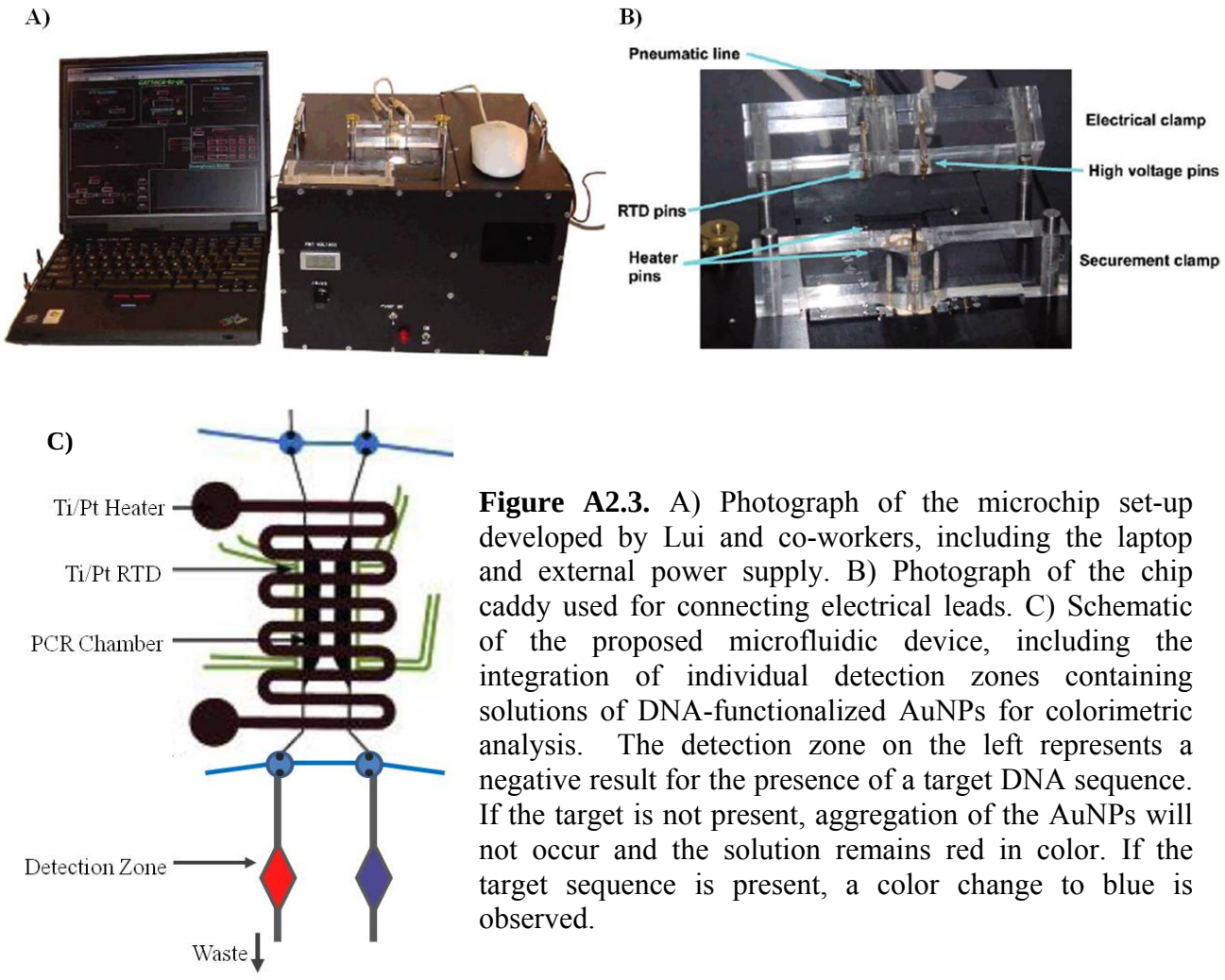

Figure A2.3. A) Photograph of the microchip set-up developed by Lui and co-workers, including the laptop and external power supply. B) Photograph of the chip caddy used for connecting electrical leads. C) Schematic of the proposed microfluidic device, including the integration of individual detection zones containing solutions of DNA-functionalized AuNPs for colorimetric analysis. The detection zone on the left represents a negative result for the presence of a target DNA sequence. If the target is not present, aggregation of the AuNPs will not occur and the solution remains red in color. If the target sequence is present, a color change to blue is observed.

A2.3.4 Analysis of Real Plasma Samples

The established PCR method and subsequent AuNP aggregation protocol will be tested with real plasma samples acquired from pregnant women in their second or third trimester. Testing samples from late-stage pregnancies will provide higher concentrations of fetal DNA in the maternal circulation than at earlier stages for preliminary studies.[7] Additionally, the accuracy of the method can be confirmed via previously acquired ultrasound results. The goal in this specific aim is to perform amplification and detection of real samples on-chip, working toward

successful analysis of samples taken in the first few weeks of gestation (5-7 weeks). In testing real plasma samples, all committees on campus have been satisfied.

Based on Akolekar's findings, detection of all three Y-chromosome specific sequences, indicated by a color change from red to blue in the three detection zones, will confirm a male fetus. Detection of one or none of the Y-chromosome sequences will confirm a female fetus. If only two sequences are detected, the sample will be considered inconclusive at this time and require retesting.[19] In rare cases, female fetuses could be falsely classified as male due to the homology of some X-chromosome specific sequences to Y-chromosome specific sequences. The use of three Y-chromosome specific markers enhances selectivity and sensitivity, avoiding false positive results.

Another situation that could generate inconclusive results is in the case of twins. Plasma samples from pregnancies with confirmed identical and fraternal twins will be investigated. Most likely, the sex of female identical twins and male identical twins could be confirmed easily with the proposed method; however, the presence of twins may be more challenging to identify. In the case of fraternal twins, the detection of Y-chromosome specific genes will confirm the presence of a male fetus, but the female twin may go undetected. To address this issue, additional assays for the PCR amplification and detection of autosomal polymorphic loci will be developed in the next phase of this research, providing more selective detection of female fetuses.[8]

A2.4 CONCLUSIONS

The development of a microfluidic device for on-chip PCR amplification of cff-DNA from maternal plasma with subsequent colorimetric detection of Y-chromosome specific sequences using AuNP aggregation would provide a simple, cost-effective means of fetal sex determination

within the first trimester of pregnancy. Such a device could greatly reduce the need for invasive and potentially dangerous CVS procedures and the number of expensive karyotyping analyses conducted. The proposed device would provide a simple, qualitative platform for confirmation of fetal sex, using an easily interpreted colorimetric detection scheme. The small footprint of microfluidic devices allow for faster, less expensive analyses as well as implementation in point-of-care applications.

A2.5 REFERENCES

1. Mazza, V.; Falcinelli, C.; Percesepe, A.; Paganelli, S.; Volpe, A.; Forabosco, A. *Prenat. Diagn.* **2002,** *22* (10), 919-924.
2. Miura, K.; Higashijima, A.; Shimada, T.; Miura, S.; Yamasaki, K.; Abe, S.; Jo, O.; Kinoshita, A.; Yoshida, A.; Yoshimura, S.; Niikawa, N.; Yoshiura, K.-i.; Masuzaki, H. *J Hum Genet* **2011,** *56* (4), 296-299.
3. Cederholm, M.; Haglund, B.; Axelsson, O. *BJOG: An International Journal of Obstetrics & Gynaecology* **2005,** *112* (4), 394-402.
4. Tabor, A.; Madsen, M.; Obel, E.; Philip, J.; Bang, J.; Gaard-Pedersen, B. *The Lancet* **1986,** *327* (8493), 1287-1293.
5. Smidt-Jensen, S.; Philip, J.; Lundsteen, C.; Permin, M.; Zachary, J. M.; Fowler, S. E. *The Lancet* **1992,** *340* (8830), 1237-1244.
6. Costa, J.-M.; Benachi, A.; Gautier, E. *New England Journal of Medicine* **2002,** *346* (19), 1502-1502.
7. Lo, Y. M. D.; Corbetta, N.; Chamberlain, P. F.; Rai, V.; Sargent, I. L.; Redman, C. W. G.; Wainscoat, J. S. *The Lancet* **1997,** *350* (9076), 485-487.
8. Pertl, B.; Sekizawa, A.; Samura, O.; Orescovic, I.; Rahaim, P. T.; Bianchi, D. W. *Human Genetics* **2000,** *106* (1), 45-49.
9. Lo, Y. M. D.; Tein, M. S. C.; Lau, T. K.; Haines, C. J.; Leung, T. N.; Poon, P. M. K.; Wainscoat, J. S.; Johnson, P. J.; Chang, A. M. Z.; Hjelm, N. M. *The American Journal of Human Genetics* **1998,** *62* (4), 768-775.
10. Invernizzi, P.; Biondi, M.; Battezzati, P.; Perego, F.; Selmi, C.; Cecchini, F.; Podda, M.; Simoni, G. *Human Genetics* **2002,** *110* (6), 587-591.
11. Bartlett, J. M. S.; Stirling, D., *A Short History of the Polymerase Chain Reaction* *PCR Protocols.* Bartlett, J. M. S.; Stirling, D., Eds. Humana Press: **2003**; Vol. 226, pp 3-6.
12. Lagally, E. T.; Emrich, C. A.; Mathies, R. A. *Lab on a Chip* **2001,** *1* (2), 102-107.
13. Jung, C.; Chung, J. W.; Kim, U. O.; Kim, M. H.; Park, H. G. *Biosensors and Bioelectronics* **2011,** *26* (5), 1953-1958.
14. Elghanian, R.; Storhoff, J. J.; Mucic, R. C.; Letsinger, R. L.; Mirkin, C. A. *Science* **1997,** *277* (5329), 1078-1081.
15. Han, M. S.; Lytton-Jean, A. K. R.; Oh, B.-K.; Heo, J.; Mirkin, C. A. *Angewandte Chemie International Edition* **2006,** *45* (11), 1807-1810.
16. Li, H. X.; Rothberg, L. J. *Journal of the American Chemical Society* **2004,** *126* (35), 10958-10961.
17. Bellan, L. M.; Wu, D.; Langer, R. S. *Wiley Interdisciplinary Reviews: Nanomedicine and Nanobiotechnology* **2011,** *3* (3), 229-246.
18. Akolekar, R.; Farkas, D. H.; VanAgtmael, A. L.; Bombard, A. T.; Nicolaides, K. H. *Prenat. Diagn.* **2010,** *30* (10), 918-923.
19. Liu, C. N.; Toriello, N. M.; Mathies, R. A. *Analytical Chemistry* **2006,** *78* (15), 5474-5479.
20. Grover, W. H.; Skelley, A. M.; Liu, C. N.; Lagally, E. T.; Mathies, R. A., Monolithic *Sensors and Actuators B: Chemical* **2003,** *89* (3), 315-323.